UNIVERSITÀ DEGLI STUDI DI MILANO – BICOCCA
Facoltà di Scienze Matematiche, Fisiche e Naturali
Scuola di dottorato di Scienze
Dottorato di ricerca in Biotecnologie Industriali - XXV ciclo

K-ras cancer cell fate under glucose deprivation is influenced by alteration of bioenergetic metabolism

Dott. ssa Roberta Palorini

Tutor: Dott. Ferdinando Chiaradonna

Coordinatore: Prof. Marco Vanoni

Anno Accademico 2012

ABSTRACT

Several cancer cells, in order to generate ATP and sustain different anabolic processes, rely mainly on glycolysis instead of Oxidative Phosphorylation (OXPHOS). Thus, glucose assumes a critical role for cancer cell survival and proliferation. Moreover, through the penthose phospate pathway glucose leads to production of NADPH contributing to maintenance of cellular oxidative equilibrium. Besides, glucose can also enter Hexosamine Biosynthesis Pathway (HBP), sustaining lipid and protein N- and O-glycosylation that cover an important role in cancer development.

Taking in consideration the essential role of glucose in cancer, one important anticancer therapeutic approach is to target its metabolism namely glycolysis and the other processes in which it is involved. On this regard, glucose deprivation and consequent analysis of cancer cell fate both at phenotypical and molecular level can be a useful strategy to unmask all mechanisms that participate to glucose-mediated cancer cell growth and survival. Such a strategy could be subsequently exploited to provide new targets and to set new anticancer therapies.

Although there is evidence that tumors originate from cells with persistent defects in the mitochondrial respiratory system, inhibition of OXPHOS activity seems to be an adaptation to cancer metabolism reprogramming rather than a cause. In this scenario, reversible post-translational modifications of mitochondrial components could assume an important regulatory role. Among the most important post-translational modifications there is Ser/Thr phosphorylation and, on this regard, the protein kinase PKA has numerous mitochondrial targets being involved in the regulation of the biogenesis, the

import and the activity of mitochondrial Complex I or IV as well as of mitochondrial morphology. Since it has been observed that oncogenic *K-ras* may lead to a depression of genes encoding for components of the cAMP/PKA signaling pathway, in *K-ras*-transformed cells the deregulation of cAMP/PKA pathway could cause OXPHOS depression and "glucose addiction" of cancer cells. In agreement with such a hypothesis, *K-ras*-transformed cells show lower PKA activity as compared to normal cells. Moreover, exogenous stimulation of PKA activity, achieved by Forskolin (FSK) treatment, protects mouse and human *K-ras*-transformed cells from apoptosis induced by glucose deprivation, by enhancing Complex I activity, intracellular ATP levels and mitochondrial fusion and by decreasing intracellular ROS levels. Worth noting, several of these effects are almost completely prevented by inhibition of PKA activity. Moreover, short time treatment with Mdivi-1, a molecule that favors mitochondrial fusion, strongly decreases the cellular ROS levels especially in transformed cells, indicating a close relationship between mitochondrial morphology and activity. These findings support the notion that glucose shortage-induced apoptosis, specific of *K-ras*-transformed cells, is associated to a derangement of PKA signaling that leads to mitochondrial Complex I decrease, reduction of ATP formation and prevalence of mitochondrial fission over fusion. Such a discovery can thereby open new approaches for the development of anticancer drugs.

Given that glucose shortage is often encountered in the tumor microenvironment, it can be exploited to potentiate the action of specific agents, such as the mitochondrial OXPHOS activity modulators, that in condition of glucose deprivation could be lethal for cancer cells. Accordingly, it is shown that glucose deprivation and Complex I inhibitors, i.e., rotenone, piericidin A and

capsaicin, synergize in inducing cancer cell death. In particular, low doses of Complex I inhibitors, ineffective on normal cells and on cells grown in high glucose, become specifically cytotoxic on cancer cells cultured in low glucose. Importantly, the cytotoxic effect of Complex I inhibitors is strongly enhanced when mitochondrial OXPHOS activity is stimulated by FSK. These findings demonstrate that the reactivation of the mitochondrial function associated with glucose depletion and low doses of mitochondrial Complex I inhibitors strongly affect cancer cell survival. This therapeutic approach might be valuable to eradicate cancer cells.

As above indicated, glucose is implicated in numerous processes in cancer cells. Transcriptomic and proteomic analyses applied to mouse *K-ras*-transformed cells as compared to normal cells show that glucose deprivation modulates the expression of several genes linked to endoplasmic reticulum stress and the Unfolded Protein Response (UPR). The activation of such a response, as confirmed by mRNA and protein expression, is observed in both cell lines, but only in transformed cells is strictly associated to their death. In fact, its attenuation by protein translation inhibitor cycloheximide or chemical chaperone 4-Phenyl-butyrate specifically rescues transformed cells from death. Moreover, glucose deprivation-induced transformed cell death is also prevented by inhibition of an UPR downstream pro-apoptotic kinase, JNK, whose activation is observed specifically in transformed cells as compared to normal cells. Interestingly, UPR activation and death of transformed cells is completely prevented by addition of a specific HBP substrate, namely N-Acetyl-D-glucosamine, suggesting a strict relation between the two processes. Notably, also oncogenic *K-ras* expressing human glycolytic cells show similar effects after UPR modulating treatments. Thus, we show that glucose deprivation can

induce an UPR-dependent transformed cell death mechanism, which is activated by harmful accumulation of unfolded proteins, probably as consequence of N-glycosylation protein reduction. The full elucidation of this response could be relevant to design new therapeutic strategies.

Today the new challenge of anticancer research and therapy is the total eradication of the cancer, targeting cancer stem cells (CSCs). Considering the important role of metabolism and metabolic reprogramming in cancer development, also the definition of CSCs metabolism can be considered an important tool for future strategies targeting these cells. Recently, a human osteosarcoma 3AB-OS CSC-like line has been developed. Therefore we have decided to characterize its metabolic features as compared to the parental osteosarcoma MG63 cells, from which 3AB-OS cells were previously selected. 3AB-OS cells depend on glycolytic metabolism more strongly than MG63 cells. Indeed, addition to the growth medium of galactose and pyruvate -mitochondrial specific substrates- instead of glucose markedly reduces 3AB-OS growth, as compared to MG63 cells. In line with these findings 3AB-OS cells, compared to MG63 cells, are strongly sensitive to glucose depletion, glycolysis inhibition and less sensitive to respiratory inhibitors. Additionally, in contrast to MG63 cells, 3AB-OS display mainly fragmented mitochondria, particularly in low glucose. Overall, these findings suggest that 3AB-OS energy metabolism is more similar either to normal stem cells or to cancer cells characterized by a glycolytic metabolism. Interestingly, the transcriptional profile of CSCs is similar to that of *K-ras*-transformed cells, confirming a possible similarity to glycolytic cancer cells. Therefore, some strategies developed for glucose addicted cancer cells could be used also to treat specific CSCs.

RIASSUNTO

Molte cellule tumorali, al fine di generare ATP e sostenere i processi anabolici, si servono principalmente della glicolisi piuttosto che della respirazione mitocondriale. Di conseguenza, il glucosio assume un ruolo critico per la sopravvivenza e la proliferazione delle cellule tumorali. Inoltre, attraverso la via dei pentosi fosfati, il glucosio porta alla formazione di NADPH, contribuendo al mantenimento nelle cellule dell'equilibrio ossidativo. Nondimeno, il glucosio può entrare anche nel *pathway* biosintetico delle esosammine (HBP), sostenendo la N- e O-glicosilazione di lipidi e proteine, importante per lo sviluppo tumorale. Considerando l'essenziale ruolo del glucosio, un possibile approccio per la terapia antitumorale è l'utilizzo del metabolismo del glucosio come *target*, non solo attraverso la glicolisi ma sfruttando anche gli altri processi glucosio-dipendenti. A tal proposito, la deprivazione di glucosio e la seguente analisi del destino cellulare a livello fenotipico e molecolare possono costituire una strategia utile per smascherare tutti i meccanismi mediati dal glucosio che partecipano alla crescita e alla sopravvivenza delle cellule tumorali. Tale strategia potrebbe essere poi sfruttata per offrire nuovi *target* e progettare nuove terapie antitumorali.

Sebbene alcuni dati indichino che i tumori originino da cellule con persistenti difetti alla catena respiratoria mitocondriale, l'inibizione della fosforilazione ossidativa (OXPHOS) sembra una condizione di adattamento più che una causa della riprogrammazione metabolica delle cellule tumorali. In questo scenario, i meccanismi di regolazione post-traduzionali, di natura essenzialmente reversibile, a carico di proteine mitocondriali potrebbero assumere un importante ruolo regolatorio. Una delle principali modificazioni post-traduzionali è la

fosforilazione dei residui Ser/Thr e, a tal proposito, la chinasi PKA presenta numerosi *target* a livello mitocondriale ed è coinvolta nella regolazione di biogenesi, trasporto e attività dei Complessi I e IV e della morfologia mitocondriale. Poiché è stato osservato che *K-ras* può causare la diminuzione dell'espressione di geni codificanti per componenti della via cAMP/PKA, nelle cellule *K-ras*-trasformate la deregolazione di tale via potrebbe portare alla disfunzione mitocondriale ed allo *switch* metabolico caratteristico delle cellule tumorali. A conferma di questa ipotesi, le cellule *K-ras*-trasformate mostrano minori livelli di attività dell'enzima PKA rispetto alle cellule normali. Inoltre, la stimolazione esogena della attività della PKA, ottenuta mediante trattamento con forskolina (FSK), protegge le cellule *K-ras*-trasformate, sia murine sia umane, dalla morte indotta dalla deplezione di glucosio. Tale protezione è dovuta alla stimolazione dell'attività del Complesso I, all'aumento dell'ATP intracellulare e della fusione mitocondriale e alla riduzione dei livelli di ROS. L'inibizione specifica di PKA previene quasi completamente molti di questi effetti. Inoltre, il breve trattamento con Mdivi-1, molecola in grado di favorire la fusione mitocondriale, riduce fortemente i livelli di ROS specialmente nelle cellule trasformate, indicando una stretta relazione tra morfologia e attività mitocondriale. Queste osservazioni supportano l'idea che l'apoptosi indotta dalla deprivazione di glucosio nelle cellule *K-ras*-trasformate è associata alla deregolazione della via cAMP/PKA che a sua volta causa la diminuzione dell'attività del Complesso I, la riduzione della produzione di ATP e la prevalenza della fissione mitocondriale rispetto alla fusione. Tale scoperta può aprire nuovi scenari per lo sviluppo di farmaci antitumorali.

Poiché la carenza di glucosio si può riscontrare nell'ambiente in cui cresce e si sviluppa il tumore, tale condizione può essere sfruttata per potenziare l'azione di

specifici agenti, come alcuni modulatori dell'OXPHOS. Infatti, l'inibizione delle funzioni mitocondriali in condizioni di deprivazione di glucosio potrebbe risultare letale per le cellule tumorali. In accordo, in questo lavoro viene mostrato che la deprivazione di glucosio e gli inibitori del Complesso I, come rotenone, piericidina A e capsaicina, hanno un effetto sinergico nell'indurre la morte delle cellule tumorali. Nello specifico, basse dosi d'inibitori del Complesso I, inefficaci sulle cellule normali e su cellule cresciute in alto glucosio, diventano citotossiche per le cellule tumorali cresciute in basso glucosio. L'effetto citotossico degli inibitori del Complesso I sulle cellule tumorali è ulteriormente e fortemente aumentato quando l'attività OXPHOS viene stimolata tramite il trattamento con FSK. Queste osservazioni dimostrano che la riattivazione della funzione mitocondriale associata alla deplezione di glucosio e al trattamento con basse dosi di inibitori del Complesso I riduce fortemente la sopravvivenza delle cellule tumorali e potrebbe quindi essere valutato come approccio terapeutico.

Come indicato in precedenza, nelle cellule tumorali il glucosio è implicato in numerosi processi. L'analisi trascrittomica e proteomica di cellule murine *K-ras*-trasformate e della loro controparte normale mostra che la deprivazione di glucosio modula l'espressione di molti geni legati allo stress del reticolo endoplasmatico e all'*Unfolded Protein Response* (UPR). L'attivazione di tale risposta si osserva in entrambe le linee cellulari ma più fortemente nelle cellule trasformate, dove è associata anche alla morte cellulare. Infatti, la sua attenuazione tramite l'inibitore della traduzione proteica, cicloesimide, o lo *chaperone* chimico, 4-fenil-butirrato, protegge specificatamente le cellule trasformate dalla morte cellulare in basso glucosio. Anche l'inibizione della chinasi proapoptotica JNK, attivata a valle dell'UPR, previene specificatamente

la morte delle cellule trasformate. Questa osservazione è in accordo col fatto che in basso glucosio le cellule trasformate mostrano una maggiore attivazione di JNK rispetto alle cellule normali. Inoltre, l'attivazione dell'UPR e la morte glucosio-dipendente delle cellule trasformate è completamente prevenuta dall'aggiunta nel terreno di coltura di un substrato dell'HBP, N-Acetyl-D-glucosammina, cosa che suggerisce una stretta relazione tra i due processi. È interessante notare che anche cellule umane esprimenti l'oncogene *K-ras* e caratterizzate da un fenotipo iperglicolitico mostrano simili effetti in seguito alla modulazione dell'UPR o dell'HBP. Quindi, la deprivazione di glucosio nelle cellule *K-ras*-trasformate può indurre un meccanismo di morte cellulare UPR-dipendente, attivato dall'eccessivo accumulo di proteine mal foldate, probabilmente come conseguenza della riduzione della N-glicosilazione delle proteine. La piena delucidazione di questa risposta potrebbe essere importante per progettare nuove strategie terapeutiche antitumorali.

Oggi la nuova sfida della ricerca e della terapia antitumorale è il totale sradicamento del tumore, uccidendo anche le cellule staminali tumorali (*cancer stem cells*, CSCs). Considerando l'importante ruolo del metabolismo e della sua riprogrammazione nello sviluppo tumorale, la caratterizzazione del metabolismo delle CSCs può essere considerata un importante mezzo per lo sviluppo di nuove strategie antitumorali. Recentemente, è stata ottenuta la linea cellulare staminale di osteosarcoma umano, 3AB-OS. In questo lavoro di tesi ho svolto una prima caratterizzazione del suo profilo metabolico, paragonato a quello delle cellule tumorali MG63, da cui le cellule 3AB-OS sono state selezionate. Si è osservato che le cellule 3AB-OS dipendono più fortemente dalla glicolisi rispetto alle cellule MG63. Infatti, quando cresciute in presenza di galattosio e piruvato (substrati mitocondriali) le cellule 3AB-OS riducono maggiormente la propria

capacità proliferativa rispetto alle cellule MG63. Esse risultano anche essere fortemente sensibili alla deprivazione di glucosio e al trattamento con inibitori della glicolisi mentre sono insensibili all'inibizione della catena respiratoria. Inoltre, diversamente dalle cellule MG63, le cellule 3AB-OS presentano principalmente mitocondri frammentati, in particolare in basso glucosio. Tutte queste osservazioni suggeriscono che il metabolismo energetico delle cellule 3AB-OS presenti caratteristiche paragonabili a quello delle cellule staminali normali e delle cellule tumorali caratterizzate da un metabolismo glicolitico. Può essere interessante notare che il profilo trascrizionale delle cellule 3AB-OS è simile a quello delle cellule *K-ras*-trasformate, confermando la similitudine tra le CSCs e le cellule tumorali glicolitiche. Quindi, alcune strategie sviluppate per il trattamento delle cellule tumorali glucosio-dipendenti potrebbero essere usate anche per trattare specifiche CSCs.

Chapter 1

Introduction

CHAPTER 1. INTRODUCTION

The hallmarks of cancer comprise different biological capabilities acquired during the multistep development of human tumors. In the last decade also energy metabolism reprogramming has emerged as a hallmark. In fact, the chronic and often uncontrolled cell proliferation that represents the essence of neoplastic disease involves not only deregulated control of cell proliferation but also corresponding adjustments of energy metabolism in order to fuel cell growth and division (Hanahan and Weinberg, 2011).

Cancer metabolism

Many cancer cells have a remarkable different metabolism from that of the tissues of origin, which allows them to sustain higher proliferative rates. In fact, they are characterized by an intense glycolytic activity that leads to a large production of lactic acid maintained also in conditions of normal oxygen tension (aerobic glycolysis), the so called "Warburg effect" (Chiaradonna *et al.*, 2012; Kroemer and Pouyssegur, 2008; Tennant *et al.*, 2010).

Metabolic reprogramming in cancer cells

In order to maintain the altered metabolism cancer cells, exploiting different strategies, reprogram numerous processes as compared to normal cells (**figure 1**).

Cancer cells frequently show an increased capacity for glucose uptake. This ability is the result of glucose transporters up-regulation. In particular, up-regulation of glucose transporter isoform 1 (GLUT-1), which is the transporter with the largest tissue distribution, has been observed in several types of tumors (gastrointestinal carcinoma, breast carcinoma, squamous cell carcinoma of head

and neck, renal cell carcinoma, ovarian and gastric cancers) (Brown and Wahl, 1993; Mellanen *et al.*, 1994; Nagase *et al.*, 1995). In addition, tumors are able to express at high levels some isoforms of Glut transporters, i.e., GLUT-3 or GLUT-5, that are normally not expressed in the most normal tissues (Chan *et al.*, 2004; Vander Heiden, 2011; Yamamoto *et al.*, 1990; Younes *et al.*, 1997).

Most cancer cells present increased expression or activity of glycolytic enzymes. Many cancer cells, in fact, overexpress hexokinase (HK), which catalyze the first step of glycolysis (conversion of glucose into glucose-6-phosphate, G6P, with consumption of ATP), ensuring in this way an increase of glycolytic flux. While most normal cells express the isoform HK1, cancer cells frequently express the form HK2 (Mathupala *et al.*, 2006). Notable, HK2 is located on the outer mitochondrial membrane protein VDAC (Voltage-Dependent Anion Channel). In this position HK2 gains both preferential access to mitochondrial generated ATP via the mitochondrial Adenine Nucleotide Translocator (ANT) and protection by its product G6P that normally at high concentration inhibits the enzyme. Thus, expressing and overproducing HK2, tumors can produce G6P at a high rate (Mathupala *et al.*, 2006).

Also the enzyme phosphofructokinase-1 (PFK-1), which irreversibly converts fructose-6-phosphate to fructose-1,6-bisphosphate (FBP), is overexpressed in various human cancer cell lines (Vora *et al.*, 1985). Since PFK-1 protein is allosterically inhibited by high levels of ATP, cancer cells have developed different strategies to relieve this ATP inhibition and, as consequence, to increase glucose metabolism in proliferating cells. For example, increased ATP consumption by UDPase ectonucleoside triphosphate diphosphorylase 5 (ENTPD5), involved in protein N-glycosylation, lowers ATP/AMP ratio and relieves allosteric inhibition of PFK-1 (Fang *et al.*, 2010). PFK-1 inhibition by ATP is diminished also by fructose-2,6- bisphosphate (F2,6BP), a metabolite

synthesized from fructose-6-phosphate. In particular, F2,6BP is produced and held at steady-state levels by the action of the bifunctional enzyme 6-phosphofructokinase/fructose-2,6-bisphosphatase (PFK2/FBPase). There are 4 isoforms of this enzyme; while PFKFB1, PFKFB2, and PFKFB4 display equal PFK2 and FBPase activities under basal conditions, PFKFB3 has high PFK2 and almost no FBPase activity (Okar and Lange, 1999; Okar *et al.*, 2001). Different tumors show high expression of the latter isoform, favoring the production of F2,6BP (Atsumi *et al.*, 2002; Tennant *et al.*, 2009). Moreover, studies performed in rat thyroid carcinomas and human gliomas, have shown that the PFK subunits expressed in these tumors are less sensitive to the allosteric inhibitors ATP and citrate (Meldolesi *et al.*, 1976; Oskam *et al.*, 1985; Staal *et al.*, 1987).

Lactate dehydrogenase (LDH) is the enzyme that interconverts pyruvate and NADH with lactate and NAD+, respectively. Levels of this enzyme are upregulated in tumor cells. In particular, differently to non-cancerous tissues, many cancer cells express and enhance activity of the isoform LDH-A (Fan *et al.*, 2011; Kroemer and Pouyssegur, 2008). LDH-A plays a key role in tumor maintenance, in fact its knocking down impairs cancer cell proliferation both *in vitro* and *in vivo* (Fantin *et al.*, 2006; Shim *et al.*, 1997). Moreover, to sustain the high rate of lactate production, also lactate transporters are upregulated in cancer cells, in particular the lactate-extruding enzyme monocarboxylate transporter 4 (MCT4) (Kroemer and Pouyssegur, 2008).

Not only enzymatic levels are regulated in cancer cells but also the selective expression of enzymatic isoforms that give specific advantages to cancer cells.

An example is the enzyme pyruvate kinase (PK) that catalyzes the reaction of glycolysis that converts phosphoenolpyruvate (PEP) to pyruvate. Many cancer cells exclusively express the M2 isoform of PK (Mazurek *et al.*, 2005), and PKM2 expression is important for tumor growth (Christofk *et al.*, 2008).

Although PKM2 is less active than PKM1 both *in vitro* and in cells (Vander Heiden *et al.*, 2010), probably it is selected by cancer cells because it can switch between active and inactive forms to switch rapidly from metabolites biosynthesis to promotion of mitochondrial ATP production (Lunt and Vander Heiden, 2011). An inactive PKM2 would support increased biosynthesis during periods that require higher concentrations of the glycolytic intermediates for amino acid, lipid and nucleotide synthesis. In contrast, active PK promotes oxidative phosphorylation (Lunt and Vander Heiden, 2011). Paradoxically, proliferating cells that selectively express the less active isoform of PK (M2) produce more lactate. The overall increase in glycolytic flux results in higher flux through PK despite expression of the less active isoform (Vander Heiden *et al.*, 2010). A possible explanation is that the expression of PKM2 can provide an efficient way to produce pyruvate in a PK-independent manner, therefore avoiding that PK generates ATP that can itself inhibit upstream steps of glycolysis. In fact, when PKM2 is in the inactive state, cells accumulate PEP and a phosphate group from PEP can be transferred to the glycolytic protein phosphoglycerate mutase 1 (PGAM1) what would therefore increase its mutase activity generating pyruvate without directly producing ATP (Vander Heiden *et al.*, 2010).

In many cancer cells also the expression of pyruvate dehydrogenase kinase 1 (PDK1) is increased, in particular as result of activation of hypoxia-inducible factor (HIF). This enzyme can phosphorylate and inactivate the pyruvate dehydrogenase complex, reducing the flow of pyruvate used by the TCA cycle and therefore favoring glycolytic flux (Hitosugi *et al.*, 2011; Schulze and Downward, 2011). Inhibition of PDK1 by dichloroacetate has been shown to shift metabolism from glycolysis to glucose oxidation and strongly reduce cancer cell viability and tumor growth (Bonnet *et al.*, 2007).

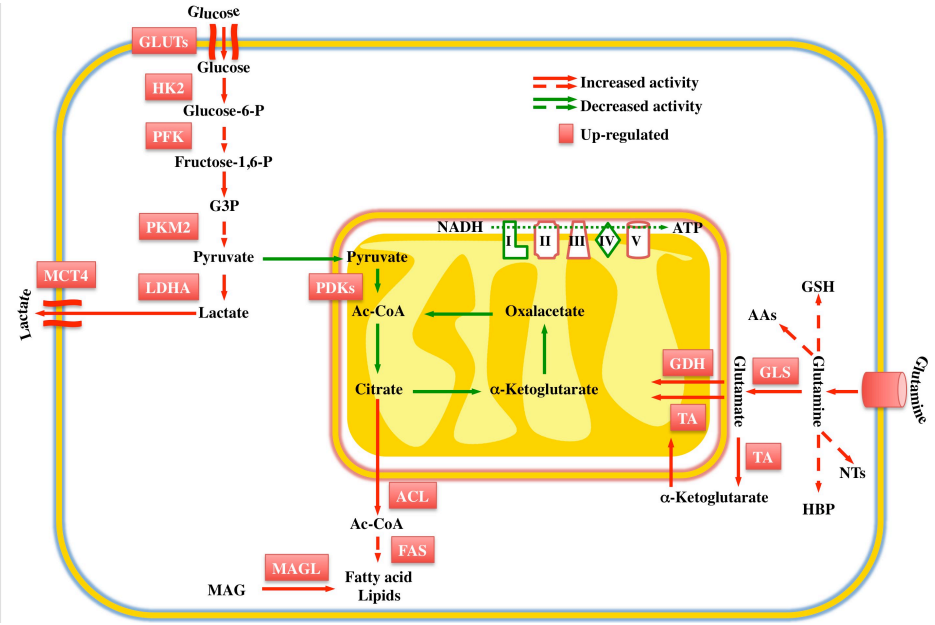

Figure 1. Metabolic pathways altered in cancer cells. Schematic representation of principal alterations identified in glycolysis, glutamine utilization and fatty acid metabolism of cancer cells. *Adapted from Chiaradonna et al., 2012.*
GLUT: glucose transporter; Glucose-6-P: glucose-6-phosphate; Fructose-6-P: fructose-6-phosphate; Fructose-1,6-P: fructose-1,6-bisphosphate; G3P: Glyceraldehyde-3-phosphate; HK: Hesokinase; PFK: Phosphofructokinase; PK: Pyruvate kinase; LDH: Lactate deyhdrogenase; MCT: monocarboxylate transporter; PDK: Pyruvate dehydrogenase kinase; Ac-CoA: Acetyl-CoenzymeA; ACL: ATP citrate lyase; FAS: Fatty acid synthase; MAGL: Monoacylglycerol lipase; MAG: Monoacylglycerol; GDH: Glutamate dehydrogenase; TA: transaminase; GLS: glutaminase; AAs: amino acids; GSH: Glutathione; NTs: nucleotides; HBP: Hexosamine Biosynthesis Pathway.

The importance of aerobic glycolysis for proliferating cells likely extends beyond rapid ATP production to allow nutrient assimilation into biosynthetic precursors and facilitate biomass accumulation (Lunt and Vander Heiden, 2011). Through glycolysis, glucose can provide the precursors for the chemical constituents (e.g., nucleotides, amino acids, and lipids) that are used to build macromolecules essential for cell division. Therefore, a main function of up-regulated glycolysis in proliferating cells may be to maintain the levels of

glycolytic intermediates needed to support biosynthesis (Lunt and Vander Heiden, 2011).

At the same time, also other metabolic reprogramming occur in cancer cells to provide building blocks for anabolic processes.

A metabolic pathway regulated in cancer cells is the metabolism of glycogen. In fact, in a recent paper (Favaro *et al.*, 2012) it has been shown that cancer cells, grown in hypoxia, increase the expression of both glycogen synthase (GYS1) and glycogen phosphorylase (PYGL). Glycogen degradation by PYGL is important for the optimal function of the pentose phosphate pathway (PPP) that leads to generation of NADPH, nucleotides, amino acids and lipids required for continuous cell proliferation. Worth noting is that PYGL depletion markedly impairs tumorigenesis *in vivo* (Favaro *et al.*, 2012).

Recently the tendency to increase glutamine consumption has been described as another metabolic feature of cancer cells. Indeed especially some types of cancer cells cannot survive in the absence of glutamine, exhibiting "glutamine addiction" (DeBerardinis and Cheng, 2010; Wise and Thompson, 2010). An intense use of glutamine reflects its importance as source both of energy and also of carbon and nitrogen (**figure 1**). Catabolism of glutamine, namely glutaminolysis, can provide carbons for TCA cycle intermediates that serve as precursors of many nonessential amino acids. Moreover, glutamine carbons also contribute to fatty acid biosynthesis, through the generation of acetyl-CoA by reductive carboxilation (DeBerardinis *et al.*, 2007; Metallo *et al.*, 2011). Glutamine is also a nitrogen source for amino acids (α-nitrogen) and for nucleotides and hexosamines like glucosamine, a precursor for protein glycosylation (γ-nitrogen). Glutamine metabolism also provides precursors for synthesis of glutathione, the major thiol-containing endogenous antioxidant. Reactions that use either the α-nitrogen or the carbon skeleton of glutamine,

specifically use glutamate as substrate; therefore glutamine must be primarily converted to glutamate by glutaminase (GLS). GLS results upregulated in many cancer cells and is essential for the metabolic phenotype of many tumors (Chiaradonna *et al.*, 2012) (**figure 1**).

Together with increased glucose, glutamine and glycogen metabolism, also fatty acid (FA) synthesis occurs at very high rates in tumor cells and this increase is reflected in the over expression and hyperactivity of some lipogenic enzymes such as ATP citrate lyase (ACL), Monoacylglycerol lyase (MAGL), acetyl-CoA carboxylase (ACC) and fatty acid synthase (FASN) (**figure 1**). The latter enzyme strongly supports cancer growth because it increases the synthesis of both cell membranes and lipids containing molecules involved in cell signaling. Moreover, enhanced lipogenesis in cancer cells is also required to balance the redox potential via the utilization of NADPH (Chiaradonna *et al.*, 2012).

OXPHOS dysfunctions in cancer cells

Primary defects in Oxidative Phosphorylation (OXPHOS) have been invoked to explain the Warburg effect, as originally proposed by Otto Warburg himself (Kroemer and Pouyssegur, 2008; Lopez-Rios *et al.*, 2007; Warburg, 1956). Cancer cell proliferation as well as tumor aggressiveness, in fact, correlates with a low mitochondrial respiratory chain activity (Chiaradonna *et al.*, 2006a), and the enhancement of OXPHOS activity appears to reduce tumor growth (Hervouet *et al.*, 2005; Schulz *et al.*, 2006).

Since mtDNA is localized near to Reactive Oxygen Species (ROS) production sites, namely the respiratory chain, it can be exposed to high mutations rates (Higuchi, 2007; Richter *et al.*, 1988). Such a deleterious effect is further worsened for the less efficient DNA protection and repair machinery present in mitochondria as compared to the nucleus (Richter *et al.*, 1988). Moreover, the

rate of mtDNA mutation can be greatly accelerated by mutations impinging on respiratory chain activity that eventually cause a chronic increase of mitochondrial ROS levels (Indo *et al.*, 2007). These circumstances can lead to the impairment of OXPHOS and have been proposed to be involved both in initiating and promoting cancer development (Lee and Wei, 2009; Penta *et al.*, 2001). As example, in thyroid oncocytic carcinoma mtDNA mutations in genes encoding a Complex I subunit and cytochrome b have been identified (Bonora *et al.*, 2006). More recently, point mutations of ND6 gene, encoding for a Complex I subunit, have been associated to highly metastatic potential of cancer cells (Ishikawa *et al.*, 2008). In fact, all these mutations produce a deficiency in Complex I activity and an overproduction of ROS that ultimately induce up-regulation of nuclear genes (as MCL-1, HIF-1α and VEGF) closely linked to enhancement and alteration of cellular metabolism as well as to metastatic potential (Ishikawa *et al.*, 2008).

There is also evidence of alteration of the expression of several respiratory chain subunits. The down-regulation of the catalytic subunit of the mitochondrial H+-ATP synthase (β-F1-ATPase) is considered a hallmark of many human carcinomas. In fact, it has been found in liver, kidney, colon, breast, stomach, squamous esophagus and lung human carcinomas (Cuezva *et al.*, 2002; Isidoro *et al.*, 2004). Also alterations of Complex I and IV subunits have been associated with tumor-altered metabolism (Baracca *et al.*, 2010; He and Cao, 2010; Krieg *et al.*, 2004; Zimmermann *et al.*, 2009).

Role of mitochondrial morphology in the appearance of cancer cell mitochondria dysfunction

Mitochondria are continuously submitted to morphological rearrangements as consequence of both fission and fusion processes (Westermann, 2010).

Mitochondria morphology appears strictly linked to their activity, since fragmentation and interconnection have been associated with specific bioenergetic and functional features of mitochondria (**figure 2**).

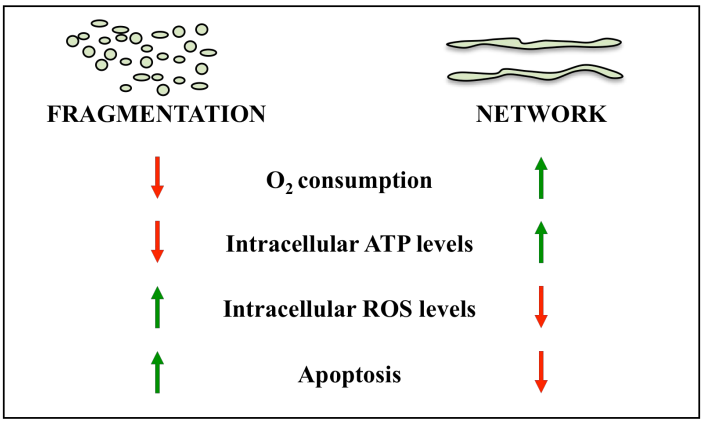

Figure 2. Scheme of the main bioenergetic and functional variations of mitochondria associated with their fragmentation or interconnection (network), as described by literature data (Benard *et al.*, 2007; Chen *et al.*, 2005; Grandemange *et al.*, 2009). Green arrows indicate decrease of the indicated parameters, red arrows indicate increase.

Several studies have identified either the ability of OXPHOS complexes to influence the mitochondrial morphology or the ability of mitochondrial dynamics to regulate OXPHOS complexes activity (Grandemange *et al.*, 2009; Sauvanet *et al.*, 2010; Chiaradonna *et al.*, 2012). In this regard it has been shown that the lack of mitochondrial fusion (caused by null mutations in Mfn1 or Mfn2 or by disruption of OPA1, the main proteins involved in the fusion process) causes poor cell growth, widespread heterogeneity of mitochondrial membrane potential and decreased cellular respiration (Chen *et al.*, 2005). On the other hand, patients with defects in Complex I, diversely from healthy subjects, display fragmented mitochondria and enhanced ROS levels (Koopman *et al.*, 2007). In accordance, the inhibition of Complex I activity by using rotenone

alters mitochondrial network organization, leading to vesicularization of the tubules and the appearance of numerous donut-like interdigitations (Benard *et al.*, 2007). These findings suggest a possible role also of mitochondrial morphology alterations in cancer cell energy metabolism linked to OXPHOS dysfunction. *K-ras* transformed mouse fibroblasts upon glucose depletion have a reduced ATP content in association with an inability to modify mitochondria morphology. On the contrary, mitochondria of normal mouse fibroblasts NIH3T3 upon glucose depletion are able to form interconnected and filamentous mitochondrial structures in relation to a higher content of ATP as compared to transformed cells (Chiaradonna *et al.*, 2006a). Similar results have been obtained also in rat normal gastric cell line (RGM-1) as compared to human gastric cancer cell line (AGS). AGS cells present smaller total numbers and cross-sectional sizes of mitochondria that appear to consume less oxygen (Kim *et al.*, 2007b). Furthermore, mitochondrial morphology can also play an active role in tumorigenesis. In fact mitochondrial dynamics alterations may participate in tumorigenesis by contributing to the accumulation of damaged mitochondria (Grandemange *et al.*, 2009) leading to mtDNA instability (Chen *et al.*, 2010b) and to the accumulation of dysfunctional mitochondria (Twig *et al.*, 2008).

Reversible alterations of mitochondria: the putative role of post-translational modifications of mitochondrial proteins in the regulation of mitochondria function and energetic metabolism in cancer cells

Mitochondrial proteins are subjected to post-translational modifications, among that the most relevant are O-linked-β-N-acetylglucosamine glycosylation (O-GlcNAcylation), phosphorylation, S-nitrosylation (SNO), glutathiolation, sumoylation, ubiquitination. Therefore, such modifications and the pathways aimed at their regulation could be involved in the modification and

rearrangement of mitochondria function and energetic metabolism in cancer cells.

O-glycosylation of proteins by the monosaccharide β-N-acetyl-D-glucosamine (O-GlcNAc) is a dynamic, inducible post-translational modification. O-GlcNAcylation dramatically alters the fate and function of target proteins. Indeed, O-GlcNAcylation may compete with phosphorylation for certain Ser/Thr target sites. O-GlcNAc transfer is the terminal step in the Hexosamine Biosynthesis Pathway (HBP), which consists of two parts: synthesis of UDP-GlcNAc and transfer and removal of O-GlcNAc. The precursors for UDP-GlcNAc synthesis are nutrient-derived: glutamine, acetyl–CoA, glucose and uridine and the levels of UDP-GlcNAc are responsive to nutrient levels, suggesting that hexosamine biosynthesis could serve as a cellular sensor of nutrient levels. Therefore, this pathway is a good candidate for the role of integration between metabolic signaling and mitochondrial regulation. Although O-GlcNAcylation of mitochondrial proteins has been explored in a limited fashion, recent papers have shown that the event is possible and is regulated by glucose availability (Hu *et al.*, 2009). In fact, high glucose increases mitochondrial protein O-GlcNAcylation e.g. of Complex I, III and IV, which in turn contributes to impaired mitochondrial function (Hu *et al.*, 2009). Thus, GlcNAcylation is emerging as an important regulator of mitochondria function and could have an essential role also in cancer cells.

Mitochondrial tyrosine phosphorylation is emerging as an important mechanism in regulating mitochondrial function. Indeed, various members of Src family, for example, Fgr, Fyn, Lyn and c-Src, are constitutively present in the internal structure of mitochondria as well as Csk, a key enzyme in the regulation of the activity of this family. The activation of Src kinases in mitochondria is associated with the proliferative status where several mitochondrial proteins are

specifically tyrosine-phosphorylated (Tibaldi *et al.*, 2008). Since Src family members have been recognized as important oncogenes (Parsons and Parsons, 2004), their role in cytoplasmic signaling as well as in regulation of mitochondrial activity may represent a further mechanism of controlling mitochondrial activity especially in cancer cells (Chiaradonna *et al.*, 2012).

The role of phosphorylation in serine and threonine as mitochondrial regulatory mechanism in response to different stimuli has been reported (Hopper *et al.*, 2006) and at least 25 kinases and eight phosphatases, belonging to different group or family, have been reported to localize to mitochondria and to regulate their functions (Pagliarini and Dixon, 2006). Protein kinase A (PKA) is a ubiquitous serine-threonine kinase that is activated by adenylcyclase-mediated cAMP. cAMP/PKA pathway has an important role in mitochondria regulation, since evidence has been accumulated that PKA regulates biogenesis (De Rasmo *et al*., 2010), import (De Rasmo *et al*., 2008), activity of Complex I or IV (Acin-Perez *et al*., 2009; Papa *et al*., 2008) and mitochondrial morphology (Chang and Blackstone, 2007). Therefore has been suggested that cAMP/PKA pathway is directly involved in the regulation of several mitochondrial functions. Besides, this pathway controls several other aspects of cellular metabolism, exerting a stimulatory effect on glucose transport and utilization, glycolysis, glycogen breakdown and glucose oxidation (Carlucci *et al*., 2008; Fang *et al*., 2000). The complex role of cAMP/PKA pathway on mitochondria and cellular metabolism, through reversible phosphorylation, as well as its extraordinary evolutionary conservation, make this pathway a good candidate for the role of integration between environmental signaling and mitochondrial regulation. Therefore, cAMP/PKA pathway could be strategic in mammalian cells and particularly in cancer cells.

Despite the prominent role of glycolysis and OXPHOS-independent metabolism, mitochondria cover an important role also in cancer cells i.e., through the maintenance of mitochondrial potential and oxidative equilibrium, necessary for cell viability and apoptosis control, and for the different anabolic processes that use precursors produced in this organelle, such as lipid, amino acids and nucleotides synthesis.

Moreover, mitochondria can also maintain partial capability for energy production also in cancer cells, in fact it has been observed in a compilation of 31 cancer cell lines/tissues that the average percentage of ATP contribution from glycolysis is 17% (Zu and Guppy, 2004). Moreover, mitochondria, although depressed in their activity, are not defective or mutated in most proliferating cells and can generate the majority of ATP not only in normal cells but also in cancer cells (Lunt and Vander Heiden, 2011; Zu and Guppy, 2004). The contribution of glycolysis to ATP production varies greatly among both normal and cancer cells and some cancer cells can even survive *in vitro* without glucose if supplied with glutamine and nucleosides (Linker *et al.*, 1985; Reitzer *et al.*, 1979).

In accordance with their manifold and essential role, mitochondria are emerging as chemotherapeutic targets and cancer cells result susceptible to mitochondrial inhibitors (Fantin and Leder, 2006). There are, in fact, a series of compounds targeting mitochondria, named mitocans, which are being tested as anticancer drugs. They lead to cancer cell death by inducing mitochondria destabilization with a consequent increase of reactive oxygen species and activation of apoptotic signals (Biasutto *et al.*, 2010; Ralph *et al.*, 2006). Different classes of mitocans exist and can be classified into eight groups, more specifically hexokinase inhibitors, Bcl-2 homology-3 (BH3) mimetics, thiol redox inhibitors, drugs targeting the voltage-dependent anionic channel (VDAC) or the adenine

nucleotide translocator (ANT), agents interfering with the electron transport chain (ETC), lipophilic cations targeting the inner membrane, agents interfering with the mitochondrial DNA and drugs acting on not well defined sites (Biasutto *et al.*, 2010). Among the compounds acting on the ETC, vitamin E analogues that in particular target complex II have been tested as anti-cancer agents (Neuzil *et al.*, 2007). Complex I inhibitors have shown anticancer properties as well. For example the acetogenins, such as rollinistatin and bullatacin, and also rotenone itself, which exhibits anti-tumor activity in animal models (Pathania *et al.*, 2009).

Causes of the metabolic switch in cancer cells

Warburg, the discoverer of the hyperglycolytic phenotype of cancer cells, suggested that tumor originated from cells with persistent defects in the mitochondrial respiratory system (Warburg, 1956). There are evidences that this is partially true, in fact cancer cell proliferation as well as tumor aggressiveness correlate with a low mitochondrial respiratory chain activity (Chiaradonna *et al.*, 2012). Nevertheless, inhibition of mitochondrial respiration by stimulated glycolysis is a common phenomenon known as Crabtree effect (Gogvadze *et al.*, 2008; Ibsen, 1961), therefore inhibition of OXPHOS activity seems to be an adaptation to cancer metabolism reprogramming rather than a cause. In this scenario, reversible post-translational modifications could assume an important regulatory role, more than irreversible mutations of respiratory chain.

Adaptation of cancer cells to their microenvironment is an important driving force in the clonal selection that leads to invasive and metastatic disease. Variation of oxygen content is frequently observed in normal tissues as in tumors. However, in tumors, the gradient is much steeper as oxygen concentrations can drop to near zero in necrotic core areas (Harris, 2002). In

fact, cells closest to a perfused blood vessel are exposed to relatively high oxygen concentrations, which decline as distance from the vessel increases. In addition to physical gradients, temporal fluctuations in oxygenation also commonly occur within tumors (Dewhirst *et al.*, 2008). One main mechanism allowing cells to adapt to hypoxia is mediated through the stabilization of the transcription factor HIF-1. HIF-1 is a heterodimeric protein composed by subunits HIF-1β, constitutively expressed, and HIF-1α, whose levels are strictly dependent on oxygen concentration. In fact, in high oxygen concentrations its half-life is brief, as it is degraded by an ubiquitin-proteasome system (Salceda and Caro, 1997), and as consequence its levels are negligible. On the other hand, under hypoxia its levels rapidly increase because of the block of its degradation. HIF-1 controls the expression of hundreds of genes including several glycolytic enzymes, glucose transporters and LDH-A, and can activate PDK-1 (Kim *et al.*, 2006; Semenza, 2010a) (**figure 3**). Therefore, in conditions where HIF-1α is stabilized the capacity of tumor cells to carry out glycolysis rather than OXPHOS is increased. Also glycogen metabolism is up-regulated in cancer cells in response to hypoxia, which induces an early accumulation of glycogen followed by a gradual decline (Favaro *et al.*, 2012).

Many tumors present metabolic reprogramming also in presence of oxygen, indicating that hypoxia cannot totally explain it. In fact, even under normoxic conditions, HIF-1α can be induced by the glycolytic metabolites pyruvate and lactate (McFate *et al.*, 2008), mTOR activation, NAD+ levels, ROS, nitric oxide, many TCA cycle metabolites (Semenza, 2010b), and oncogene gain of function or tumor suppressor gene loss of function (Lunt and Vander Heiden, 2011; Semenza, 2010a).

Several authors have demonstrated the involvement of oncogenes in the Warburg effect (Bartrons and Caro, 2007; Levine and Puzio-Kuter, 2010). In

particular, there are many findings showing that the expression of oncogenes can favor the up-regulation of glycolysis (**figure 3**) and of glutamine utilization (Bartrons and Caro, 2007; Deberardinis *et al.*, 2008).

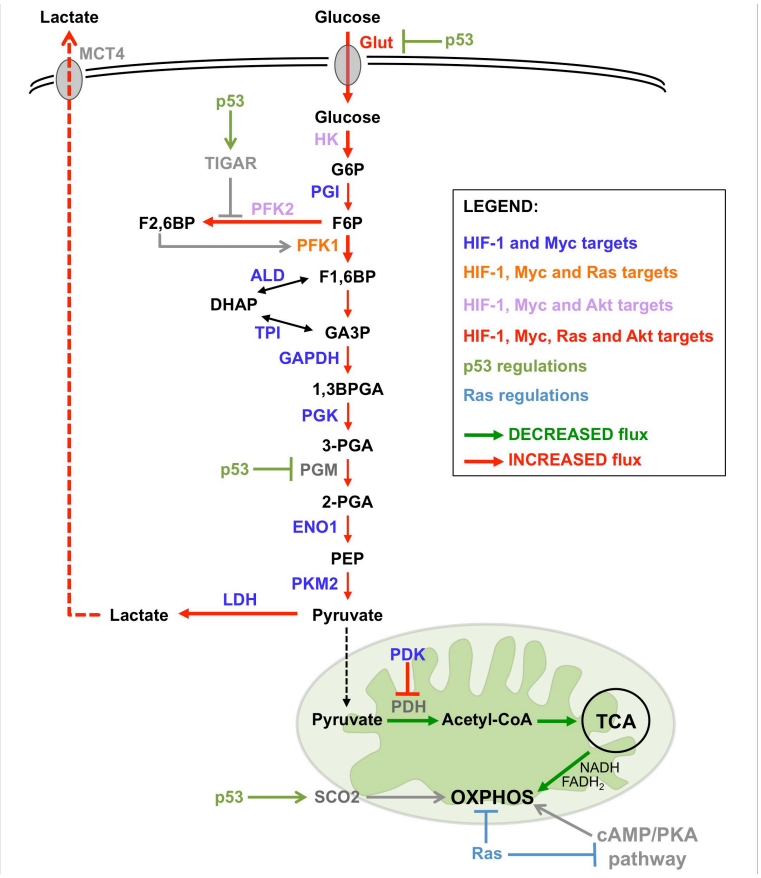

Figure 3. Role of oncogenes and oncosuppressors in the metabolic reprogramming of cancer cells. In cancer cells the flux throughout glycolysis is increased, while OXPHOS activity is inhibited. Oncogenes and oncosuppressors have an important role in regulating such a metabolic switch. HIF-1 is induced under hypoxia but can be activated also by oncogenes, such as *Myc* and *Ras*. *Ras*, as the other oncogenes, regulates glycolytic enzymes but has also negative effect on OXPHOS; such a negative role could be explained also by *Ras*-mediated depression of cAMP/PKA pathway. The oncosuppressor p53 normally favors mitochondrial respiration instead of glycolysis, therefore loss of p53 can induce Warburg effect.

G6P: glucose-6-phosphate; F6P: fructose-6-phosphate; F1,6BP: fructose-1,6-bisphosphate; F2,6BP: fructose-2,6-bisphosphate; DHAP: dihydroxyacetone phosphate; GA3P: Glyceraldehyde-3-phosphate; 1,3-BPG: 1,3-bisphosphoglycerate; 3-PGA: 3-phosphoglycerate; 2-PG: 2-phosphoglycerate; PEP: phosphoenolpyruvate. Glut: glucose transporters; MCT: monocarboxylate transporter. HK: hexokinase; PGI: phosphoglucoisomerase; PFK: Phosphofructokinase; ALD: Aldolase; TPI: triose phosphate isomerase; GAPDH: Glyceraldehyde 3-phosphate dehydrogenase; PGK: phosphoglycerate kinase; PGM: phosphoglycerate mutase; ENO1: enolase 1; PK: pyruvate kinase; LDH: lactate dehydrogenase; PDH: Pyruvate dehydrogenase; PDK: Pyruvate dehydrogenase kinase. TCA cycle: Trycarboxilic acid cycle; OXPHOS: Oxidative phosphorylation.

The PI3K/Akt pathway leads to increased glycolysis promoting the expression and membrane localization of GLUT-1 and stimulating PFK-2 activity and the association of HK1 and HK2 with the mitochondria (Barthel *et al.*, 1999; Gottlob *et al.*, 2001) (**figure 3**). Moreover, downstream of Akt, activation of mammalian Target of Rapamycin kinase complex I (mTORC1) is sufficient to stimulate specific metabolic pathways, including glycolysis, the oxidative arm of the pentose phosphate pathway, and de novo lipid biosynthesis. Therefore, in addition to promoting protein synthesis, mTORC1 activates specific bioenergetic and anabolic cellular processes that are likely to contribute to cancer cell physiology (Duvel *et al.*, 2010). Myc promotes transcription of glucose transporters and glycolytic enzymes (Ahuja *et al.*, 2010; Osthus *et al.*, 2000) and enhances the expression of LDH-A (Shim *et al.*, 1997) (**figure 3**). Moreover, Myc has been shown to regulate glutamine uptake and utilization in several ways (Wise *et al.*, 2008). For instance, through the repression of miR-23a and miR-23b, which leads to the induction of their target enzyme mitochondrial GLS1 (Gao *et al.*, 2009). Finally, also Ras seems to promote glucose metabolism (see below and **figure 3**).

The tumor suppressor p53 has a role in the regulation of cellular metabolism and is involved in the Warburg effect (Levine and Puzio-Kuter, 2010) by regulating both glycolysis and mitochondrial respiration and hence modulating the balance between the two processes (Chiaradonna *et al.*, 2012) (**figure 3**). p53 is able to

regulate transcription of the SCO2 gene, a critical regulator of respiratory chain complex IV (COX) activity, being required for its correct assembly (Matoba *et al.*, 2006) (**figure 3**). In fact, after disruption of SCO2 gene, wild-type p53 human cancer cells present the glycolytic metabolism normally characterizing p53-deficient cells (Matoba *et al.*, 2006). In addition, p53 protein can inhibit the expression of the glucose transporters GLUT-1 and GLUT-4 (Schwartzenberg-Bar-Yoseph *et al.*, 2004), decrease the levels of the glycolytic enzyme phosphoglycerate mutase (PGM) (Kondoh *et al.*, 2005) and increase the expression of TIGAR (TP53-induced glycolysis and apoptosis regulator) that in turn leads to a decrease of PFK-1 activity (Bensaad *et al.*, 2006) (**figure 3**). Thus, glycolysis can be promoted by loss of p53 function.

Ras pathway in cancer cells

In various human tumors (up to 35%) the oncogenic *RAS* gene has been found mutated (Rodenhuis, 1992) and these mutations play a critical role in the onset of different malignant phenotypes. Mainly, constitutive activation of Ras stimulates hyperproliferation and inhibits apoptotic processes. In fact, constitutively active *Ras* signaling drives uncontrolled proliferation and enhances survival of cancer cells through the activation of its downstream signaling pathways, such as the MAPK and PI3K-mTOR pathways (Gysin *et al.*, 2011). On the other hand, oncogenic *Ras* can promote glucose metabolism and seems implicated in the regulation of aerobic glycolysis. In accordance, transfection with oncogenic *H-ras* stimulates glycolysis and inhibits oxygen consumption, for example lowering mitochondrial biogenesis and the expression of genes encoding for OXPHOS components (Biaglow *et al.*, 1997; Ramanathan *et al.*, 2005). It can also promote increased glucose uptake and lactate production up-regulating PFK-1 activity through induction of F2,6BP (Telang *et al.*, 2006)

(**figure 3**). Pharmacologic inhibition of *Ras* results in a substantial down-regulation of glycolytic components, including GLUT-1 (Gillies *et al.*, 2008) (**figure 3**). In fact, GLUT-1 is consistently upregulated in cells with *KRAS* mutations and, as consequence, such cells exhibit enhanced glucose uptake and glycolysis (Yun *et al.*, 2009). Moreover, *Ras* is also involved in impairment of mitochondrial function (**figure 3**). Normal human cells expressing oncogenic *Ras* increase ROS production and accumulate dysfunctional mitochondria around the nucleus in parallel with their entrance in senescence (Moiseeva *et al.*, 2009). Accordingly, functional OXPHOS defects are induced by oncogenic H-rasQ61L transformation (Yang *et al.*, 2010). In recent years, the group of Dr. Chiaradonna has developed and deeply analyzed an *in vitro* model of cellular transformation. Such a model is represented by two NIH3T3-derived stable cell lines, NIH3T3 cells expressing an oncogenic *K-ras* (Transformed cell line) and NIH-ras cells expressing a GEF-DN, a protein able to down regulate *Ras* activation and to phenotipically revert transformed cells (Reverted cell line) (Bossu *et al.*, 2000; Chiaradonna *et al.*, 2006a). *K-ras* cell line has been extensively characterized and found to have several metabolic alterations (Chiaradonna *et al.*, 2006a; Chiaradonna *et al.*, 2006b; Gaglio *et al.*, 2009). It has been shown that the enhanced proliferation potential of *K-ras*-transformed cells requires a high initial glucose and glutamine concentrations in the medium. The selective growth advantage of transformed cells is lost in sub-optimal glucose or glutamine growth conditions. Glucose- and glutamine-dependent growth correlates with an altered metabolic pattern namely increased glucose utilization and lactate production, increased utilization of glutamine through the TCA cycle, increased expression of glycolytic genes, depressed expression of mitochondrial genes, altered mitochondrial morphology and reduced ability of ATP production (Chiaradonna *et al.*, 2006a; Chiaradonna *et al.*, 2006b; Gaglio

et al., 2011). Transformed cells produce large amount of ROS associated with decreased activity of mitochondrial Complex I (Baracca *et al.*, 2010) and increased cell death in glucose deprivation (Chiaradonna *et al.*, 2006a). Remarkably, several metabolic phenotypes induced by oncogenic *K-ras* expression, are almost completely reverted by the GEF-DN expression (Chiaradonna *et al.*, 2006b; Gaglio *et al.*, 2011), suggesting a main role of oncogenic *Ras* signaling in the induction and maintenance of metabolic alterations.

Finally, oncogenic *Ras* can also influence the transcription pattern of cancer cells, in turn modulating specific pathways. For example, *K-ras* dependent tumor cell lines of the NCI-60 collection (Shoemaker, 2006), analyzed by transcriptional profiling, show a down-regulation of many transcripts of the cAMP/PKA pathway (Balestrieri *et al.*, 2009), thereby indicating that *K-ras*-dependent oncogenic transformation may involve reduction of cAMP/PKA pathway activity. In accordance, different groups have reported that active forms of the Ras family members lead to a depression of genes encoding for components of the cAMP/PKA signaling pathway (Baratta *et al.*, 2009; Chiaradonna *et al.*, 2008; Feliciello *et al.*, 1996; Gallo *et al.*, 1995; Ross *et al.*, 2000). Considering the important role of cAMP/PKA pathway in regulating mitochondria activity and morphology (see before), *Ras*-dependent deregulation of cAMP/PKA pathway could cause OXPHOS depression and "glucose addiction" of cancer cells (**figure 3**).

Role of glucose in proliferating cancer cells

Proliferation represents a significant bioenergetic challenge for a cell and requires that bioenergetic resources and biosynthetic activity be redirected toward the duplication of all macromolecular components (DNA, membranes,

and proteins) to ensure successful passage through the cell cycle. To meet this challenge, metabolic activities are reorganized in proliferating cells resulting in an anabolic shift in cellular metabolism (Lunt and Vander Heiden, 2011). In this scenario, glucose assumes a critical role, being involved in different and various mechanisms aimed at ensure cancer cell survival and proliferation (**figure 4**).

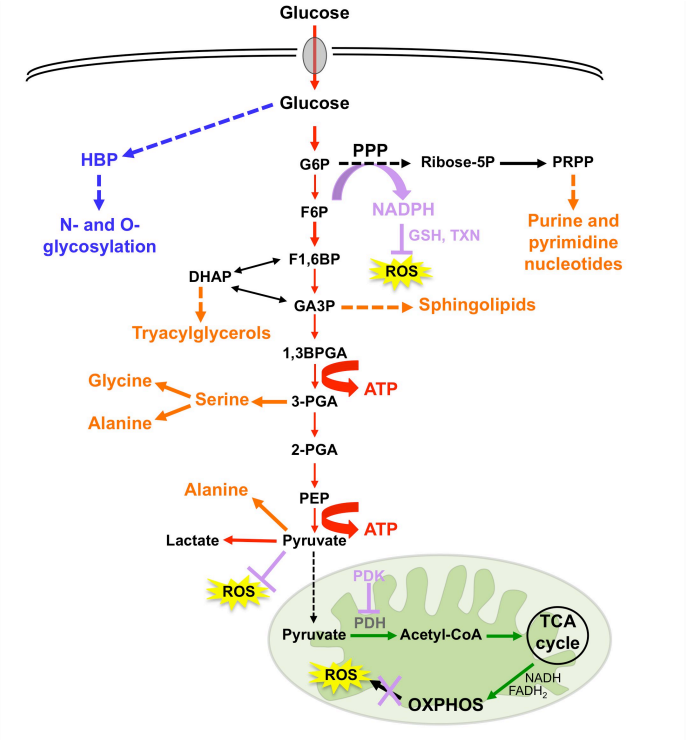

Figure 4. Role of glucose in proliferating cancer cells. Glucose is involved in the production of ATP (represented in red), anabolic processes (orange), maintenance of oxidative equilibrium (violet), fuelling of Hexosamine Biosynthesis Pathway (HBP) (blue). See the text for details.
G6P: glucose-6-phosphate; F6P: fructose-6-phosphate; F1,6BP: fructose-1,6-bisphosphate; F2,6BP: fructose-2,6-bisphosphate; DHAP: dihydroxyacetone phosphate; GA3P: Glyceraldehyde-3-phosphate; 1,3-BPG: 1,3-bisphosphoglycerate; 3-PGA: 3-phosphoglycerate; 2-PG: 2-phosphoglycerate; PEP: phosphoenolpyruvate; Ribose-5P: ribose-5-phosphate; PRPP: 5-phosphorybosyl-α-pyrophosphate. PPP: pentose phosphate pathway; GSH: glutathione; TXN: thioredoxin. PDH: Pyruvate dehydrogenase; PDK: Pyruvate dehydrogenase kinase. TCA cycle: Trycarboxilic acid cycle; OXPHOS: Oxidative phosphorylation.

- *ATP production (glycolysis)*

One of the primary metabolic changes associated with proliferating tumor cells is the induction of aerobic glycolysis associated with the depression of OXPHOS. In fact, in proliferating cancer cells, the majority of the pyruvate generated from glucose (>90%) is converted to lactate. Therefore, in such cells glucose is the primary substrate for ATP generation. At face value, the preferential use of glycolysis for ATP production appears to be wasteful form of metabolism. Although the energetic yield per molecule of glucose is much lower for aerobic glycolysis compared with OXPHOS, when glucose is in excess and flux through the pathway is high, glycolysis has the potential to produce ATP in greater quantities and at a faster rate (Guppy *et al.*, 1993; Jones and Thompson, 2009).

- *Anabolism (synthesis of amino acids, nucleotides, lipids)*

Glucose can provide the precursors for the chemical constituents that are used to build macromolecules essential for cell division (Lunt and Vander Heiden, 2011).

- Purine nucleotides as building blocks of nucleic acids and also for cofactor biosynthesis (FAD, NAD, coenzyme A). Each purine nucleotide (ATP, GTP, dATP, and dGTP) synthesized by the cell requires the assimilation of 10 carbon atoms from the extracellular environment. Glucose provides a minimum of five carbons and up to nine carbons through 5-phosphorybosyl-α-pyrophosphate (PRPP), an activated version of ribose-5-phosphate, and 3-phosphoglycerate, a glycolytic intermediate.

- Pyrimidine nucleotides. Glycolysis is also a major source of carbons for biosynthesis of these nucleotides, as the majority (five out of nine) of the carbons come from PRPP. Three of the remaining carbons in pyrimidine

nucleotides come from aspartate, which can be acquired directly from the environment or generated from the TCA cycle intermediate oxaloacetate. Carbons in oxaloacetate can be derived from glucose or provided by glutamine.
In accordance with its role in providing nucleotides, glycolysis seems necessary for nucleic acid synthesis and cell proliferation. In accordance, cells can grow in size using glutamine as the only major carbon source but are unable to proliferate unless a metabolite capable of entering glycolysis is available (Lunt and Vander Heiden, 2011; Wellen *et al.*, 2010).

- Lipid precursors. The glycolytic intermediate dihydroxyacetone phosphate is the precursor to glycerol-3-phosphate, which is crucial for the biosynthesis of the phospholipids and triacylglycerols, the major structural lipids in cell membranes. Similarly, the other glycolytic intermediate 3-phosphoglycerate is the precursor of sphingolipids that are important membrane components and also play a role in signaling, being implicated in cell growth, differentiation, senescence, apoptosis, and cancer (Futerman and Hannun, 2004; Ogretmen and Hannun, 2004). Moreover, Acetyl-CoA provides the carbon for synthesis of fatty acyl chain components of the various lipid classes and of mevalonate, a precursor for cholesterol and related molecules. Glucose can be a major source of acetyl-CoA production, although acetyl-CoA derived from glucose is not a direct product of glycolysis.

- Amino acids. Glycolytic intermediates are direct precursors for the biosynthesis of some amino acids. 3-phosphoglycerate provides the carbons for cysteine, glycine, and serine; pyruvate provides the carbons for alanine.

- *Oxidative equilibrium*

Several studies have focused on glycolysis role in the detoxification of hydroperoxides as byproducts of oxygen metabolism. Glucose-6-phosphate

(G6P), produced from glucose through the enzyme HK, through glycolysis can form pyruvate, which has been shown to scavenge H_2O_2 and other hydroperoxides directly (Das, 2006; Nath *et al.*, 1995; Wang *et al.*, 2007). On the other hand, G6P can enter into penthose phosphate pathway, permitting the regeneration of NADPH. NADPH, being the source of reducing equivalents for the glutathione and thioredoxin antioxidant systems, has also been shown to participate in the detoxification of H_2O_2 and organic hydroperoxides (Berggren *et al.*, 2001; Nomura *et al.*, 1999). Therefore, glucose metabolism appears to be directly related to the detoxification of intracellular ROS.

Moreover, the increased fuel of glucose through aerobic glycolysis and consequent depression of OXPHOS can avoid oxidative stress produced by dysfunctional respiratory chain. In fact, it is proved that limiting the conversion of pyruvate to acetyl-CoA and its entry into mitochondria metabolism (for example, through activity of PDK-1) reduces electron flux through OXPHOS, and, as a result, reduces oxidative stress derived from mitochondrial metabolism.

- *Hexosamine pathway*

Under physiological conditions, 1–3% of intracellular glucose is shunted from the glycolytic pathway to the Hexosamine Biosynthesis Pathway (HBP) (McClain, 2002) and flux through the HBP is mainly modulated on glucose availability although it requires also glutamine, acetyl-CoA, and UTP. Main product of HBP is UDP-N-acetylglucosamine, an important donor molecule for post-translational modifications, such as N- and O-glycosylation (Slawson *et al.*, 2010). Although its function during tumorigenesis is poorly understood, recent studies indicate that the HBP is important for the coordination of nutrient uptake, partially through modulating the glycosylation and membrane localization of growth factor receptors (Wellen *et al.*, 2010). Moreover, protein

and lipid glycosylation plays fundamental regulatory roles in tumor cell proliferation, invasion/metastasis, angiogenesis, and immune evasion (Fuster and Esko, 2005; Hart and Copeland, 2010). Akt stimulates N-glycosylation, in turn favoring glycolysis (Fang *et al.*, 2010). Also *Ras* oncogenes have been shown to induce N-glycosylation (Bolscher *et al.*, 1988; Dennis *et al.*, 1989; Rak *et al.*, 1991; Wojciechowicz *et al.*, 1995). In a recent study it has been shown that the expression of Glutamine-Fructose-6-phosphate-Transaminase 1 (Gfpt1), the first and rate-limiting step of HBP, is strongly downregulated upon K-rasG12D inactivation (Ying *et al.*, 2012). This study has provided additional evidence that oncogenic *K-ras* signaling plays a prominent role in the flux of glucose into the HBP sustaining protein O-glycosylation during tumor maintenance (Ying *et al.*, 2012)**.**

Glucose deprivation in cancer cells

Considering the essential role of glucose, it is not surprising that deprivation of this source can induce growth arrest and death in cancer cells. Different authors have investigated the effects of glucose deprivation in cancer cells (Chiaradonna *et al.*, 2006a; Simons *et al.*, 2009).

One cause of glucose deprivation-induced cell death can be the drop of the intracellular ATP levels. In fact, as indicated before, in cancer cells glucose consumption through glycolysis can be the main mechanism of ATP production. Therefore, in absence of the principal energetic source cells can undergo energetic crisis and die. Moreover, the decrease of intracellular ATP levels can also cause the loss of the mitochondrial potential ($\Delta\Psi m$), in particular in cancer cells where OXPHOS is still functional but repressed (for example through regulatory pathways) or completely or particularly dysfunctional and complex V is used in reverse. In fact, Complex V, namely ATP synthase, can work in two

opposite directions and the directionality of the enzyme is dictated by the balance between the bioenergetic parameters of free energy available from the phosphorylation potential and from ΔΨm. In normally respiring mitochondria, the high ΔΨm favors ADP phosphorylation (i.e., ATP synthesis). However, when mitochondrial homeostasis is compromised, the situation can be the reverse. In fact in order to maintain a high mitochondrial potential, complex V can hydrolyze ATP generated by glycolysis to pump protons from the mitochondrial matrix to the intermembrane space. Therefore, during mitochondrial dysfunction, the complex V can run 'backwards', in reverse, acting as an ATP-consuming proton pump (Campanella *et al.*, 2009). In many transformed cells that exhibit high rates of glycolysis, high levels of Adenine Nucleotide Translocase 2 (ANT2) and depressed OXPHOS, ATP generated by glycolysis powers ANT2 and the β-subunit of Complex V to function in reverse. In this way, glycolysis supports the mitochondrial membrane potential (Campanella *et al.*, 2009). It has been suggested that this contributes to the aggressive growth of cancer cells (Chevrollier *et al.*, 2005). Therefore, in absence of glucose, low levels of intracellular ATP cannot sustain ΔΨm. Loss of mitochondrial potential leads to apoptosis inducing the release of cytocrome C and Apoptosis Inducing Factor (AIF) from mitochondria.

Moreover, there is experimental evidence that during glucose deprivation mitochondrial O_2^- and H_2O_2 cause oxidative stress, significantly contributing to cytotoxicity of human cancer cells (Ahmad *et al.*, 2005). In particular, cancer cells appear more susceptible to glucose-deprivation-induced cytotoxicity and oxidative stress, as compared to their normal counterpart. Over-expression of manganese superoxide dismutase and mitochondrially targeted catalase significantly protect cancer cells from glucose-deprivation-induced cytotoxicity and oxidative stress (Aykin-Burns *et al.*, 2009). Recently, Graham *et al.* (2012)

extended our understanding of this phenomenon demonstrating that the cellular microenvironment (i.e., nutrient availability) can alter the cellular redox balance, provoking a signaling-based positive feedback loop that amplifies ROS levels above a toxicity threshold resulting in cell death. Specifically, they demonstrated that glucose deprivation initiates a positive feedback amplification loop driven by NOX- and mitochondria-derived ROS generation resulting in cell-wide consequences on phospho-tyrosine signaling and protein tyrosine phosphatases (PTP) activity, ultimately resulting in cell death (Graham *et al.*, 2012). In accordance with previous evidence, also *K-ras*-transformed NIH3T3 cells in glucose deprivation produce large amount of ROS associated with cell death (Chiaradonna *et al.*, 2006a).

Glucose deprivation can also disrupt protein folding in the endoplasmic reticulum (ER). The accumulation of unfolded proteins in the ER induces ER stress and activates the Unfolded Protein Response (UPR). This complex network of physiological responses to ER stress is regulated by only few ER transmembrane proteins: inositol requiring 1 (IRE1), PKR-like endoplasmic reticulum kinase/pancreatic eIF2 kinase (PERK/PEK) and activating transcription factor 6 (ATF6) (Ron and Walter, 2007). Primarily, activation of the UPR is aimed at enhancing cell survival by limiting accumulation of unfolded or misfolded proteins in the ER (Kaufman *et al.*, 2002). In fact, the main responses induced by UPR include expansion of the ER membrane to improve its function, selective synthesis of key components of protein folding and quality control, such as molecular chaperones, to refine and ameliorate protein folding, and also attenuation of protein influx into the ER in order not to saturate this organelle (Hetz, 2012). If these adaptive responses are not sufficient to relieve the unfolded protein load and ER stress, the cells undergo apoptosis or necrosis (Kaufman *et al.*, 2002). Thus, UPR may lead to either cell survival or

cell death depending on the strength and duration of the stimulus (Tabas and Ron, 2011).

Despite the numerous works investigating mechanisms and events involved in cancer cell response to glucose deprivation, whole picture is not clear and all the mechanisms and their interconnections are not yet fully understood.

Targeting glucose metabolism for anticancer therapy

Considering the complex metabolic reprogramming of cancer cells, it could possible to interfere with tumor metabolism at multiple levels: either depleting tumor cells of their preferred nutrients or inhibiting intracellular catabolic or biosynthetic pathways altered in tumors (El Mjiyad *et al.*, 2011; Kroemer and Pouyssegur, 2008; Pathania *et al.*, 2009; Pelicano *et al.*, 2006; Tennant *et al.*, 2010). One possible approach for anticancer therapy is the use of the glucose metabolism as target.

It is postulated that the metabolic adaptation of cancer cells eventually renders them highly addictive to and dependent on the glycolytic pathway, as consequence they become vulnerable to glycolytic inhibition (Gatenby and Gillies, 2004). On the contrary, normal cells with intact mitochondria are able to use alternative energy sources such as fatty acids and amino acids to produce metabolic intermediates channeled to the TCA cycle for ATP production through respiration. As such, normal cells are expected to be less sensitive to agents that inhibit glycolysis (Pelicano *et al.*, 2006). Therefore, glycolytic inhibitors appear promising as anticancer drugs.

In the last years many different glycolytic inhibitors have been developed and tested *in vitro* and *in vivo* as anticancer agents. The most known is 2-deoxyglucose (2-DG). This compound is a glucose analog and acts as a

competitive inhibitor of glucose metabolism (Brown, 1962). Upon transport into the cells, 2-DG is phosphorylated by HK to 2-DG-P. However, unlike G6P, 2-DG-P cannot be further metabolized by phosphohexose isomerase, which converts G6P to fructose-6-phosphate. 2-DG-P is trapped and accumulated in the cells, leading to the inhibition of glycolysis. Although the efficacy of this compound has been demonstrated *in vitro* (Maher *et al.*, 2004; Zhang *et al.*, 2006), inducing ATP depletion and cancer cell death, some studies have evidenced that 2-DG alone does not exhibit significant anticancer activity *in vivo* (Maschek *et al.*, 2004). In addition to 2-DG, other anti-glycolytic compounds have been individuated, such as 3-bromopyruvate (inhibitor of HK) and lonidamine (inhibitor of mitochondrially bound HK, approved as antitumor drug). Although they have been shown to have promising anticancer activity, all these compounds are not very potent and required to be used in combination to inhibit tumor growth (Choi and Lee, 2011; Pelicano *et al.*, 2006). The reason for that could be that, although cancer cells exhibit increased glycolysis and depend more on this pathway for ATP generation, inhibition of glycolysis alone may not be sufficient to effectively kill the malignant cells (Pelicano *et al.*, 2006). It has been suggested that ATP depletion should reach certain thresholds in order to trigger cell death by apoptosis or necrosis processes, with a depletion of 25–70% ATP leading to apoptosis, and an over 85% ATP depletion causing necrosis (Lieberthal *et al.*, 1998). Since all cancer cells contain mitochondria, some degree of ATP generation through oxidative phosphorylation is still possible when glycolysis is inhibited. This may compromise the efficiency of glycolytic inhibitors to deplete cellular ATP (Pelicano *et al.*, 2006). In fact, cancer cells can partially exploit compensatory mechanisms, such as glutamine or glycogen catabolism (Favaro *et al.*, 2012; Lunt and Vander Heiden, 2011), to produce ATP and anabolites and hence survive also when glycolysis is inhibited.

Moreover, glucose have different roles in cancer cells (as described above) that guarantee cancer cell proliferation and survival, for this reason for a strongly efficient therapy could be necessary to target not only glycolytic pathway but also the other glucose-dependent processes. On this regard, glucose deprivation and consequent analysis of cancer cell fate both at phenotypical and molecular level can be a useful strategy to unmask all mechanisms that participate to glucose-mediated cancer cell growth and survival. Such strategy could be subsequently exploited to provide new targets and to set new combined anticancer therapies. Examples of combined treatments between glycolysis inhibitors and other specific compounds, such as metformin or tephrosin, are reported to induce cancer cell death (Cheong *et al.*, 2011; Choi and Lee, 2011).
On the other hand, glucose shortage together with hypoxia is a deficiency encountered in tumor microenvironment (Nam *et al.*, 2002; Yun *et al.*, 2009); therefore it can be exploited to potentiate the action of other specific agents, such as the OXPHOS modulators. In fact, targeting mitochondria in condition of glucose deprivation could be lethal for cancer cells. As experimental evidence, it has been already observed that glucose deprivation in the presence of the inhibitor of respiratory chain Complex III, Antimycin A, significantly enhances oxidative stress and cytotoxicity in different human cancer cell lines (Ahmad *et al.*, 2005).

Emerging role of cancer stem cells

Tumors are no longer viewed as homogenous masses of proliferating cells, each with identical genetic alterations, but more as a heterogeneous tissue that contains a hierarchy of cells, perhaps originating from a single cancer stem cell (CSC) (Hanahan and Weinberg, 2011). For this reason CSCs are also called cancer initiating cells. Although the evidence is still fragmentary, CSCs may be

a common constituent of many if not most tumors, albeit being present with widely varying abundance (Hanahan and Weinberg, 2011). CSCs are defined operationally through their ability to efficiently seed new tumors upon inoculation into recipient host mice (Cho and Clarke, 2008). CSCs are a population of cells with self-renewal and differentiation capacity, and for this reason they are considered similar to normal stem cells (Tang *et al.*, 2007). In fact, often express markers that are also expressed by the normal stem cells in the tissue of origin (Al-Hajj *et al.*, 2003). Moreover, CSCs are believed to be fundamental for the promotion and maintenance of several types of cancer as well as for acquiring chemo- and radio-resistance and disease recurrence (O'Brien *et al.*, 2010). Although our knowledge regarding CSC biology is still limited, the possibility of using a combination of CSC-specific therapeutic approaches with traditional cancer treatment strategies is rapidly growing (Clarke *et al.*, 2006; Diehn and Clarke, 2006). Indeed, current therapies preferentially kill differentiated cancer cells, which eventually may result in preservation and enrichment of CSCs (Cheng *et al.*, 2011). Thus, a better understanding of CSC biology is becoming urgent to provide therapies able to offer significant clinical benefit.

Some studies have been done on the metabolism of stem cells. Undifferentiated embryonic stem cells as well as adult stem cells have recently been shown to have a different energetic metabolism as compared to fully differentiated cells. In fact, stem cells rely mostly on anaerobic metabolism rather than on OXPHOS (Varum *et al.*, 2011). In addition, it has been shown that undifferentiated stem cells have a reduced number of mitochondria, that appear also more immature, a low content of mtDNA, a reduced consumption of oxygen and a low level of intracellular ATP and ROS as compared to more differentiated cells (Chen *et al.*, 2010a; Chen *et al.*, 2008). With regard to this, recent observations have

correlated energetic cell metabolism to self-renewal and differentiation potential of stem cells. Human embryonic pluripotent stem cells (hESCs) as well as induced pluripotent stem cells (iPSCs) show high glycolytic flux (Prigione and Adjaye, 2010; Prigione *et al.*, 2010), while stem cells, i.e., embryonic, hematopoietic and mesenchymal, that undergo differentiation, increase mitochondrial biogenesis and function, relying mainly on OXPHOS for energy supply (Chen *et al.*, 2010a). Accordingly, inhibition of mitochondrial respiratory chain has recently been found associated with enhancement of hESC pluripotency (Varum *et al.*, 2009) as well as over-expression of mitochondrial protein UCP2 favoring glycolysis interferes with human pluripotent stem cells differentiation (Zhang *et al.*, 2011). Therefore it is becoming clear that energetic metabolism could be used for stem cell recognition and characterization as well as a way of modulating their fate.

Up to now energy metabolism in CSCs remains to be explored. In fact, it is unknown whether the metabolic profile of CSCs is similar to that observed in embryonic stem cells and whether it is able to originate the alterations observed in somatic cancer cells. Since recent observations indicate a link between cellular metabolism and cellular differentiation and since cancer stem cells induced to differentiate become less tumorigenic i.e., as a consequence of a reduced proliferation (Beug, 2009; Varum *et al.*, 2009; Zhang *et al.*, 2011), manipulation of cell metabolism for possible therapeutic targets in tumors is very intriguing.

So far, the main limitations in studying CSC biology have been their identification, characterization, isolation and mostly important the fact that they are only a small fraction of the total cancer cells. Therefore an attractive alternative source of cells for CSC research has been the identification and isolation of established cancer stem cell subpopulations from cancer cells that

retain stem cell patterns of behavior. Nowadays, CSCs have been successfully separated from cell lines derived from various solid cancers including glioma (Qiang *et al.*, 2009), breast cancer (Fillmore and Kuperwasser, 2008), lung cancer (Ho *et al.*, 2007), head and neck squamous carcinomas (Huang *et al.*, 2009).

Recently, a novel stable cancer stem-like cell line, namely 3AB-OS, has been irreversibly selected from human osteosarcoma MG63 cells (Di Fiore *et al.*, 2009). These CSC-like line have been shown to express a number of pluripotent embryonic and mesenchymal stem cell marker genes (Di Fiore *et al.*, 2012a; Di Fiore *et al.*, 2009) and, as confirmed by a transcriptional profiling in comparison with MG63, an enrichment of different pathways involved in the maintenance of stemness phenotype (Di Fiore *et al.*, 2012a). Its plurilineage differentiation potential has been demonstrated *in vitro*, with the production of derivatives of the three primary germ layers: endoderm, mesoderm, and ectoderm (manuscript in preparation). Moreover, when injected in athymic mice, these cells recapitulate *in vivo* various features of human osteosarcoma CSCs (Di Fiore *et al.*, 2012b). Noteworthy is the fact that such a stem-like phenotype, both in terms of morphological and antigenic features, is retained after prolonged serial passages (up to now, more than 200 passages) (unpublished observations). Therefore, 3AB-OS may be useful for investigating metabolic features of CSCs compared to differentiated cells and obtain information for new therapeutic approaches against osteosarcomas.

In general, the continuous deeper investigation of cancer and cancer stem cell metabolism has become really relevant in order to project new efficient anticancer therapies.

Chapter 2

Materials and methods

CHAPTER 2. MATERIALS AND METHODS

Cell cultures

Mouse fibroblast NIH3T3 cells (ATCC, Manassas, VA, USA), *K-ras*-transformed NIH3T3-derived cell line 226.4.1 (Pulciani *et al.*, 1985), Reverted NIH3T3 (Bossu *et al.*, 2000), human breast cancer MDA-MB-231, human pancreatic cancer MIA PaCa-2, human lung cancer A549, human osteosarcoma MG63 and 3AB-OS stem cells (Di Fiore *et al.*, 2009) were routinely cultured in Dulbecco's modified Eagle's medium containing 4 mM L-glutamine, 100 U/mL penicillin and 100 mg/mL streptomycin (complete medium), supplemented with 10% newborn calf serum (mouse cells) or 5–10% fetal bovine serum (human cells). All reagents for media were purchased from Life Technologies (Carlsbad, CA, USA).

For experiments cells were plated in complete growth medium. After 16 hours cells were washed twice with Phosphate Buffer Saline (PBS) and incubated in specific growth medium (time 0) without glucose and sodium pyruvate, supplemented with different sources, typically 25 mM, 1 mM or 0.5 mM glucose, 25 mM galactose, 5 mM fructose, 10 mM methyl-pyruvate as required for each experiment. Glucose, galactose, fructose and methyl-pyruvate were purchased from Sigma-Aldrich Inc. (St Louis, MO, USA). For some specific analyses cells at time 0 were incubated in growth medium with 25 mM glucose supplemented with 4 or 0.5 mM glutamine (Life Technologies). Cells were then collected for further analyses at 24, 48, 72, 96 or 120 hours of culture.

To measure cell proliferation, harvested cells were counted using the Burker chamber. Where indicated, cell viable count was performed using Trypan Blue Stain 0.4% (Life Technologies).

Treatments

Forskolin, H89 (N-[2-p-bromocinnamylamino)ethyl]-5-isoquinolinesulfonamide dihydrochloride), Mdivi-1 (3-(2,4-dichloro-5-methoxyphenyl)-2,3-dihydro-2–thioxo-4(1H)-quinazolinone), rotenone, oligomycin, N-Acetyl-L-Cysteine, N-Acetyl-D-Glucosamine and oxamate were purchased from Sigma-Aldrich Inc. (St. Louis, MO, USA). Capsaicin, piericidin A, cycloheximide, sodium 4-phenylbutyrate and thapsigargin were purchased from Vinci-Biochem (Florence, Italy). SP600125 from Santa Cruz Biotechnology Inc. (Santa Cruz, CA, USA).

Intracellular ATP quantification

Intracellular ATP levels were measured using CellTiter Glo luciferin-luciferase assay (Promega, Madison, WI, USA) according to the manufacturer's protocol. In particular, 100 μL of cell suspension containing 10^4 cells were added to an equal volume of Cell Titer Glo reagent in a single well of 96-well plate. The emitted luminescence was collected at 560 nm using Cary Eclipse spectrofluorimeter (Varian, Palo Alto, CA, USA) and the luminescence values were converted in ATP quantities after the setting of a calibration curve.

Flow cytometric analyses

All flow cytometric analyses were performed using a FACScan flow cytometer (Becton-Dickinson, Franklin Lakes, NJ, USA) with CellQuest software (Becton-Dickinson). Analysis of flow cytometric data was carried out using the freely available WinMDI software.

Propidium Iodide (PI)/Annexin V-FITC staining was performed using Apoptosis assay kit from Immunological Sciences (Rome, Italy). In particular, $5x10^5$ cells were collected in 50 μL of binding buffer and stained with 1 μL of Annexin V-

FITC and 1 μL of PI, as provided, for 15 minutes. After the incubation, samples were diluted in an appropriated volume of binding buffer and analyzed.

ROS levels were measured by staining plated cells with 5 μM dichloro-dihydro-fluoresceine-diacetate ($DCFH_2$-DA, Life Technologies) for 30 minutes at 37°C. After staining, the cells were trypsinized, collected in PBS + serum and analyzed.

Mitochondrial potential was analyzed staining cells with 20 nM JC-1 (5,5',6,6'-tetrachloro-1,1',3,3'-tetraethylbenzimidazolylcarbocyanine iodide**,** from Life Technologies) for 10 minutes. After staining, flow cytometric analysis was performed acquiring FL1 (JC-1 monomers, low potential) and FL2 (JC-1 aggregates, high potential) signals. For each sample the ratio FL2/FL1 was calculated and used to compare different samples.

Glucose uptake assay was performed using the fluorescent glucose analogue 2-[*N*-(7-nitrobenz-2-oxa-1,3-diazol-4-yl)-amino]-2-deoxy-D-glucose (2-NBDG, Life Technologies). The cells were washed twice with PBS, then their medium was replaced with a glucose-containing medium supplemented with 60 μM 2-NBDG for 30 min at 37°C. After staining, cells were trypsinized, collected in PBS + serum and analyzed.

D-Glucose and L-Lactate measurement

D-Glucose and L-Lactate levels in culture medium were determined using spectrophotometric enzyme assay kits (R-Biopharm, Darmstadt, Germany) as specified by manufacturer's datasheet.

RNA extraction and semiquantitative RT-PCR analysis

RNA was extracted from cultured cells using Trizol reagent (Life Technologies). Total RNA was reverse-transcribed with oligo dT by using the Superscript™ III

RT-PCR First-Strand Synthesis System for RT-PCR (Life Technologies). 0.2 μg of the RT product were amplified with primer pairs specific for the studied genes. As internal control of PCR assays specific primers for beta-actin and 18s transcripts were designed. Agarose gel images were visualized, processed and quantified by using ImageJ software.

Primers used are listed in the table below:

	Forward	**Reverse**
GRP78	AGTGGTGGCCACTAATGGAG	CAATCCTTGCTTGATGCTGA
ATF4	TCGATGCTCTGTTTCGAATG	GGCAACCTGGTCGACTTTTA
XBP1	CTGACGAGGTTCCAGAGGTG	AGCAGACTCTGGGGAAGGAC
CHOP	CATACACCACCACACCTGAAAG	CCGTTTCCTAGTTCTTCCTTGC
CAR6	GCCCTCCATGTACCTTGAAA	GACGGCTAACACAGCTAGGC
TRIB3	GATGCCAAGTGTCCAGTCCT	CTTGCTCTCGTTCCAAAAGG
GADD34	AGGACCCCGAGATTCCTCTA	CCTGGAATCAGGGGTAAGGT
PDIA3	TCTGAACCCATCCCAGAGTC	GTGGCATCCATCTTGGCTAT
NDUFA9	CAGATTGTTCCTCCCATTCC	TGCATCCGCTCCACTTTATC
GRIM19	AGATGCTTCGGGAGAACCTG	GGCCTACGTGTACCACATGA
ND1	CCCTGGTCAACCTCAACCTA	CTAGTTCGGACTCCCCTTCG
ND6	GGTGTGGTCGGGTGTGTTAT	CCAATAGGATCCTCCCGAAT
COXI	ACGTTGTAGCCCACTTCCAC	AGCGAAGGCTTCTCAAATCA
COXII	TTCATGATCACGCCCTCATA	CGGGAATTGCATCTGTTTTT
COXIII	GGCCTTCGATACGGGATAAT	GGAAGCCTGTGGCTACAAAA
COXIV	TTCGCTCCCAGCTTATATGG	GCTTCTGCCACATGATAACG
ACTIN B	AAACTGGAACGGTGAAGGTG	CTCAAGTTGGGGGACAAAAA
18S	GTTGGTGGAGCGATTTGTCT	GGCCTCACTAAACCATCCAA

Western blot analyses

For the analysis of protein expression, or 2×10^5 cells were harvested and lysed in Laemli buffer or all the cells were disrupted in an appropriated lysis buffer to collect at least 30 μg of the total extract. Samples were then resolved by sodium dodecyl sulfate–polyacrylamide gel electrophoresis and transferred to nitrocellulose membrane, which was incubated overnight with specific antibodies. Total CREB, phospho-CREB Ser133, phospho-Drp1 Ser637, phospho-JNK Thr183/Tyr185, total JNK and Caspase 3 were obtained from Cell Signaling Technology Inc., Danvers, MA, USA; total Drp1 from BD Biosciences, Franklin Lakes, NJ, USA; Vinculin, Grp78 and CHOP (GADD153) from Santa Cruz Biotechnology Inc.; Bcl-2 from Calbiochem (Merck Millipore, Darmstadt, Germany); O-Linked-N-Acetylglucosamine from Abcam (Cambridge, UK).

Clonogenic assay

For each sample $3x10^3$ cells were plated in 100 mm dish. After ≥12 days colonies were fixed with PBS-formaldehyde 5%, stained with Crystal Violet 1% and then counted.

Mitochondrial morphology analysis

To study mitochondrial morphology, NIH3T3, *K-ras*-transformed NIH3T3, MDA-MB-231, MG63 and 3AB-OS cells were transfected with pEYFP-Mito construct (6115-1, BD Biosciences) and stably transfected clones were isolated. Images of mitochondrial morphology were collected under a Nikon ECLIPSE 90i fluorescence microscope (Nikon, Tokyo, Japan) equipped with a b/w CCD camera (Hamamatsu-CoolSnap, Hamamatsu Corporation, Hamamatsu City, Japan) or using a laser scanning confocal microscope MRC-600 (Bio-Rad

Microscience Division, Hemel Hempstead, UK) coupled to an Optiphot-2 Epi Fluor microscope (Nikon). Images were then visualized, processed and classified by using the freely available ImageJ software.

PKA activity determination

Vmax was obtained from Lineweaver-Burk plots of enzymatic PKA activity. In all, 15 µg proteins of sonicated cellular extract were incubated in 50 µL of 10 mM Tris–HCl, pH 7.5, 8 mM $MgCl_2$, 20 mM NaF, 0.25 mM phenylmethylsulfonyl fluoride and 3 µg of oligomycin in the presence of [γ-^{32}P]ATP (1000 c.p.m./pmol), 1 µM cAMP and histone H2B (2.5 µg), as substrate, at different ATP concentration (30–190 µM). After 15 min at 30°C, proteins were subjected to sodium dodecyl sulfate–polyacrylamide gel electrophoresis. After electrophoresis, the gels were stained with Comassie blue and dried. Radioactive protein bands of phosphorylated histone were detected by Personal FX at 'phosphorus imager' (Bio-Rad, Hercules, CA, USA) and quantified by VERSADOC (Bio-Rad).

cAMP cellular levels measurement

cAMP assay was performed as described in (De Rasmo *et al.*, 2011). For cAMP assay the culture medium was removed and 1 mL of 0.1 M HCl was added to the cell layer. After 10 min at 37°C, the lysed cells were scraped. The samples were centrifuged at 1300 × g for 10 min at 4°C. The supernatants were used to determine cAMP concentration using a direct immunoassay kit (Assay Designs, Ann Arbor, Michigan, USA) as described by the manufacturer. Total protein concentration was determined by BioRad protein assay (BioRad). The cAMP level in the sample was normalized to the protein concentration and expressed as pmol/mg proteins.

OXPHOS Complex I and complex IV activity determination

Analyses were performed with little differences as described in (De Rasmo *et al.*, 2011). The isolated mitoplasts were frozen and thawed three times and then exposed to ultrasound energy for 15s at 0°C. The NADH-ubiquinone oxidoreductase (Complex I) activity was performed in 40 mM potassium phosphate buffer, 2 mM K-EDTA, pH 7.4, 2 mM $MgCl_2$, in the presence of 3 mM KCN, 1 μg/ml antimycin, 100 μM decylubiquinone, using 30 μg of mitoplast proteins, by following the oxidation of 2,5-11 μM NADH at 360–374 nm ($\Delta\varepsilon$ = 2.01 mM^{-1} cm^{-1}). The activity was corrected for the residual activity measured in the presence of 1 μg/ml rotenone. Vmax values were obtained from Lineweaver–Burk plots. Cytochrome *c* oxidase (Complex IV) activity was measured by following the oxidation of ferrocytochrome c at 550–540 nm ($\Delta\varepsilon$ = 19.1 mM^{-1} cm^{-1}). Enzymatic activity was estimated in 25 mM phosphate buffer, pH 7.4, and 2 mM $MgCl_2$ using 15 μg of mitoplast proteins.

Transcriptomic analysis

The cRNA was generated by using the Affymetrix One-Cycle Target Labeling and Control Reagent kit (Affymetrix Inc., Santa Clara, California, USA), following the manufacturer's protocol. Total RNA was extracted from biological duplicate samples and analyzed using Affymetrix Genechips (Mouse Genome 430 2.0 Array) to determine the global gene expression patterns. The Mouse Genome 430 2.0 Array contains more than 45000 probe sets including approximately over 34000 well-substantiated mouse genes. Chips were washed and scanned on the Affymetrix Complete GeneChip® Instrument System and processed into CEL files. The complete array data are available at the GEO database under accession GSE29962.

Data elaboration, all statistical analyses and cluster analysis were performed

using GeneSpring GX 11.5 software (Agilent Technologies, Santa Clara, CA, USA).

Proteomic analysis

After extraction, proteins were subjected to labeling, 2-D separation and image acquisition, performed as previously described (Vigano *et al.*, 2011). Only proteins with spot volumes consistently different in all replicates were considered differentially expressed and identified by matrix-assisted laser desorption/ionization (MALDI) time-of-flight (TOF) utilizing the method previously described (Vigano *et al.*, 2011).

Chapter 3

Results (I)

CHAPTER 3. RESULTS (I)

Oncogenic *K-ras* expression is associated with derangement of the cAMP/PKA pathway and forskolin-reversible alterations of mitochondrial dynamics and respiration.

From Palorini *et al.*, Oncogene (2012)

The Warburg effect in cancer cells has been proposed to involve several mechanisms, including adaptation to hypoxia, oncogenes activation or loss of oncosuppressors and impaired mitochondrial function (Lee and Wei, 2009; Levine and Puzio-Kuter, 2010; Semenza, 2010b). In previous papers, it has been shown that *K-ras*-transformed mouse cells are much more sensitive as compared with normal cells to glucose withdrawal (undergoing apoptosis) and present a high glycolytic rate and a strong reduction of mitochondrial complex I (Baracca *et al.*, 2010; Chiaradonna *et al.*, 2006a). Recent observations suggest that transformed cells have a derangement in the cyclic adenosine monophosphate/cAMP-dependent protein kinase (cAMP/PKA) pathway (Balestrieri *et al.*, 2009), which is known to regulate several mitochondrial functions (Acin-Perez *et al.*, 2009; Chang and Blackstone, 2007; De Rasmo *et al.*, 2008; De Rasmo *et al.*, 2010; Papa *et al.*, 2008). Herein, the derangement of the cAMP/PKA pathway and its impact on transformation-linked changes of mitochondrial functions is investigated.

Results

Oncogenic K-ras stimulates glycolysis leading to glucose-dependent cell proliferation

NIH3T3 cells are a genetically well-characterized immortalized cell line that has long been established as a model of 'normal' cells for the study of cell transformation, as these cells undergo contact inhibition, exhibit no growth in soft agar and do not form tumors in immunocompromised mice (Yamamoto and Perucho, 1984), in contrast to isogenic transformed lines as *K-ras*-NIH3T3 cells (Bossu *et al.*, 2000). Besides, as previously described, oncogenic *Ras* proteins expression correlates with the appearance of several metabolic alterations distinctive of cancer cells (Chiaradonna *et al.*, 2006a; Vizan *et al.*, 2005; Weinberg *et al.*, 2010; Yun *et al.*, 2009).

Given that both Ras and cAMP/PKA pathways are able to control cellular metabolism and proliferation (Gerits *et al.*, 2008), we decided to test the relationship between the cAMP/PKA system and the proliferation ability of NIH3T3 and *K-ras*-NIH3T3 cells on alteration of glucose availability.

Asynchronous NIH3T3 (Normal) and *K-ras*-NIH3T3 (Transformed) cell lines were cultured in normal growth medium (25 mM glucose), in a low glucose medium (1 mM glucose), in glucose-free medium supplemented with 25 mM galactose, an obligate mitochondrial oxidative substrate, or in 5 mM fructose.

The growth of normal cells declined after 72 hours in both 25 and 1 mM glucose and at 48 hours in galactose (**figures 1A and C**) and fructose (**figure 2A**). Transformed cells maintained a vigorous growth for at least 96 hours in 25 mM glucose but lost their proliferative ability in 1 mM glucose (**figure 1B**), in 25 mM galactose (**figures 1B and C**) and in 5 mM fructose (**figure 2B**).

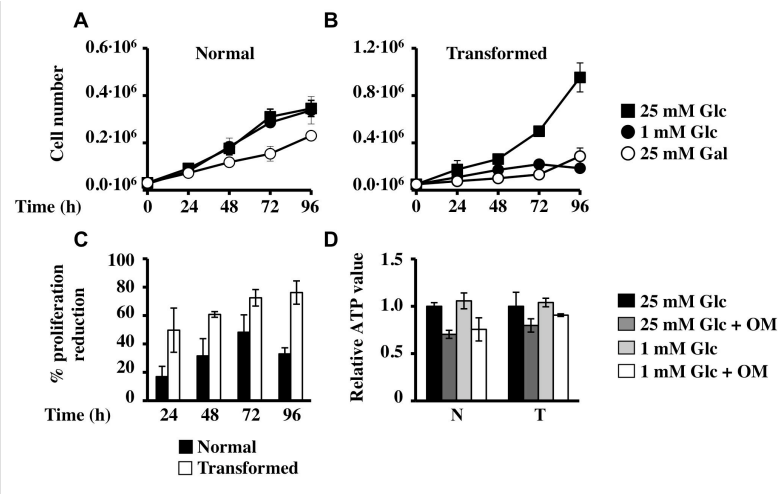

Figure 1. *K-ras*-transformed cells are strongly sensitive to glucose availability. Proliferation curves of Normal (N) **(A)** and Transformed (T) **(B)** cells cultured at 25 mM glucose (Glc), at 1 mM Glc or at 25 mM galactose (Gal) were determined counting cells at indicated time points. Note the different scale for the two cell lines. **(C)** Percentage of proliferation reduction in 25 mM Gal as compared with 25 mM Glc at each time point for N and T cells. **(D)** Total intracellular ATP levels were measured in N and T cells grown at 25 and 1 mM Glc, treated or not with 5 μM oligomycin (OM) at 24 hours of culture. Values are relative to the sample 25 mM Glc. All data represent the average of at least three independent experiments (± s.d.).

Addition to the culture medium of oligomycin (OM) (**figure 1D**), a specific inhibitor of the mitochondrial FoF1 ATP synthase (Papa *et al.*, 1996), in Normal cells reduced the ATP levels by around 30% both at 25 and 1 mM glucose. Thus, this fraction represents the contribution of mitochondrial oxidative phosphorylation to ATP production under the prevailing cultivation conditions. In Transformed cells, cultivated in 25 mM glucose, OM addition resulted in a smaller reduction of the ATP levels as compared with normal cells that was significantly smaller at 1 mM glucose. Thus, these data show that in Transformed cells the mitochondrial oxidative phosphorylation contributes only marginally to cellular ATP production, which is essentially contributed by glycolysis (Chiaradonna *et al.*, 2006a).

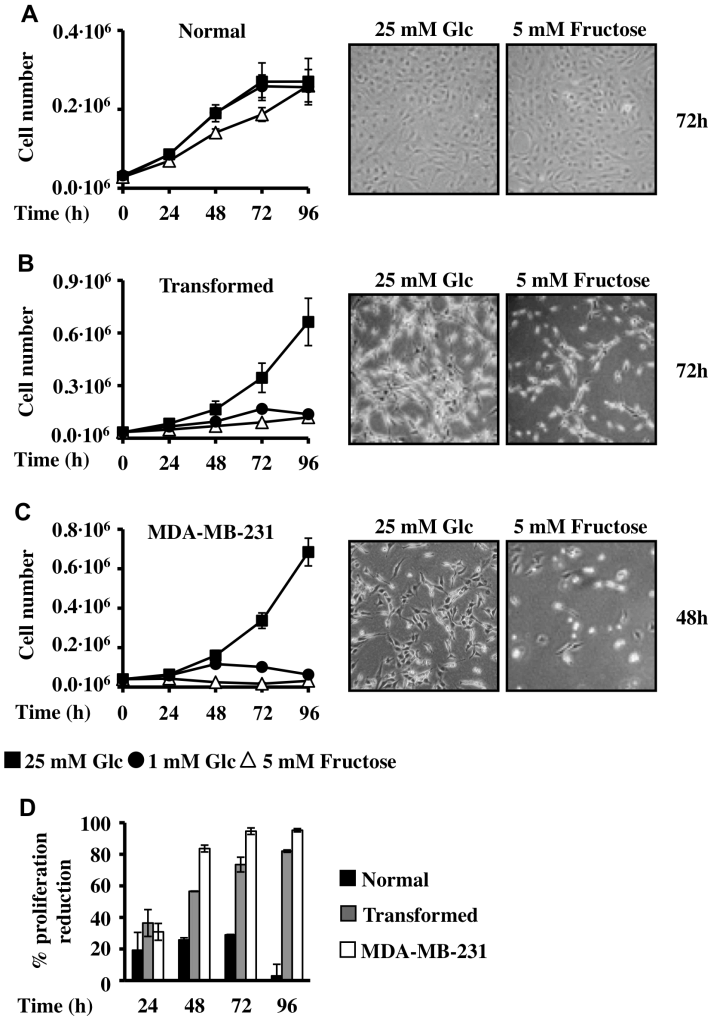

Figure 2. Transformed cell growth is strongly reduced in fructose-enriched medium. (A-C) Proliferation curves of Normal (**A**), Transformed (**B**) and MDA-MB-231 (**C**) cells cultured at 25 mM glucose (Glc), at 1 mM Glc or at 5 mM fructose were determined counting cells at indicated time points. Note the different scale for the three cell lines. Representative phase contrast microscopy images of all cell lines were collected and reported on the right of the proliferation curves. **(D)** Percentages of proliferation reduction at 5 mM fructose as compared to 25 mM Glc at each time point for Normal, Transformed and MDA-MB-231 cells. All data represent the average of at least three independent experiments (± s.d.).

K-ras-Transformed cells present altered cAMP/PKA pathway as compared to Normal cells

Direct determination of basal endogenous levels of cAMP along a time course of 72 hours in cells grown at 25 and 1 mM glucose (**figures 3A and B**) showed a time-dependent increase in cAMP levels in both cell lines.

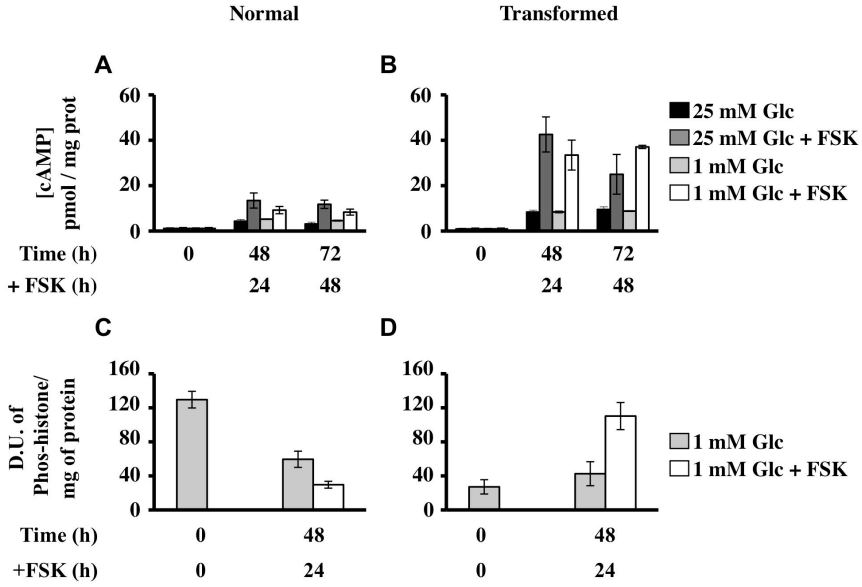

Figure 3. FSK treatment largely increases intracellular cAMP levels and PKA activity in transformed cells as compared with normal ones. (a, b) The cAMP levels were measured at indicated time points in Normal **(a)** and Transformed **(b)** cells grown at 25 and 1 mM glucose (Glc), untreated and + FSK. **(c, d)** PKA activity was measured as described in Materials and methods at indicated time points in Normal **(c)** and Transformed **(d)** cells grown at 1 mM Glc (untreated and + FSK). All data represent the mean ± s.e.m. of three independent determinations. *These data were obtained by Papa's group.*

In Transformed cells, at both 48 and 72 hours, cAMP levels were higher than in Normal cells (**figures 3A and B**). The addition of forskolin (FSK, an activator of the adenylyl cyclases) increased, as expected, the level of cAMP, but such an

increase was much larger in Transformed cells as compared with Normal ones (**figures 3A and B**).

Kinetic analysis of the PKA activity in cell extracts showed in Transformed cells a constitutive (time 0 of the growth curve) depressed activity of the enzyme as compared with Normal cells, which slightly increased in 48 hours growth and was greatly enhanced by FSK addition to the cultivation medium (**figure 3D**). In Normal cells, the PKA activity decreased significantly during cell growth and was further depressed by FSK (**figure 3C**).

Direct immunochemical analysis revealed an increase in the cellular content of the catalytic subunit of PKA in 48 hours of growth of Normal and Transformed cells, which in both type of cells was prevented by FSK addition (**data not shown**). These findings indicate that the changes in the functional capacity of PKA, rather than being due to changes in the content of the enzyme, reflect altered PKA responsiveness to cellular activator(s)/inhibitor(s).

In order to evaluate the PKA activation state as a function of glucose availability and of oncogenic *Ras* mutation, the extent of cAMP responsive element binding protein (CREB) phosphorylation was monitored in Normal and Transformed cells at both 25 and 1 mM glucose.

In Normal cells (**figure 4A**), as well in Reverted cells (**figures 5A and 5B**), phosphorylation of CREB significantly increased with the cultivation time, in particular at 25 mM glucose (**figure 4A**). On the contrary, in Transformed cells no significant time-dependent increase in CREB phosphorylation occurred either at 25 or 1 mM glucose (**figure 4B**).

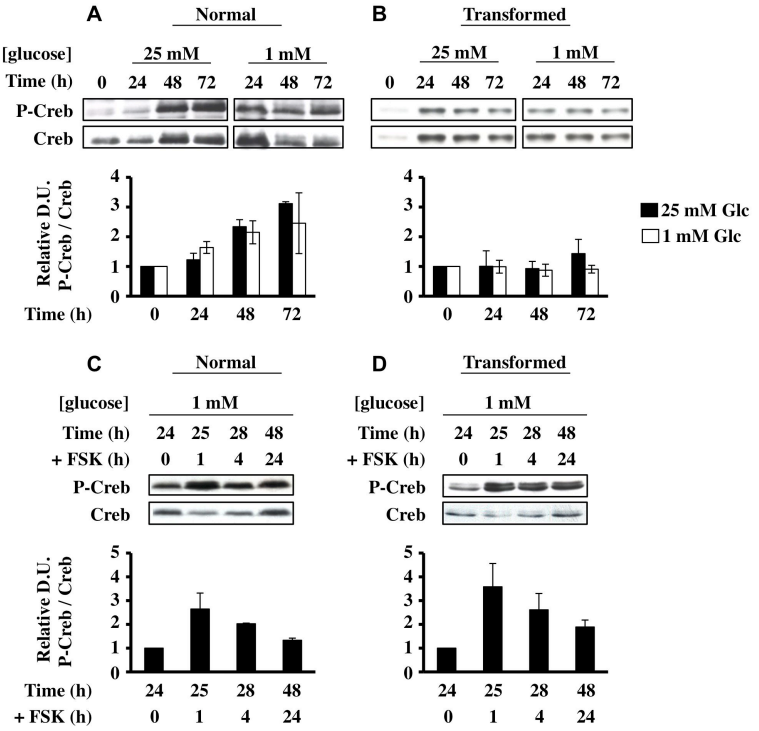

Figure 4. FSK treatment induces CREB phosphorylation especially in transformed cells. (A, B) For basal expression analysis of total CREB (Creb) and phospho-CREB Ser133 (P-Creb), Normal **(A)** and Transformed **(B)** cells were collected at indicated time points and total cellular extracts were subjected to sodium dodecyl sulfate–polyacrylamide gel electrophoresis followed by Western blot analysis with specific antibodies. Relative quantitative measurement (**A and B, bottom histograms**) of CREB phosphorylation, in both cell lines grown at 25 or 1 mM glucose (Glc), was performed by densitometric analysis of western blot films. The values obtained for P-CREB were normalized to the corresponding total CREB values, plotted as fold change from the sample 0 hours (0h=1) and indicated as relative densitometric units (DUs). **(C, D)** Western blot analysis of CREB phosphorylation (upper panels) and relative quantitative measurement (lower panels) were also performed in Normal **(C)** and Transformed **(D)** cells grown at 1 mM glucose on 24 hours of FSK treatment. Values were normalized as described above. Data represent the mean± s.e.m. of three independent determinations.

FSK treatment resulted in a transient increase in CREB phosphorylation, which was larger and more persistent in Transformed cells as compared with Normal

ones (**figures 4C and D**). Altogether, these findings show an altered regulation of the cAMP/PKA pathway in Transformed cells.

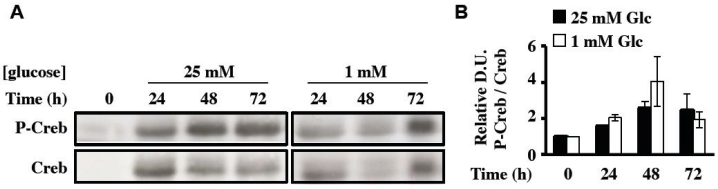

Figure 5. Basal CREB expression in Reverted cells is similar to that of Normal cells. (A, B) For basal expression analysis of Total CREB (Creb) and Phospho-CREB Ser133 (P-Creb), Reverted cells grown at 25 or 1 mM glucose (Glc) were collected at indicated time points and total cellular extract was subjected to sodium dodecyl sulfate–polyacrylamide gel electrophoresis followed by Western blot (**A**). Quantitative analysis (**B**) of CREB phosphorylation status was performed by densitometric analysis of Western blot film. The values obtained for P-CREB were normalized to the corresponding total CREB values, plotted as fold change from the sample 0 hours (0h=1) and indicated as relative densitometric units (DUs). Data represent the mean ± s.e.m of three independent determinations.

FSK regulates cell growth, apoptosis and mitochondrial morphology, with different effects in Normal and Transformed cells

To gain an insight into the impact of the above-detected alterations of the cAMP/PKA pathway on mitochondrial dynamics and functions in *K-ras*-transformed cells, the effect of adenylyl cyclase activation by FSK was tested on cell growth, apoptosis, mitochondrial structure and functions of normal and transformed fibroblasts. To this aim, the cells were daily treated with 10 μM FSK, starting from 24 hours after medium replacement.

Proliferation of Transformed cells grown at 1 mM glucose began to slow down at 48 hours and under these conditions they started to die and undergo apoptosis more significantly and faster than Normal cells (**figure 6**). Addition of FSK to the culture medium prevented the glucose-dependent death of Transformed cells (**figures 6B, D and F**).

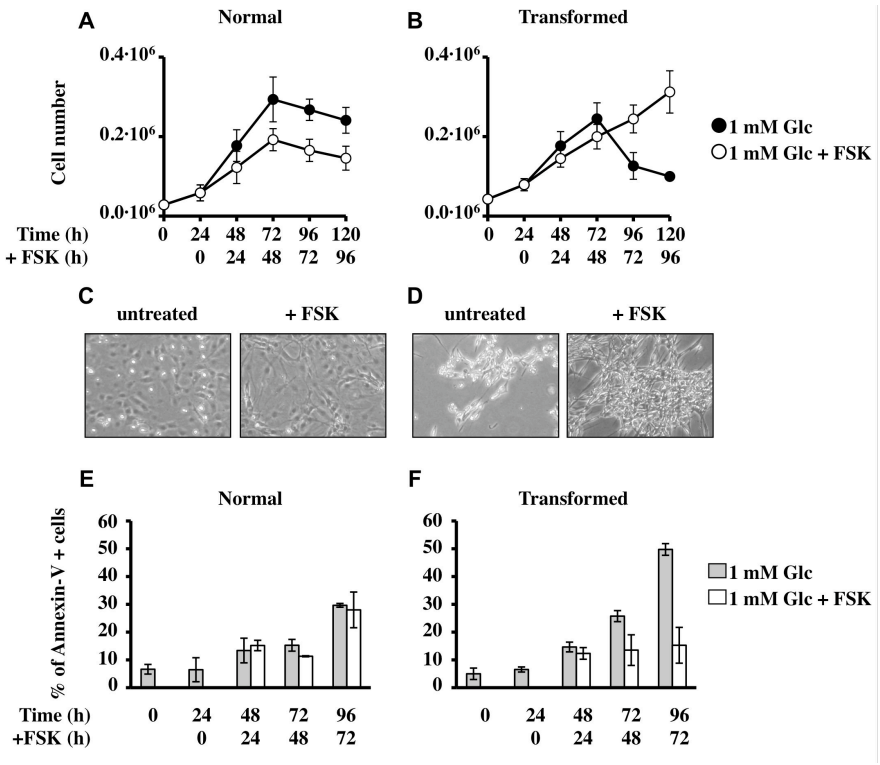

Figure 6. FSK treatment increases survival of *K-ras*-transformed cells on glucose deprivation. (A, B) Proliferation curves of Normal **(A)** and Transformed **(B)** cells grown at 1 mM glucose (Glc), treated or not with FSK, were determined counting cells at indicated time points. **(C, D)** Phase contrast microscopy images were collected for Normal **(C)** and Transformed **(D)** cells at 96 hours of cell culture. **(E, F)** Analysis of apoptosis for Normal **(E)** and Transformed **(F)** cells was evaluated by annexin-V/propidium iodide (PI) staining and calculating the percentage of annexin-V-positive cells. Data represent the average of at least three independent experiments (± s.d.).

The death-preventing effect of FSK was suppressed by the addition of H89, a specific inhibitor of PKA (Chijiwa *et al.*, 1990) (**figure 7B**).

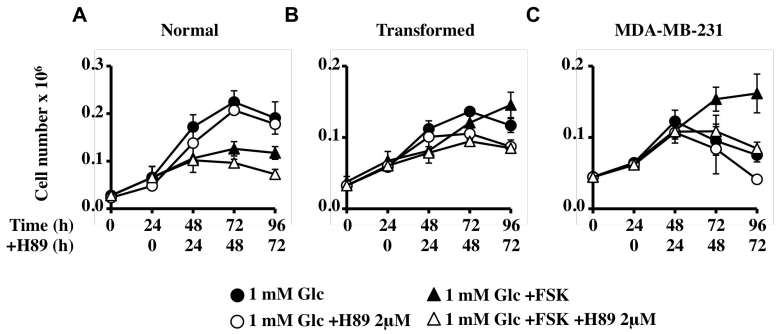

Figure 7. H89 inhibits the protective role of FSK in low glucose. (A-C) Proliferation curves of Normal **(A)**, Transformed **(B)** and MDA-MB-231 **(C)** cells cultured at 1 mM glucose (Glc), untreated or treated with FSK or/and H89 as reported, were determined counting cells at indicated time points. Note the different scale for the three cell lines. Data represent the average of at least three independent experiments (± s.d.).

In Normal (**figures 6A, C and E; figure 7A**) and Reverted cells (**figure 8**) an inhibiting effect of FSK on cell growth was observed.

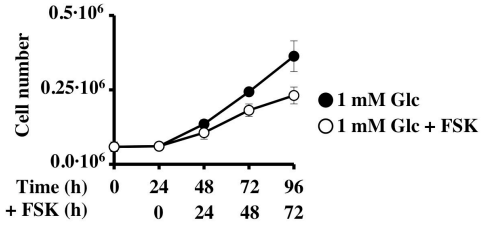

Figure 8. FSK inhibits proliferation of Reverted cells. Proliferation curves of Reverted cells grown at 1 mM glucose (Glc), treated or not with FSK, were determined counting cells at indicated time points. Data represent the average of at least three independent experiments (± s.d.).

In order to investigate whether the survival of FSK-treated cells could be consequence of a different ability of transformed cells to transport and utilize glucose, glucose utilization as well as lactate production of both cell lines grown in 1 mM glucose condition were assayed. As shown in **figures 9A and 9B**, the amounts of consumed glucose and of secreted lactate, as measured in the culture

medium, were substantially identical between untreated and FSK-treated cell lines. These findings were confirmed also by measuring both glucose and lactate on per cell basis (**data not shown**) and by measuring the rate of glucose transport into the cells, using the fluorescent derivative of glucose 2-NBDG as indicator of glucose uptake (**figures 9C and 9D**).

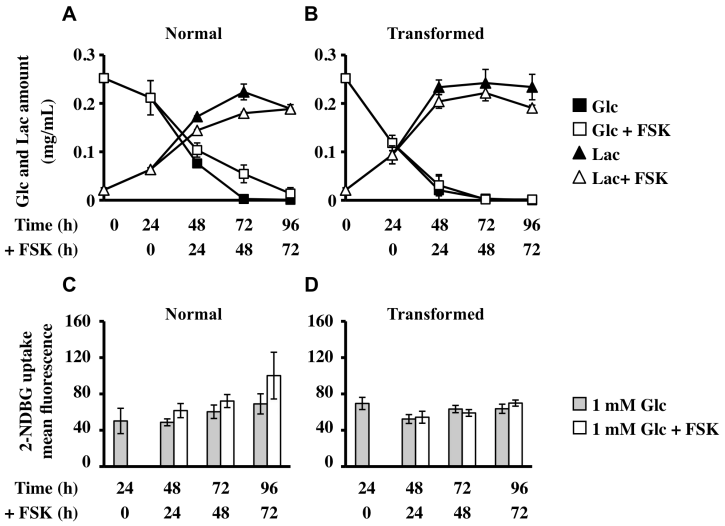

Figure 9. Glucose consumption and uptake as well as lactate production are almost identical in both untreated and FSK-treated cells. (A, B) Residual glucose (Glc) and secreted lactate (Lac) in culture medium of Normal (**A**) and Transformed (**B**) cells cultured at 1 mM initial glucose concentration and upon FSK treatment were measured by using specific enzymatic kits. (**C, D**) Glucose uptake rate was determined using the fluorescent glucose analogue 2-[*N*-(7-nitrobenz-2-oxa-1,3-diazol-4-yl) amino]-2-deoxy-D-glucose (2-NBDG) in Normal **(C)** and Transformed **(D)** cells grown at 1 mM Glc. All data represent the average of three independent experiments (± s.d.).

In stable clones of Normal and Transformed cell lines expressing a mitochondrially targeted EYFP-Mito protein, the effect of FSK treatment on mitochondrial morphology in 1 mM glucose culture condition was investigated by fluorescent microscopy (**figure 10**).

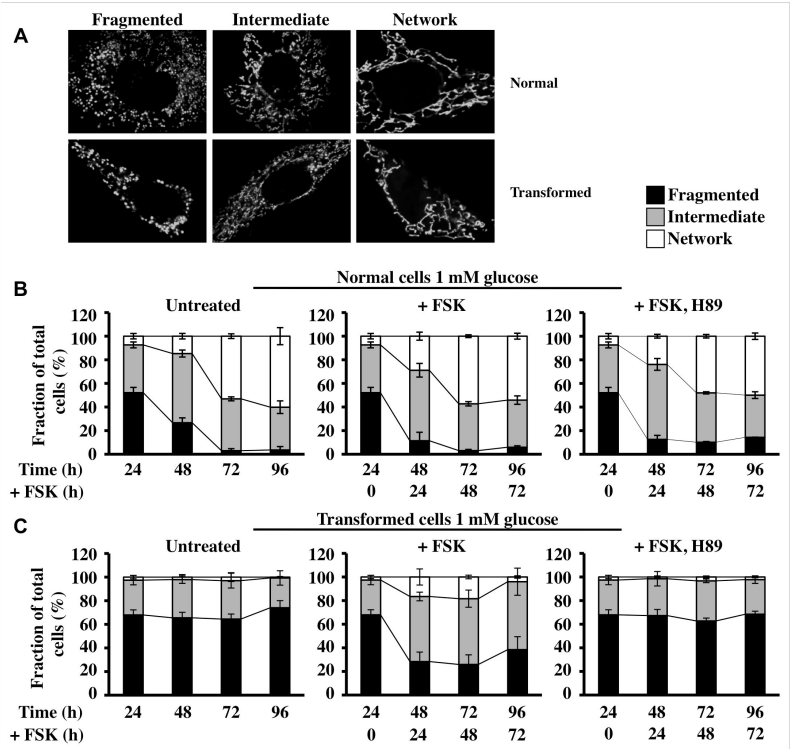

Figure 10. FSK treatment increases mitochondrial interconnections in Transformed cells. (A) Confocal microscopy images of stable EYFP-Mito expressing clones of Normal and Transformed cells sorted according their mitochondrial morphology: fragmented, intermediate and networked. **(B, C)** Mitochondrial morphology analysis was carried out at indicated time points in Normal **(B)** and Transformed **(C)** cells grown in 1 mM glucose, subjected or not to treatment with FSK and 2 μM H89. For each determination, at least 100 cells were counted and classified depending their mitochondrial morphology. Data represent the average of at least three independent experiments (± s.d.) and are indicated as percentage.

Three types of mitochondrial morphologies have been classified as fragmented, intermediate and networked (**figure 10A**). At an early cultivation time, Normal cells displayed both fragmented and intermediate mitochondria (**figure 10B, left panel**). At later cultivation time (72–96 hours), fragmented mitochondria completely disappeared and the vast majority of cells showed a networked

morphology (**figure 10B, left panel**). In Normal cells at all time points, morphology was not affected by FSK (**figure 10B, middle panel**). On the contrary, Transformed cells showed more fragmented mitochondria and intermediate mitochondria along all the time course of analysis (**figure 10C, left panel**) and were strongly sensitive to FSK, which induced a marked decrease in fragmented mitochondria with a parallel increase in intermediate and networked structures (**figure 10C, middle panel**). Mitochondrial morphological analysis, performed in both cell lines grown in 25 mM glucose, resulted in comparable data (**figure 11**).

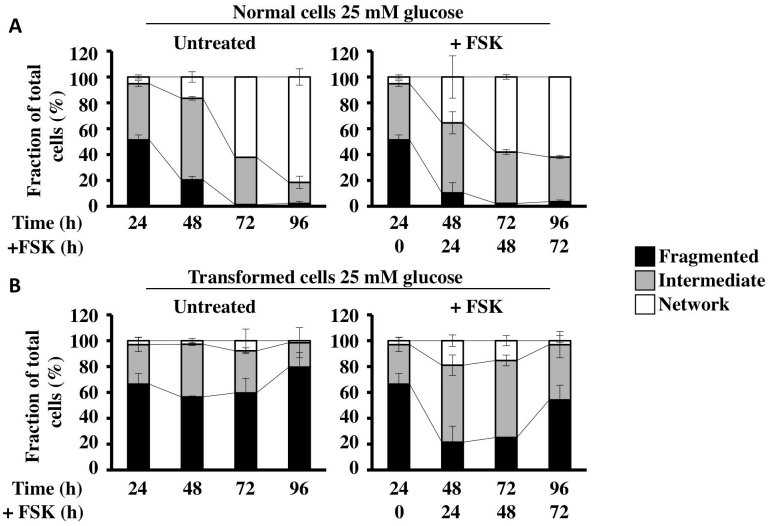

Figure 11. FSK treatment induces mitochondrial interconnections in Transformed cells even in high glucose culture. Mitochondrial morphology was analyzed in stable EYFP-Mito expressing cell clones of Normal (**A**) and Transformed (**B**) cells and classified as fragmented, intermediate and networked. The analysis was carried out in cells grown at 25 mM glucose, subjected or not to FSK treatment. For each determination at least 100 cells were counted and classified depending on their mitochondrial morphology. Data represent the average of three independent experiments (± s.d.) and are indicated as percentage.

A role of PKA on mitochondrial dynamics of transformed cells was confirmed by analysis of mitochondrial morphology upon co-treatment of the cells with FSK and H89. As shown in **figures 10B and 10C, right panels**, H89 strongly prevented the FSK-dependent formation of more interconnected and intermediate mitochondria in Transformed cells as compared with Normal ones.

FSK improves mitochondrial activity and decreases ROS levels especially in Transformed cells

In **figure 12**, the results of an analysis of the functional capacity of Complex I and IV of the respiratory chain, ATP and ROS production in Normal and Transformed cells are presented at 72 hours of growth in 1 mM glucose (48 hours of FSK treatment).

In Transformed cells, the specific activity of Complex I (NADH-ubiquinone oxidoreductase), depressed as compared with Normal cells, was stimulated by FSK treatment (**figure 12B**), but it was unaffected in Normal cells (**figure 12A**). No changes were observed in the specific activity of Complex IV (cytochrome c oxidase) (**figure 12D**). Transformed cells as compared with Normal ones showed a slight but significant increase in the respiratory activity with NAD-linked substrates, in particular in the uncoupled state, on FSK treatment (**data not shown**). No effect of FSK was observed on the respiratory activity with succinate as respiratory substrate (**data not shown**). The level of cellular ATP was increased by the presence of FSK in both cell lines (**figures 12E and F**). This increase was larger in Transformed cells (**figures 12E and F**) and was almost completely prevented by H89, especially in Transformed cells as compared with Normal cells (**figures 12E and F**). Notably, the FSK-dependent effects on Complex I activity and ATP levels were also associated with a significant decrease in ROS levels in Transformed cells (**figure 12H**).

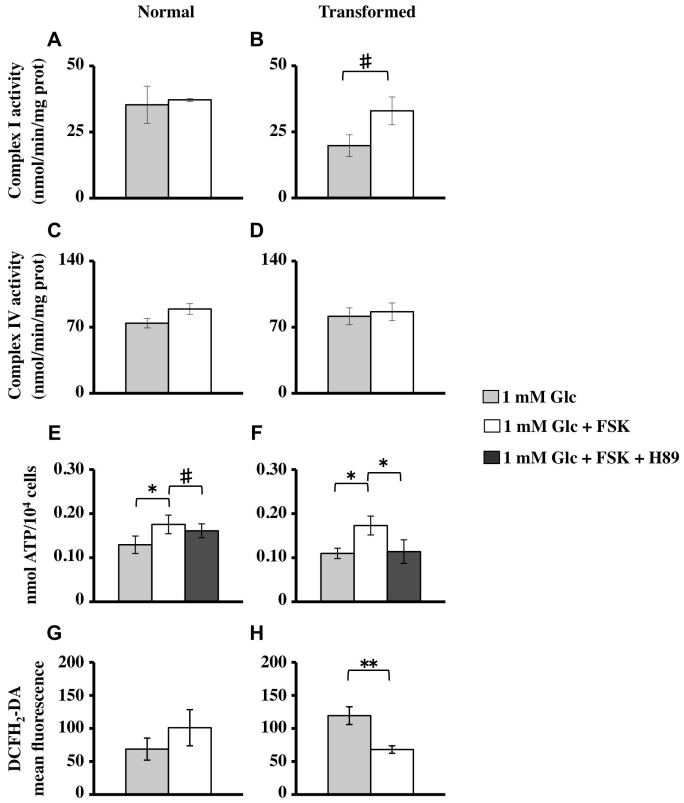

Figure 12. FSK treatment improves mitochondrial activity especially in transformed cells. The analyses were performed at 72 hours of culture at 1 mM glucose (Glc) in absence or in presence for 48 hours of FSK or FSK plus 2 μM H89 as indicated. (**A, B**) Complex I activity of mitochondrial respiratory chain was measured in daily isolated mitoplast fraction from Normal (**A**) and Transformed (**B**) cells; #P<0.02, Student's t-test. (**C, D**) Complex IV activity of mitochondrial respiratory chain was measured in daily isolated mitoplast fraction from Normal (**C**) and Transformed (**D**) cells. *These analyses were performed by Papa's group.* Total intracellular ATP was measured in Normal (**E**) and Transformed (**F**) cells; *P<0.0001 and #P<0.02, Student's t-test. (**G, H**) ROS levels were measured in Normal (**G**) and Transformed (**H**) cells; **P<0.003, Student's t-test. All data represent the average of at least three independent experiments (± s.d.).

The addition to the cultivation medium of N-acetyl-cysteine (NAC), which decreased the ROS levels in both Normal and Transformed cells, partly

sustained the growth of Transformed cells but had no effect on Normal cells (**figure 13**).

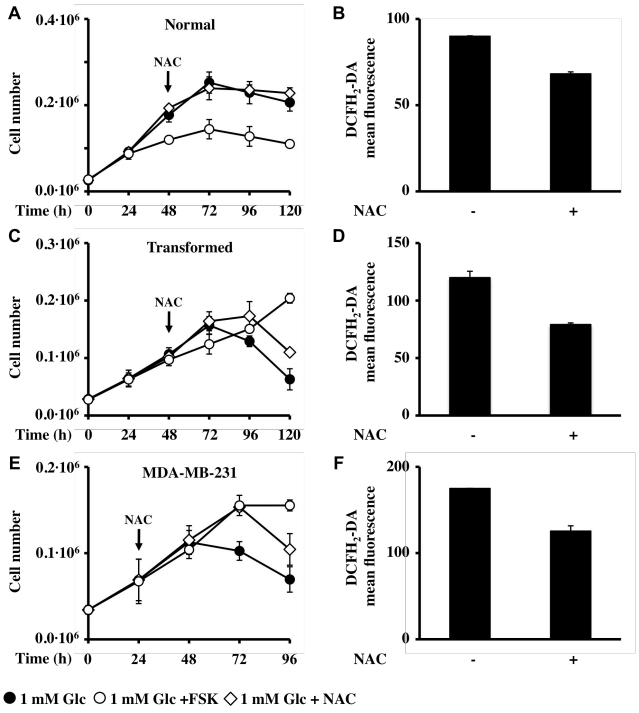

Figure 13. NAC treatment partially protects transformed cells from glucose-dependent death. (A, C, E) Proliferation curves of Normal **(A)**, Transformed **(C)** and MDA-MB-231 **(E)** cells cultured at 1 mM glucose (Glc), untreated or treated with FSK or NAC, were determined counting cells at indicated time points. Note the different scale for the three cell lines. A single treatment with 5 mM NAC was performed at indicated time point. **(B, D, F)** ROS levels were measured in Normal **(B)**, Transformed **(D)** and MDA-MB-231 **(F)** cells 4 hours after the treatment with NAC for untreated (-) and treated (+) cells. All data represent the average of three independent experiments (± s.d.).

FSK-treated Reverted cells did not show ATP levels increase and ROS levels decrease (**data not shown**). Noteworthy, the positive effect on Complex I by FSK treatment in Transformed cells was observed also when they were grown in

25 mM glucose (**data not shown**), pointing out to a general role of PKA as mitochondrial function regulator.

FSK protects also human MDA-MB-231 cells in glucose deprivation, improving their mitochondrial function

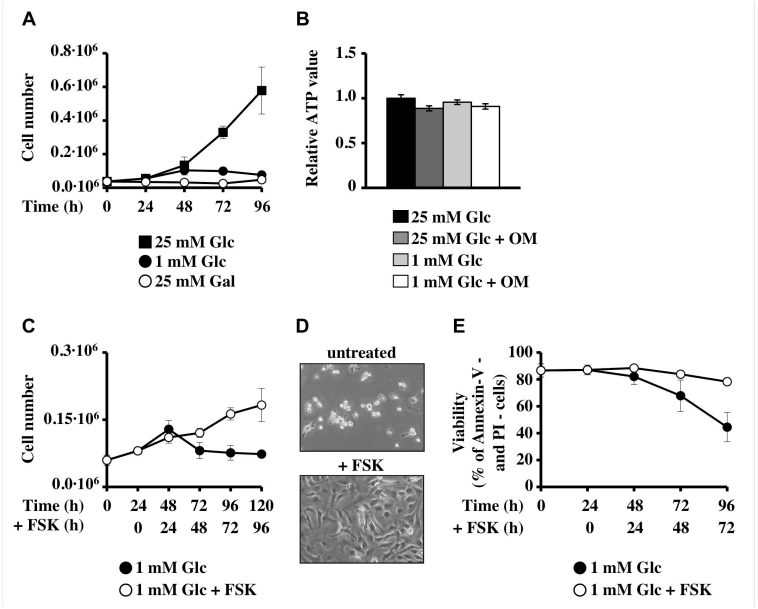

Figure 14. FSK treatment protects human MDA-MB-231 cancer cells from glucose shortage-dependent cell death. (A) Proliferation curves of MDA-MB-231 cells cultured at 25 mM glucose (Glc), at 1 mM Glc or at 25 mM galactose (Gal) were determined counting cells at indicated time points. **(B)** Total intracellular ATP was measured in MDA-MB-231 cells grown at 25 and 1 mM Glc, treated or not with 5 μM oligomycin (OM) at 24 hours of culture. Values are relative to the sample 25 mM Glc. **(C)** Proliferation curves of MDA-MB-231 cells grown at 1 mM Glc, treated or not with FSK, were determined counting cells at indicated time points. **(D)** Phase contrast microscopy images were collected for cells at 72 hours of culture. **(E)** Analysis of cell viability in MDA-MB-231 cells was evaluated by annexin-V/propidium iodide (PI) staining and calculating the percentage of annexin-V/PI-negative cells. All data represent the average of at least three independent experiments (± s.d.).

MDA-MB-231 cells, harboring a K-ras oncogenic mutation, show a cellular metabolism similar to those observed in the mouse model of *K-ras*-dependent transformation (Gaglio *et al.*, 2011). Mitochondrial and metabolic characteristics of these human cancer cells were, thus, analyzed, both in untreated and FSK-treated conditions.

MDA-MB-231 cells, grown at 1 mM glucose, 25 mM galactose (**figure 14A**) as well as at 5 mM fructose (**figure 2C**) showed a dramatic decrease in their proliferation capacity as compared with the cells grown at 25 mM glucose (**figure 14A**). Addition of oligomycin in both glucose conditions did not cause any effect on total ATP levels (**figure 14B**), showing their dependence on glycolytic activity. FSK treatment of MDA-MB-231 cells grown at 1 mM glucose rescued their proliferation ability and decreased apoptosis (**figures 14C–E**).

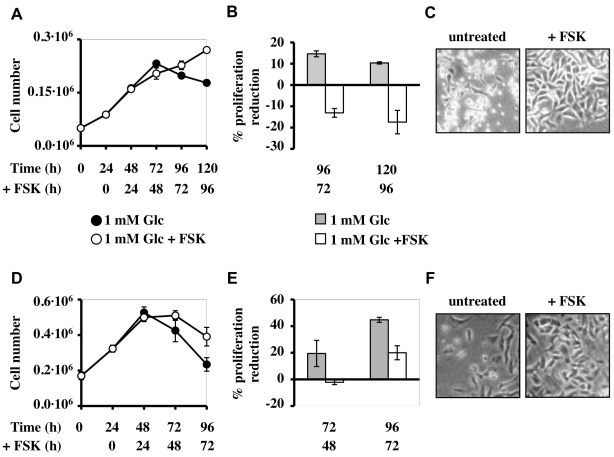

Figure 15. FSK treatment protects human *K-ras*-transformed cells from glucose-dependent apoptosis. (A, D) Proliferation curves of MIA PaCa-2 (**A**) and A549 (**D**) cells grown at 1 mM glucose (Glc), treated or not with FSK, were determined counting cells at indicated time points. **(B, E)** Percentages of proliferation reduction at indicated time point as compared to previous time point are represented for MIA PaCa-2 (**B**) and A549 (**E**) cells. **(C, F)** Representative phase contrast microscopy images of cell lines were collected at 96 hours (MIA PaCa-2, **C**) or 72 hours (A549, **F**) of culture. All data represent the average of three independent experiments (± s.d.).

Similar results were obtained in other two human cancer cell lines harboring an oncogenic *K-ras*, namely MIA PaCa-2 (pancreatic) and A549 (lung). In fact, both cell lines were sensible to glucose deprivation, undergoing to cell death, and both were, in different extend, protected by FSK treatment (**figure 15**).

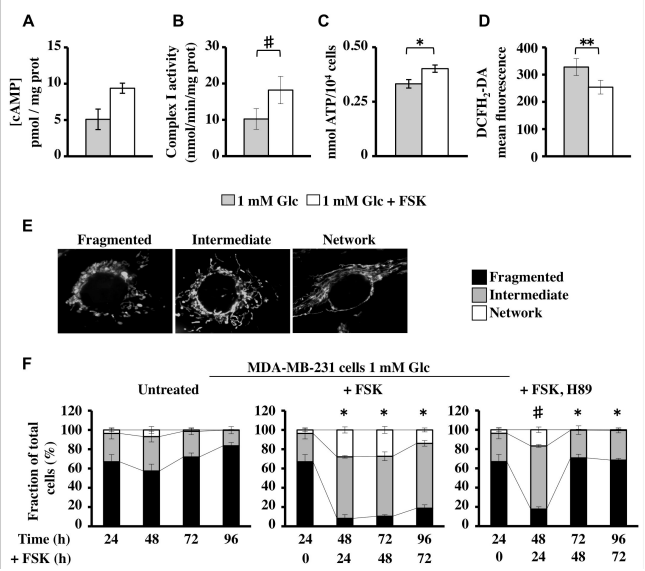

Figure 16. FSK treatment enhances several mitochondrial parameters in MDA-MB-231 cancer cells associated to increased survival on glucose shortage. cAMP levels **(A)**, Complex I activity **(B)**, ATP **(C)** and ROS **(D)** levels were measured at 48 hours of culture in MDA-MB-231 cells grown at 1 mM glucose (Glc). Panel **(A)** represents the mean ± s.e.m. of three independent determinations; all the other data represent the average of at least three independent experiments (± s.d.); #P<0.02, *P<0.0001 and **P<0.003, Student's t-test. **(E)** Examples of fragmented, intermediate and networked mitochondria in stable EYFP-Mito expressing MDA-MB-231 cells. **(F)** Analysis of mitochondrial morphology in MDA-MB-231 cells grown at 1 mM Glc, subjected or not to treatment with FSK and 5 μM H89. For each determination, at least 100 cells were counted and classified depending their mitochondrial morphology. Data represent the average of at least three independent experiments (± s.d.) and are indicated as percentage; *P<0.0001 and #P<0.05, Student's t-test; P-value is calculated on percentage of fragmented and networked mitochondria. FSK-treated samples are compared with untreated samples, while samples treated with FSK + H89 are compared with FSK-treated samples.

After 24 hours of FSK treatment, MDA-MB-231 cells showed an increase in cellular cAMP levels (**figure 16A**), in complex I activity (**figure 16B**) and in ATP levels (**figure 16C**), associated with a decrease in ROS levels (**figure 16D**) and an increase in mitochondrial interconnections (**figure 16F**).

The increase in mitochondrial interconnections (**figure 16F, right panel**) and ATP levels (**data not shown**) produced by FSK were prevented by H89 treatment, confirming the role of PKA in mitochondria regulation.

Noteworthy, the FSK-dependent positive effects on complex I activity and mitochondrial fusion were observed also in MDA-MB-231 cells grown in 25 mM glucose (**data not shown**) as well as previously described for mouse transformed cells.

Short treatment with FSK induces mitochondrial fusion, associated with the decrease of ROS levels

PKA-catalyzed phosphorylation of cellular proteins can result, in addition to long-term transcriptional effects as those mediated by CREB, in short-term regulation of mitochondrial respiration and morphology at post-translational level (Acin-Perez *et al.*, 2009; Gomes *et al.*, 2011; Piccoli *et al.*, 2006).

As reported for *K-ras*-transformed fibroblasts, no significant time-dependent CREB phosphorylation was observed in MDA-MB-231 cells grown at either 25 or 1 mM glucose (**figures 17A and B**). The addition of FSK, however, resulted in a transient increase in CREB phosphorylation, which after reaching a maximum at 1 hour declined back to the initial value at 24 hours of cultivation (**figures 17C and D**).

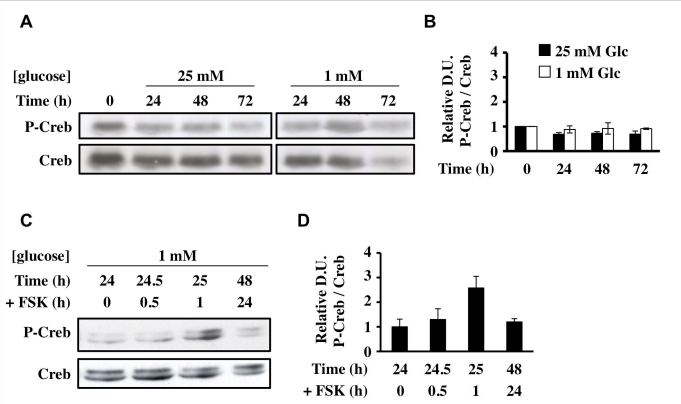

Figure 17. Expression analysis of total CREB and phospho-CREB Ser133 in MDA-MB-231 cells. (A) MDA-MB-231 cells grown at 25 or 1 mM glucose (Glc) were collected at indicated time points and total cellular extracts were subjected to sodium dodecyl sulfate–polyacrylamide gel electrophoresis followed by western blot analysis with specific antibodies against total CREB (Creb) and phospho-CREB Ser133 (P-Creb). **(B)** Quantitative analysis of CREB phosphorylation status was performed by densitometric analysis of western blot films. The values obtained for P-CREB were normalized to the corresponding total CREB values, plotted as fold change from the sample 0 hours (0h=1) and indicated as relative densitometric units (DUs). **(C, D)** Western blot evaluation **(C)** of phospho-CREB Ser133 was also performed in MDA-MB-231 cells grown at 1 mM glucose on 24 hours of FSK treatment and quantitative analysis is reported in the histogram **(D)**. Values were normalized as described above. All data represent the mean ± s.e.m. of three independent determinations.

It has been reported that PKA-mediated phosphorylation of the pro-fission protein factor Drp1 inhibits fission with consequent increase in mitochondrial fusion (Chang and Blackstone, 2007). The results presented in **figure 18A** show that FSK treatment of MDA-MB-231 cells induced phosphorylation of Drp1 between 1 and 4 hours, which then disappeared at 24-hours cultivation.

The effects of FSK and of the mitochondrial division inhibitor Mdivi-1, which prevents mitochondrial fission by inhibiting the Drp1 activity, were analyzed on mitochondrial dynamics in short-time intervals. As shown in **figure 18B**, treatment with FSK or Mdivi-1 of MDA-MB-231 cells grown at 1 mM glucose

significantly increased mitochondrial interconnections as early as 1-hour treatment. Analysis of ROS levels showed that the more interconnected mitochondria induced by FSK or Mdivi-1 were associated with a significant reduction of ROS levels (**figure 18C**).

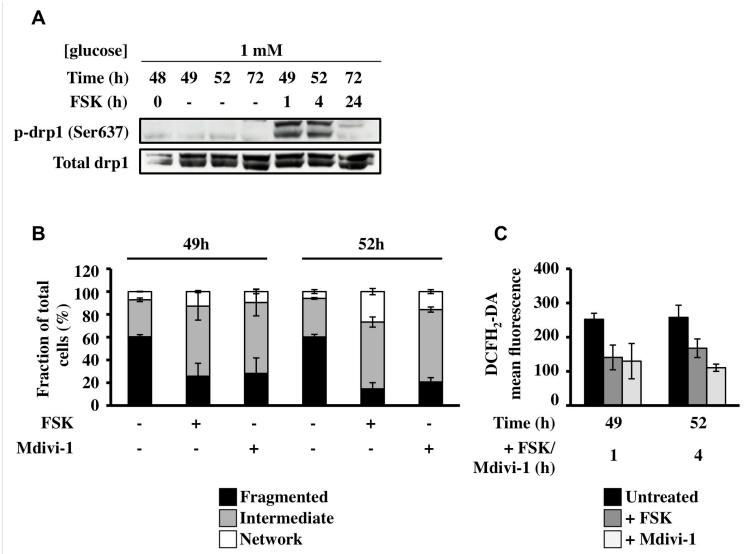

Figure 18. Networked mitochondria are less prone to ROS generation. (A) Analysis of Total Drp1 and phospho-Drp1 Ser637 (p-drp1) was performed in MDA-MB-231 cells grown at 1 mM glucose untreated (−) or treated with FSK for 1, 4 and 24 hours. Cells were collected at indicated time points and total cellular extracts were subjected to sodium dodecyl sulfate–polyacrylamide gel electrophoresis followed by western blot analysis with specific antibodies against Drp1 and phospho-Drp1. **(B, C)** MDA-MB-231 cells, cultured at 1 mM glucose, were subjected to a treatment with 10 μM FSK or 10 μM Mdivi-1 48 hours after medium change. Cells were then collected 1 hour and 4 hours after the treatment for the subsequent analyses. **(B)** Mitochondrial morphology was determined classifying mitochondria as fragmented, intermediate and networked (for major details of the procedure refer to the figure 16 legend). **(C)** Intracellular ROS levels were analyzed staining cells with $DCFH_2$-DA. Data represent the average of three independent experiments (± s.d.).

Chapter 4

Results (II)

CHAPTER 4. RESULTS (II)

Forskolin and mitochondrial Complex I inhibitors synergize in killing cancer cells under glucose deprivation.

Cancer cells generally rely mostly on glycolysis rather than Oxidative Phosphorylation (OXPHOS) for ATP production (Chiaradonna *et al.*, 2012; Kroemer and Pouyssegur, 2008; Tennant *et al.*, 2010). As consequence, they are particularly sensitive to glycolysis inhibition and glucose depletion (El Mjiyad *et al.*, 2011; Pelicano *et al.*, 2006). However, mitochondria maintain an important role for cell viability; in fact, there are a series of compounds targeting mitochondria, named mitocans, that are being tested as anticancer drugs (Biasutto *et al.*, 2010; Ralph *et al.*, 2006). Therefore, combined treatments targeting both glycolysis and mitochondria function, exploiting peculiar tumor features, might be lethal for cancer cells. Here we show that glucose deprivation and modulators of respiratory chain Complex I synergize in inducing cancer cell death.

Results

Complex I inhibition by rotenone enhances cancer cell death in glucose deprivation

MDA-MB-231 human breast cancer cells, like several other cancer cells, are dependent on glycolysis for their proliferation and survival (see **chapter 3** and Gaglio *et al.*, 2011) and in low glucose availability they undergo the reduction of proliferation and, ultimately, die. Nevertheless, mitochondria could cover an important role also in these cells, for example participating to energy production in a minimal but relevant amount, mainly in specific conditions, and contrasting apoptotic stimuli. In this scenario, we tested the ability of rotenone, a natural inhibitor of respiratory chain Complex I (Benard *et al.*, 2007), to increase sensitivity of MDA-MB-231 cells to glucose depletion. In order to evaluate the effects of OXPHOS inhibition on the cells we treated proliferating MDA-MB-231 cells, grown for 48 hours in low (1 mM) or high glucose (25 mM), with rotenone for 4 hours. The treatment was executed at 48 hours of culture because, despite a comparable proliferation rate in the two different glucose concentrations (see **chapter 3, figure 14A**), in low glucose condition external medium analysis indicated that this carbon source was almost completely depleted at this time point (**figure 1**).

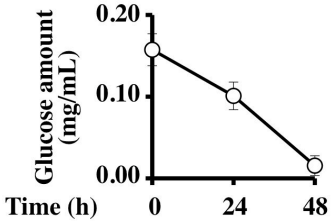

Figure 1. Glucose amount in medium of cells cultured in 1 mM glucose was measured using enzymatic kit at indicated time points. Data represent the average of at least three independent experiments (± s.d.).

Short treatment with a low concentration of rotenone (3 nM for 4 hours), in glucose-depleted condition induced a reduction of cell viability. In fact treated cells appeared circle and floating, as typical for dead cells (**figure 2A**), and Trypan Blue viable cell count showed an increase of mortality in treated sample (**figure 2B**). Such detrimental effect was associated with a rotenone-induced decrease of intracellular ATP and mitochondrial potential levels (**figure 2C** and **2D)**, confirming the direct effect of the treatment on mitochondrial function.

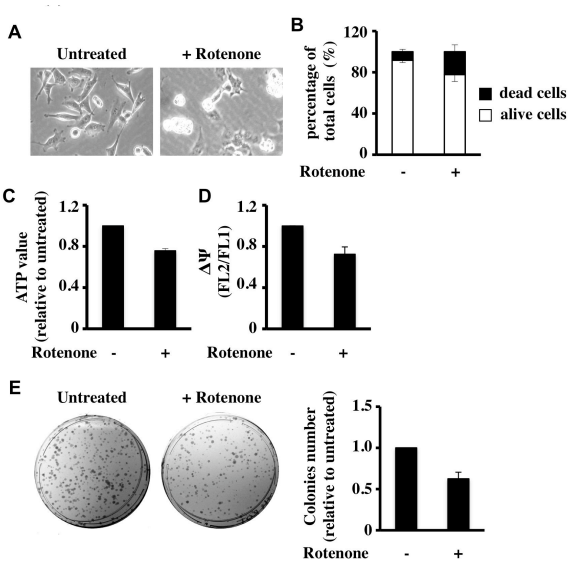

Figure 2. Rotenone enhances MDA-MB-231 citotoxicity in condition of glucose deprivation. A-E. MDA-MB-231 cells cultured 1 mM glucose were treated for 4 hours with 3 nM rotenone at 48 hours of culture. After treatment different parameters were investigated in untreated (-) and treated (+) cells: cell morphology through optical microscopy images **(A)**, viable cell count performed by using Trypan Blue staining **(B)**, intracellular ATP levels **(C)**, mitochondrial potential (ΔΨ) indicated as ratio of mean fluorescence FL2 on mean fluorescence FL1 as described in chapter 2, materials and methods **(D)**. In addition, after treatment, $3x10^3$ cells were also plated in normal growth medium for clonogenic assay and after ≥12 days colonies were stained (left images) and counted (right histogram) **(E)**. All data represent the average of at least three independent experiments (± s.d.).

Cytotoxic effect of rotenone in glucose deprivation was further supported by a clonogenic assay (**figure 2E**), which showed that treated cells, re-plated in high glucose condition (25 mM), formed less colonies (about 50% of reduction) as compared to untreated control.

Importantly, rotenone treatment in non-limiting glucose condition had no effect on cell survival (**figure 3A-D**) and on intracellular ATP levels (**figure 3E**), indicating that in high glucose availability ATP is generated essentially by glycolysis. Such limited effect is reflected also on mitochondrial potential (**figure 3F)**.

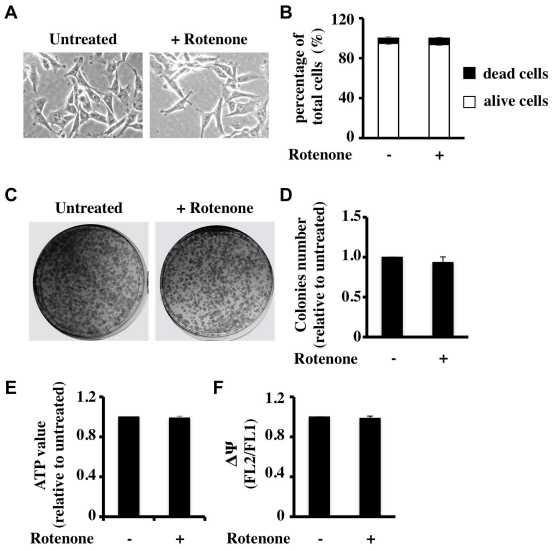

Figure 3. In high glucose MDA-MB-231 cells are insensitive to rotenone. Morphological analysis (**A**), viable cell count **(B)**, clonogenic assay **(C-D**) and intracellular ATP (**E**) and mitochondrial potential **(ΔΨ**, **F)** measurement were performed in cells grown for 48 hours in 25 mM glucose and treated with rotenone as in low glucose (figure 2). All data represent the average of at least three independent experiments (± s.d.).

Under glucose depletion combined treatment with Complex I inhibitors and forskolin increases cytotoxicity of K-ras-transformed cells

In the last year, it has been shown that inducing OXPHOS in cancer cells, for example by inhibition of PDK-1, leads them towards apoptosis (Bonnet *et al.*, 2007). Therefore it has been supposed that induction of a reversion of the Warburg effect, through OXPHOS activity enhancement and glycolysis inhibition, coupled to a treatment able to interfere with mitochondrial activity could specifically kill cancer cells at high rate. In this regard, previously we have shown that exogenous activation of PKA pathway, obtained through the treatment with forskolin (FSK, an activator of adenylyl cyclase), can improve specifically cancer cell mitochondrial activity, especially by restoration of Complex I function (see **chapter 3**). Therefore, we sought to investigate whether the combination of rotenone and FSK in glucose-depleted cells could synergistically enhance the killing of cancer cells. We treated MDA-MB-231 cancer cells, grown in low glucose, with such compounds alone or in combination. Combined treatment increased MDA-MB-231 cell death as compared to either untreated and or rotenone alone, as demonstrated by cell count (**figure 4A**) and PI/Annexin V assay (**figure 4B**). Such an increase of cell death was especially associated with reduction of ATP levels (40% less than control sample) and mitochondrial potential (less 20%) (**figure 4C and 4D**). Importantly, the combined treatment further reduced cancer cell ability to form colonies in a clonogenyc assay as compared to rotenone alone (**figure 4E**).

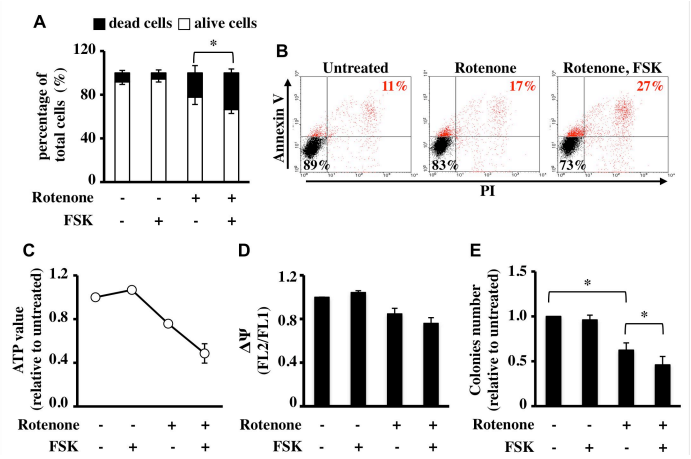

Figure 4. FSK treatment enhances the viability loss induced by rotenone alone in MDA-MB-231 cells. MDA-MB-231 cells were cultured in 1 mM glucose and treated with 3 nM rotenone, 10 μM FSK or both molecules at 48 hours of culture. Cells were pre-treated for 1 hour with FSK and then rotenone was also added for 4 hours. After treatment different parameters were investigated in untreated (-) and treated (+) cells. Viable cell count was performed using Trypan Blue **(A)**. Cell viability was also evaluated staining cells with Propidium Iodide (PI) and Annexin V-FITC; representative profiles are shown **(B)**. Intracellular ATP levels **(C)** and mitochondrial potential **(ΔΨ, D)** were measured. After treatment $3x10^3$ cells were also plated in normal growth medium for clonogenic assay and after ≥12 days colonies were stained and counted as reported in the histogram **(E)**. All data represent the average of at least three independent experiments (± s.d.); *p<0.05 (Student's *t-test*).

We performed the same analysis on NIH3T3 mouse fibroblasts (Normal cells), and NIH3T3 mouse fibroblasts expressing an oncogenic *K-RAS* gene (Transformed cells) to investigate whether the synergistic effect of rotenone and FSK in killing cancer cells had also detrimental effects on normal cells. The cells grown for 72 hours in both high and low glucose were incubated with rotenone and FSK alone or in combination. In non-limiting glucose condition rotenone had no effect on proliferation of both cell lines, confirming that such a low rotenone concentration does not inhibit mitochondrial respiration of Normal

cells (**figure 5A**) and does not induce cell death in mouse Transformed cells (**figure 5B**), as previously observed in human cancer cells.

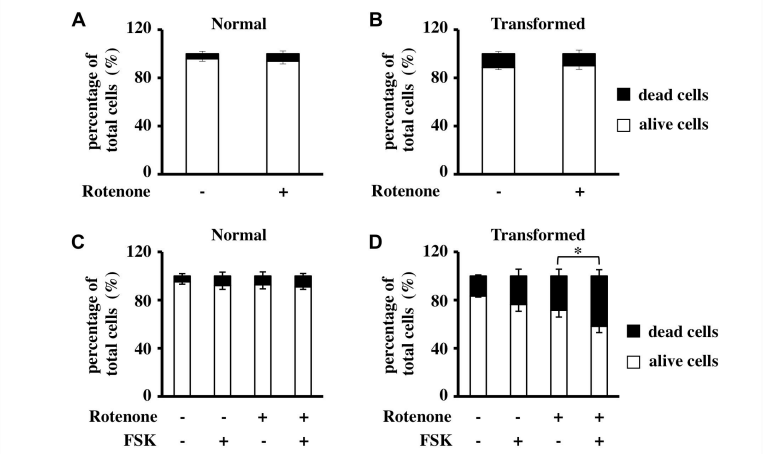

Figure 5. Normal cells are less sensitive to rotenone treatment than Transformed cells. Viable cell count using Trypan blue was performed after treatment with rotenone at 72 hours of culture in different growth conditions. **A-B.** NIH3T3 Normal **(A)** and Transformed **(B)** cells were cultured in 25 mM glucose and counted after 4 hours treatment with 3 nM rotenone. **C-D.** Normal **(C)** and Transformed **(D)** cells were cultured in 1 mM glucose and treated with 3nM rotenone, 10 μM FSK or both molecules. For the combined treatment, cells were pre-treated for 1 hour with FSK and then rotenone was also added for 4 hours. After treatment cell count was performed. All data represent the average of at least three independent experiments (± s.d.); *$p<0.05$ (Student's *t-test*).

On the contrary, cells grown in low glucose for 72 hours, time point at which both cell lines have completely consumed the glucose present in the culture medium (see **chapter 3, figure 9A-B**) showed a different response to rotenone and FSK. Normal cells were founded to be insensitive to rotenone either alone or in combination with FSK (**figure 5C**). In contrast, Transformed cells appeared to be sensitive to the treatment with rotenone (29% of cell death compared to 17% on untreated sample). FSK enhanced cytotoxic effect of Complex I inhibitor, in fact sample treated with the two combined molecules showed a

significant increase of cell death (42%) in comparison to untreated and only rotenone-treated samples (**figure 5D**).

To further confirm the role of Complex I in the cell death mechanism upon glucose depletion, we treated MDA-MB-231 cells also with two other inhibitors of this complex, namely piericidin A and capsaicin (Okun *et al.*, 1999). Both molecules inhibit Complex I binding the ubiquinone-binding site, although in different points, and are natural compounds. In fact, piericidin A is an antibiotic isolated from *Streptomyces* sp. while capsaicin is the active component of chilli peppers, plants belonging to the genus *Capsicum*.

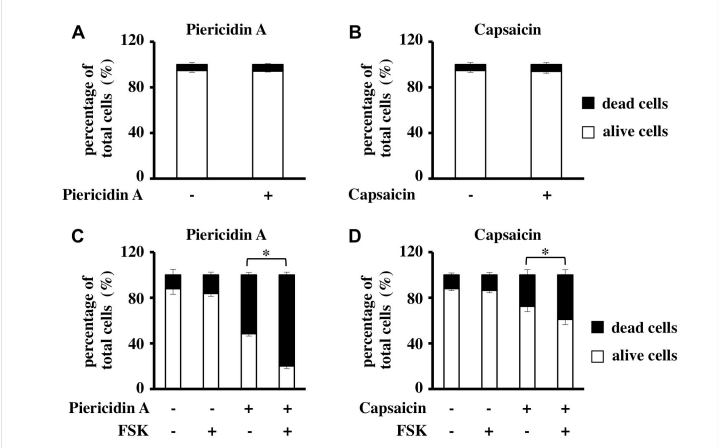

Figure 6. The two inhibitors of mitochondrial Complex I, Piericidin A and capsaicin, induce effects similar to rotenone in MDA-MB-231 cells. Viable cell count using Trypan blue was performed after treatment with 5 nM piericidin A or 100 μM capsaicin at 48 hours of culture in different growth conditions. **A-B.** MDA-MB-231 cells were cultured in 25 mM glucose and counted after 2 hours treatment with piericidin A **(A)** or capsaicin **(B)**. **C-D.** MDA-MB-231 cells were cultured in 1 mM glucose and treated with piericidin A **(C)** or capsaicin **(D)**, 10 μM FSK or FSK together with complex I inhibitors. In the last case, cells were pre-treated with FSK for 1 hour and then piericidin A **(C)** or capsaicin **(D)** were added for 2 hours. After treatment cell count was performed. All data represent the average of at least three independent experiments (± s.d.); *p<0.05 (Student's *t-test*).

As previously observed with rotenone both inhibitors did not induce cell death in MDA-MB-231 grown in high glucose. On the contrary, their addition in glucose-depleted cells led to an increase of MDA-MB-231 cell death that was much stronger in the samples treated with piericidin A (**figure 6C)** than with capsaicin (**figure 6D**). Notably, combined treatment with FSK further increased the percentage of cell death (**figure 6C-D**).

Altogether these findings indicate that, upon glucose depletion, stimulation of respiratory chain activity by FSK makes cancer cells more sensitive to Complex I inhibitors.

Chapter 5

Results (III)

CHAPTER 5. RESULTS (III)

Prolonged glucose deprivation induces cell death in *K-ras*-transformed cells by interfering with Hexosamine Biosynthesis Pathway and activating the Unfolded Protein Response

In the previous chapters it has been shown the role of the mitochondrial dysfunctions in cancer cell death under glucose deprivation. In particular, alterations of cAMP/PKA pathway, ATP depletion and ROS accumulation have been shown to have an important role in such a process. This observation, especially about the involvement of cAMP/PKA pathway, has opened new scenario for innovative anticancer therapies. Nevertheless, other processes may be associated and contribute to glucose deprivation-induced transformed cell death. Since it is relevant to exploit the mechanisms underlying these biological responses to achieve new anticancer therapies, we sought to identify them by using transcriptome and proteome analysis applied to mouse NIH3T3 fibroblasts harboring an oncogenic *K-RAS* gene (Transformed cells), compared to NIH3T3 Normal cells. Noteworthy, the analysis, performed in high and low glucose culture, indicated that reduction of glucose availability induces, especially in Transformed cells, a significant increase in the expression of several hallmarks genes of the Unfolded Protein Response (UPR). The critical role of this response in both cell survival and death led us to investigate about a link between Transformed cell death upon glucose deprivation and UPR. The full elucidation of this response could be relevant to design a new therapeutic strategy.

Results

Transcriptomic and proteomic analyses identified ER-stress as critical process in Transformed cells grown in low glucose

To investigate specific glucose deprivation-induced cell death mechanisms in Transformed cells, a time-course transcriptional analysis (between 0 and 72 hours of culture) was performed in Normal and Transformed NIH3T3 cells grown under optimal condition (HG, 25 mM as initial glucose concentration in the growth medium) or under glucose limiting condition (LG, 1 mM).

Specifically, genes, whose expression levels changed between 0 and 72 hours of culture, were identified and analyzed. In Normal cells in HG, among the most significant pathways, several wide-ranging cellular processes were identified, such as that associated to DNA, RNA and protein metabolism, signaling pathways and cell cycle regulation. In the same growth condition, few pathways in Transformed cells were identified. Pathway analysis in LG growth indicated a different response to glucose depletion of the two cell lines. In particular, in Normal cells in LG the enriched pathways were almost the same observed in HG. Conversely, Transformed cells in LG showed enrichment of specific pathways involved in cell remodeling (i.e., Focal adhesion, Cytoskeletal regulation by Rho GTPase), cell metabolism (i.e., Cholesterol biosynthesis, Biosynthesis of unsaturated fatty acids) and p53 related signaling. In addition, also a large number of genes encoded for proteins involved in ER-stress response (protein processing in endoplasmic reticulum) were identified.

The two cell lines grown in HG and LG for 72 hours were also subjected to proteomic analysis, through 2-D difference gel electrophoresis (2-DIGE), coupled with Mass Spectrometry (MS). Comparing the two cell lines, both in HG and LG, it was observed that the differentially expressed proteins were

involved in glycolysis, protein folding and synthesis and stress response. In particular, the latter process was more significant in Transformed sample in LG since the proteins resulted either specific (i.e., HSP90B1, PSMA1 and PRDX6) or more largely expressed (i.e., ESD, GSTO, SOD2 and PRDX1) in this condition, confirming the activation of a stress response under glucose depletion.

Since the two analyses identified cellular processes associated to protein folding, cellular stress and ER-stress, all the mRNA that could be involved in different form in ER-stress response were identified in the transcriptional profiles. The analysis allowed the identification of 57 genes encoding for proteins more strictly associated to ER function upon stress and 59 UPR responsive genes, encoding for proteins regulating Survival, Cell Death and other cellular processes indicated as Miscellaneous. The 57 mRNAs (colored ellipses) were used to generate a ER network (**figures 1A and 1B**) composed of five key functional ER response sub-networks, shown in the **figure 1** as dotted line boxes, namely Translational/Translocation, Unfolded Protein Binding, Quality Control, ER Associated Degradation and Translocation Block respectively. The networks indicated that the ER-stress response was activated in cells grown in LG (**figure 1A**), since in HG (**figure 1B**) the vast majority of these mRNAs appeared to be expressed at normal levels (yellow and light green color). Noteworthy, Transformed cells grown in LG as compared to Normal cells showed a significant number of up-regulated mRNAs (red color) that were, for instance, mainly involved in reducing the loading of misfolded proteins and/or increasing folding activity (**figure 1A**).

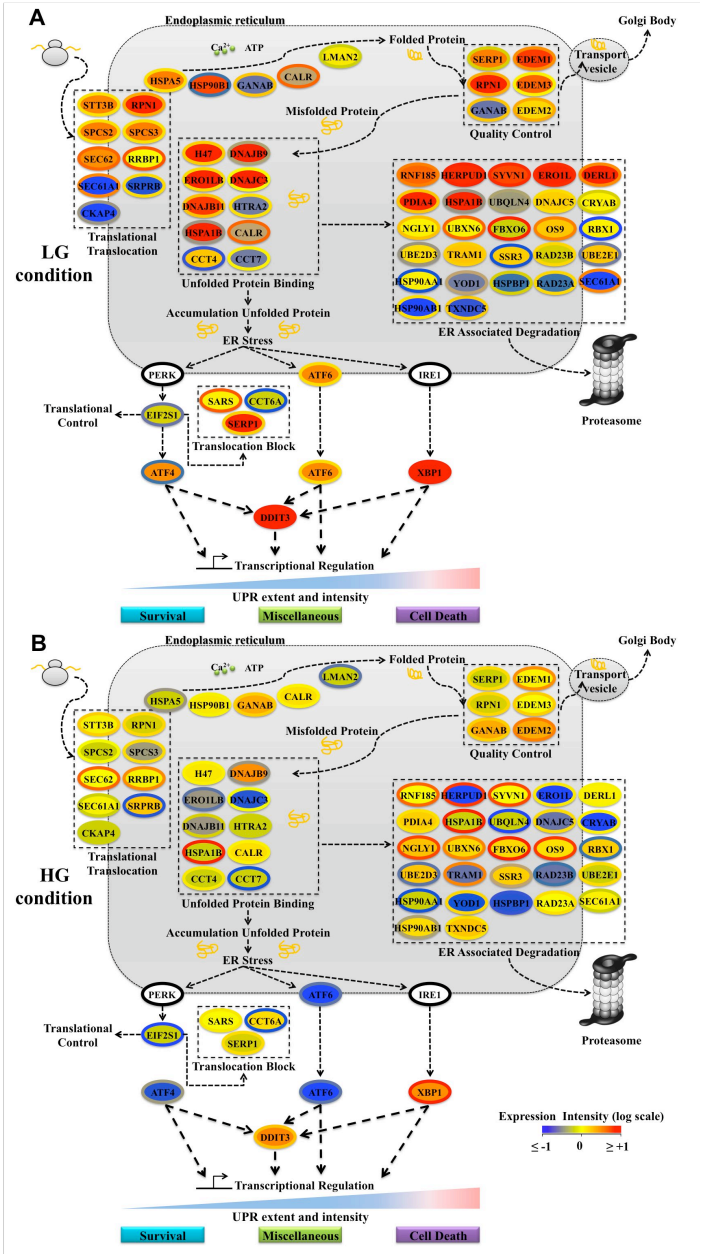

Figure 1. ER networks for Normal and Transformed cells grown in LG (A) and in HG (B), derived by using mRNA expression data at 72 hours.

Each mRNA is represented by a colored ellipse; in particular, the external ellipse represents Normal cell data and the internal ellipse represents Transformed cell data. Changes in gene expression levels are represented by a color log scale from red (high expression) to blue (low expression). Unchanged levels of expression (yellow) are considered for expression values between -0.5 and 0.5. The double colored triangle below the regulated processes indicates the relation between time and intensity of ER-stress and effect on cell homeostasis (blue as survival, red as death). *From the elaboration of transcriptional data performed by Chiara Balestrieri.*

To prove the transcriptional up-regulation of the UPR observed in the Affymetrix GeneChip data, we assessed the expression of eight UPR target genes (Grp78, Atf4, XBP1, CHOP, CAR6, Trb3, GADD34 and PDIa3) at 72 hours of culture both in HG and LG.

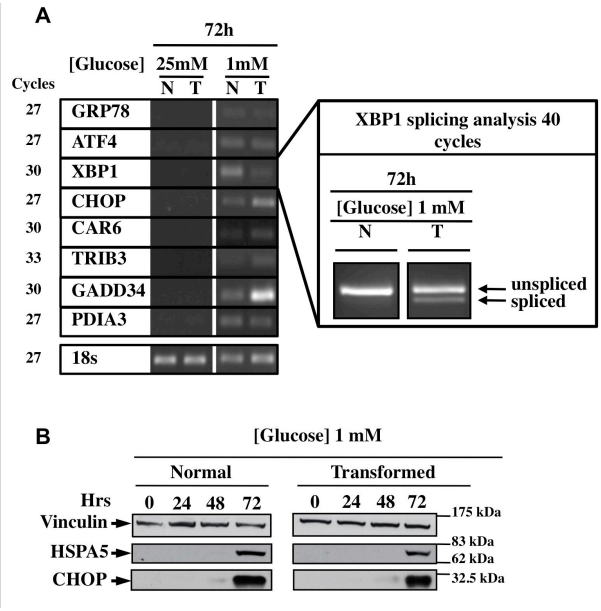

Figure 2. Semi-quantitative RT-PCR and Western blot analysis indicated that UPR is activated in LG. (A) Semi-quantative RT–PCR of the mRNAs specific for different UPR-related gene in Normal (N) and Transformed cells (T) at 72 hours of culture in HG and LG. **(B)** Western blot analysis of UPR activation upon glucose depletion. To follow UPR activation the expression of Grp78 and CHOP proteins was analyzed. As loading control the expression of Vinculin was analyzed. Figures are representative of three independent experiments.

Both cell lines showed an increase in expression of these genes only in LG and not in HG (**figure 2A**), confirming data from microarray assay. Interestingly, the presence of ER stress-induced splicing of XBP1 (X box-binding protein 1) was detectable only in Transformed cells (**figure 2A, right box**).

Also Western blot analysis was performed, monitoring Grp78 and CHOP protein levels, as early and later UPR activation hallmarks. As expected, the expression of the two proteins was elevated in LG at 72 hours of culture (**figure 2B**), while there was no evidence of expression of UPR proteins in cells grown in HG (**figure 3**).

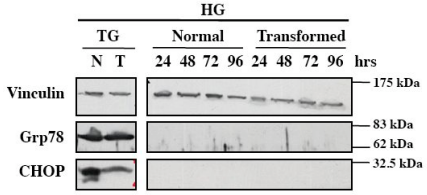

Figure 3. UPR is not activated in HG. Western blot analysis of UPR activation, through Grp78 and CHOP detection, was performed for Normal and Transformed cells grown at HG. As loading control the expression of Vinculin was analyzed. As control of UPR activation Normal and Transformed cells were treated with Thapsigargin (TG) that induces Ca^{2+} release from ER stores to the cytosol and activates UPR. Figure is representative of at least three independent experiments.

Attenuation of protein translation or increase of cell folding capacity reduce UPR activation and transformed cell death

Normal and Transformed cells grown in LG were subjected to treatments with cycloheximide (CHX), a known protein synthesis inhibitor, or 4-Phenyl butyrate (4-PBA), a chemical chaperone, at 72 hours of culture, in order to analyze the effect at 96 hours, when Transformed cells in low glucose normally die. As shown in **figures 4 and 5**, both molecules rescued Transformed cells from death in LG for 24 (**figures 4B-C and 4F-G**) or for 48 hours (**figures 5B-C**). The treatments did not affect Normal cells growth (**figures 4A and 4E**; **figure 5A**).

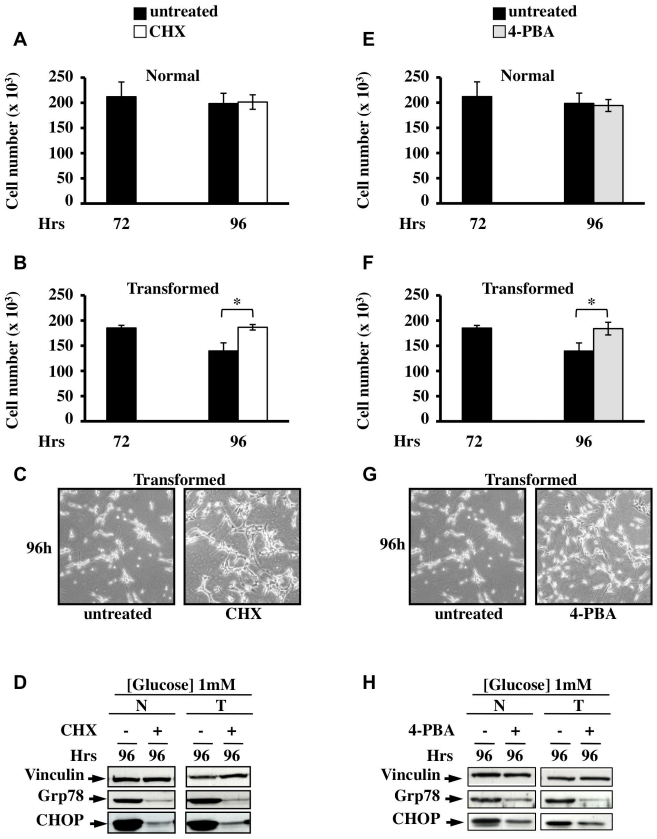

Figure 4. Attenuation of UPR by cycloheximide or Sodium 4-Phenylbutyrate protects Transformed cells from death. Cell death and UPR activation, after 24 hours of treatment with cycloheximide (CHX; **A-D**) or Sodium 4-Phenylbutyrate (4-PBA; **E-H**), were analyzed in Normal and Transformed cells grown at LG for 72 hours. The cells were counted at 72 and 96 hours of culture, after treatment for 24 hours with CHX (**A, B**) or 4-PBA (**E, F**). Data represent the average of at least three independent experiments (± s.d.); *p<0.01 Student's t-test. Phase contrast microscopy images were collected for untreated and treated (+CHX, **C**; +4-PBA, **G**) Transformed cells at 96 hours of culture. UPR activation upon CHX (**D**) and 4-PBA (**H**) treatments was followed through the expression analysis of Grp78 and CHOP proteins. As loading control the expression of Vinculin was analyzed. Figures are representative of three independent experiments.

Noteworthy, Western blot analysis of CHX and 4-PBA treated samples as compared to control (**figure 4D and 4H**) showed a strong reduction of Grp78

and CHOP protein expression, confirming the role of ER stress in glucose-dependent transformed cell death.

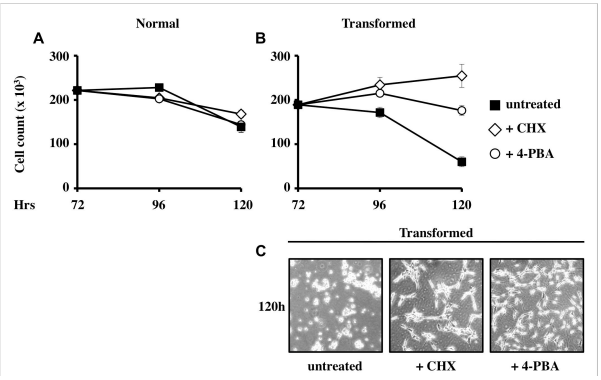

Figure 5. Cycloheximide or Sodium 4-Phenylbutyrate protect Transformed cells from death for a long time. Cell response to 48 hours of treatment with cycloheximide (CHX) or Sodium 4-Phenylbutyrate (4-PBA) was analyzed in Normal (**A**) and Transformed (**B, C**) cells grown at LG. The cells were treated once with the two molecules at 72 hours of culture and counted at indicated time points. Data represent the average of at least three independent experiments (± s.d.). Phase contrast microscopy images (**C**) were collected for untreated and treated (+CHX, +4-PBA) Transformed cells at 120 hours of culture.

Glucose deprivation induces JNK mediated cell death specifically in Transformed cells

The UPR relieves the ER stress by several mechanisms (Hetz, 2012), however, when the ER stress is prolonged or the adaptive response fails, cells undergo apoptosis or necrosis (Gorman *et al.*, 2012; Jager *et al.*, 2012). Among the different mechanisms activated by UPR to induce cell death, there is the activation of c-Jun NH2-terminal kinase (JNK) through the IRE1 kinase/XBP1 UPR branch (Urano *et al.*, 2000). Since previously we showed that glucose deprivation induced the splicing of XBP1 specifically in Transformed cells, we decided to explore a possible role of JNK activation in glucose deprivation-induced cell death. Therefore, we measured the JNK phosphorylation status,

indicative of its activation, along a time-course upon glucose deprivation. We observed that JNK phosphorylation especially increased in Transformed cells as compared to Normal cells (**figures 6A and 6B**). Importantly, its inhibition, obtained by treatment with the specific inhibitor SP600125, induced Transformed cell survival in glucose deprivation (**figures 6E-F**). No effect was observed in Normal cells (**figures 6C-D**).

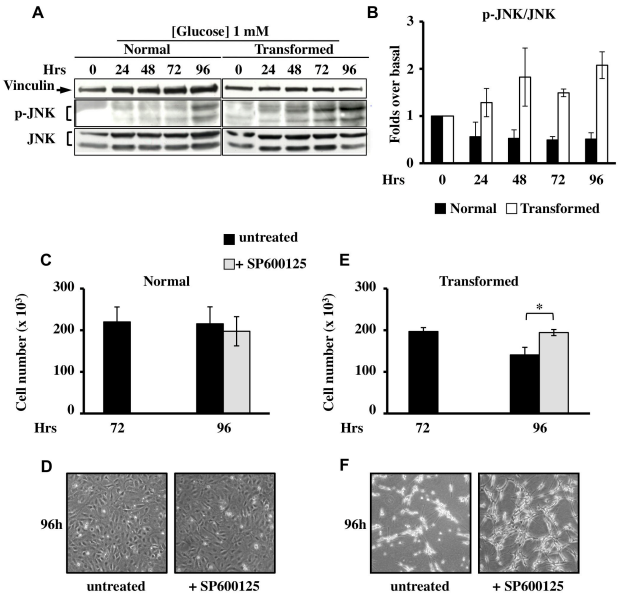

Figure 6. JNK inhibition induces survival in Transformed cells grown at LG. (**A**) For JNK expression analysis, Normal and Transformed cells, grown at LG, were collected at indicated time points and total cellular extracts were subjected to SDS-PAGE followed by Western Blot analysis with antibodies anti phospho-JNK Thr183/Tyr185 (p-JNK) and total JNK. As loading control the expression of Vinculin was analyzed. (**B**) Quantitative analysis of JNK phosphorylation status was performed by densitometric analysis of Western blot films. The values obtained for p-JNK were normalized to the corresponding total JNK values and plotted as fold changes over basal (sample 0h=1). Normal (**C**) and Transformed (**E**) cells, grown at LG, were counted at 72 and 96 hours of culture upon 24 hours-treatment with the JNK inhibitor, SP600125. Phase contrast microscopy images were collected for untreated and treated Normal (**D**) and Transformed (**F**) cells at 96 hours of culture. All data represent the average of at least three independent experiments (± s.d.); *$p<0.01$ Student's t-test.

These findings indicated that JNK activation by UPR plays a role in glucose deprivation-induced Transformed cell death.

N-Acetyl-D-glucosamine attenuates UPR activation and protects Transformed cells from death induced by glucose deprivation

Since glucose deprivation induced the expression of several UPR hallmarks, especially in Transformed cells, we sought to determine whether this activation was a consequence of a reduced flux of Hexosamine Biosynthesis Pathway (HBP) and hence a reduction of N- and O-protein glycosylation that ultimately may bring to unfolded protein accumulation (Mitra *et al.*, 2006; Romero-Fernandez *et al.*, 2011). We assayed Normal and Transformed cells for alterations in protein O-GlcNAcylation, as marker of HBP flux reduction, in response to changes in glucose concentration (**figure 7**).

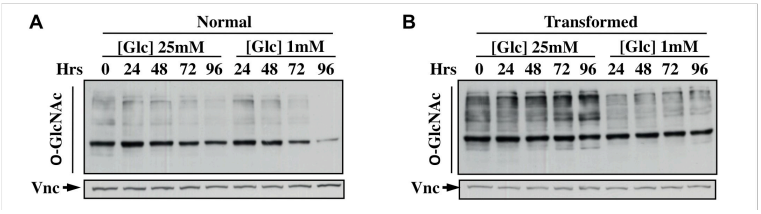

Figure 7. N-Acetyl-D-glucosamine protects Transformed cells from glucose depletion dependent cell death. Normal (**A**) and Transformed (**B**) cells, grown at HG and LG, were subjected to Western Blot analysis with anti O-glycosylation antibody (O-GlcNAc). As loading control the expression of Vinculin and Ponceau staining (data not shown) were analyzed. Image is representative of three independent experiments.

Normal cells presented a time-dependent decrease of O-GlcNAc protein modification levels, more evident in cells grown in LG (**figures 7A and 7C**). Noteworthy, Transformed cells showed in both glucose concentrations and at all analyzed time points a higher level of O-GlcNAc as compared to Normal cells, confirming previous evidence (Ying *et al.*, 2012). Besides, a severe reduction of

total O-GlcNAc post-translational modification in LG was observed (**figures 7B and 7D**). These data indicated that in Transformed cells, and in lower extend in Normal cells, the levels of O-GlcNAc are dependent on glucose availability.

Hence, we evaluated whether the addition of N-Acetyl-D-glucosamine (GlcNAc), which can enter HBP downstream to entry point of glucose, affected ER stress-induced Transformed cells death under glucose depletion (**figure 8**).

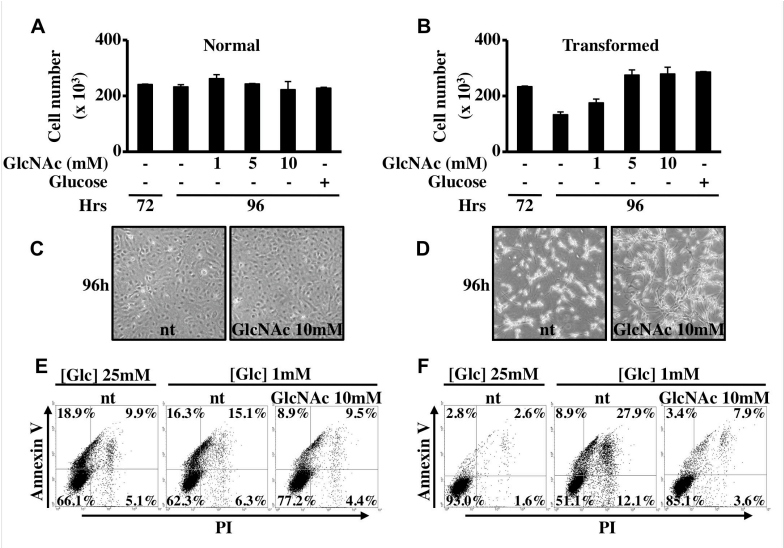

Figure 8. N-Acetyl-D-glucosamine protects Transformed cells from glucose depletion dependent cell death. Normal **(A)** and Transformed (**B**) cells, grown at LG, were counted at 72 and 96 hours of culture upon 24 hours-treatment with different concentrations of N-Acetyl-D-glucosamine (GlcNAc) or 1 mM glucose (Glc). Data represent the average of at least three independent experiments (± s.d.). Microscopy images were collected for Normal (**C**) and Transformed (**D**) cells treated and not treated with 10 mM GlcNAc. (**E-F**) FACS analysis of Annexin-V plus PI labeled Normal (**E**) and Transformed (**F**) cells, grown in HG (left panels), LG (middle panels) and LG + 10 mM GlcNAc (right panels). Figures are representative of three independent experiments.

In particular, this addition could allow us to ascertain whether stimulation of HBP was sufficient to promote UPR attenuation and cell survival. To confirm that GlcNAc enters HPB, we evaluated the O-GlcNAcylation protein status after

treatment with O-GlcNAc. Both cell lines presented a GlcNAc concentration-dependent change of O-glycosylation pattern (**data not shown**). Treatment with GlcNAc between 72 and 96 hours rescued Transformed cell survival in dose-dependent manner (**figures 8B and 5D**). Notable, a single treatment with GlcNAc, prolonged Transformed cells survival until 120 hours of culture (**data not shown**). Remarkable, GlcNAc treatment did not affect Normal cell number (**figures 8A and 8C**), further suggesting the ability of Normal cells to re-program their metabolism in order to cope alterations of HBP flux as well as ER-stress. Moreover, Annexin V plus PI staining (**figures 8E and 8F**) showed that in response to GlcNAc both cell lines displayed a decrease of apoptotis, that was more consistent in Transformed cells, since the percentage of alive cells appeared almost similar to that observed in cells grown in HG.

In addition, in both cell lines, a dose-dependent effect of GlcNAc on the expression of Grp78 and CHOP was observed (**figures 9A and 9B**).

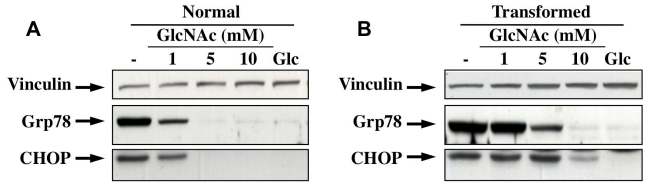

Figure 9. N-Acetyl-D-glucosamine attenuates UPR activation. UPR activation after N-Acetyl-D-glucosamine (GlcNAc) or glucose (Glc) treatment was followed through the expression analysis of Grp78 and CHOP proteins in Normal (**A**) and Transformed (**B**) cells. As loading control the expression of Vinculin was analyzed. Figures are representative of three independent experiments.

Importantly, glucose re-addition induced the same effects as GlcNAc, confirming its fundamental role as main substrate for HBP flux and protein folding (**figures 8A and 8B; figures 9A and 9B**, Glc samples).

To confirm the previous evidence (Wellen *et al.*, 2010) that GlcNAc can fuel HBP without contributing significantly to glycolysis, we treated Transformed cells with 10 mM GlcNAc combined to 5mg/mL oxamate, a glycolytic inhibitor (Wilkinson and Walter, 1972) (**figure 10**).

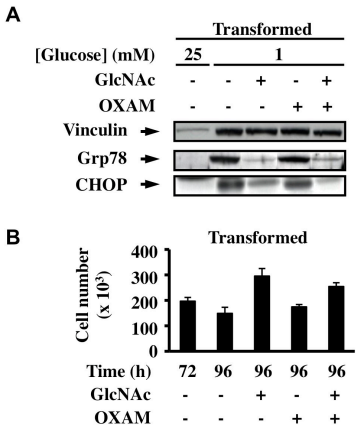

Figure 10. Oxamate does not influence protective role of N-Acetyl-D-glucosamine. (**A**) UPR activation was followed through the expression analysis of Grp78 and CHOP proteins in Transformed cells at 96 hours of culture, 24 hours after N-Acetyl-D-glucosamine (GlcNAc) or/and oxamate (OXAM) treatment. As loading control the expression of Vinculin was analyzed. Figure is representative of three independent experiments. (**B**) Transformed cells, grown at LG, were counted at 72 and 96 hours of culture upon 24 hours-treatment with GlcNAc or/and OXAM. Data represent the average of at least three independent experiments (± s.d.).

As shown in **figure 10**, oxamate did not affect protective role of GlcNAc on Transformed cells, both as cell viability (**figure 10A**) and UPR activation (**figure 10B**).

UPR attenuation by N-Acetyl-D-glucosamine protects also glycolytic human cancer cells from glucose-dependent apoptosis

Our findings indicated that glucose deprivation, leading to a reduction of HBP flux, induces UPR activation, most likely as consequence of accumulation of

unfolded proteins, and hence cell death. In order to evaluate whether this mechanism was also effective in a glucose-addicted human cancer cell line, namely MDA-MB-231, we tested UPR activation in these cells grown for 96 hours in LG, as compared to HG (**figure 11**).

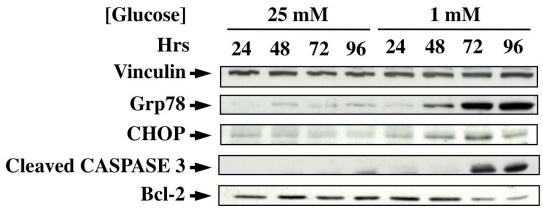

Figure 11. Glucose deprivation induces apoptosis in human cancer cells MDA-MB-231. Western blot analysis of UPR and cell death activation in MDA-MB-231 grown at HG and LG. To follow the UPR and cell death processes, the expression levels of Grp78 and CHOP as well of cleaved Caspase 3 and Bcl-2 were analyzed, respectively. As loading control the expression of Vinculin was evaluated. Figure is representative of three independent experiments.

As shown in **figure 11**, Grp78 and CHOP protein levels increased only in LG, in correlation with the complete glucose depletion from culture medium (at 48 hours of culture, see **chapter 3, figure 1**). In association, caspase-3 activation as well as Bcl-2 reduction were observed, indicating that glucose depleted cells were progressing to apoptotic cell death.

We next treated MDA-MB-231 cells grown in LG with SP600125. Since an early activation of UPR was observed in these cells, we decided to treat the cells between 48 and 72 hours of culture. JNK inhibition induced an increase of cell survival (**figures 12A and 12B**), associated with a significant decrease of Caspase-3 activation (**figure 12C**), confirming the role of UPR in mediating MDA-MB-231 cell death.

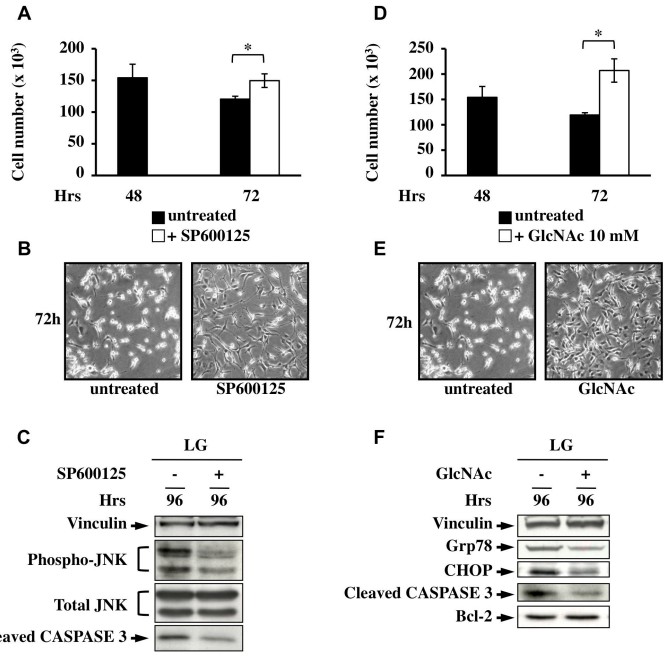

Figure 12. Glucose addicted human cancer cells are protected from cell death by N-**Acetyl-D-glucosamine and JNK inhibitor.** MDA-MB-231 cell survival was analyzed by counting the cells, grown at LG for 72 hours and after treatment with SP600125 (**A**) or 10 mM N-Acetyl-D-glucosamine (GlcNAc, **D**). Data represent the average of at least three independent experiments (± s.d.); *$p<0.01$ Student's t-test. Phase contrast microscopy images were collected for untreated and treated (+SP600125, **B**; +GlcNAc, **E**) cells at 72 hours of culture. (**C**) JNK inhibitor effect on cell survival was followed by western blot analysis of JNK phosphorylation, as control, and Caspase 3 activation. (**F**) UPR activation and cell death, at LG and upon GlcNAc treatment, were followed through the expression analysis of Grp78, CHOP, cleaved caspase-3 and Bcl-2. Figures are representative of three independent experiments.

Finally, we evaluated the effect of GlcNAc addition to cells in LG. GlcNAc increased cell survival (**figures 12D and 12E**) and led to a clear decrease of the two UPR markers and of Capsase-3 activation as well as a slightly increase of Bcl-2 expression (**figure 12F**), confirming that the treatment was able to attenuate UPR and protect cells from apoptosis.

Chapter 6

Results (IV)

CHAPTER 6. RESULTS (IV)

Energy metabolism characterization of a novel cancer stem cell-like line 3AB-OS

Cancer stem cells (CSCs) have a central role in driving tumor growth. Since metabolism is becoming an important diagnostic and therapeutic target, characterization of CSC line energetic properties is an emerging need. Embryonic and adult stem cells, compared to differentiated cells, exhibit a reduced mitochondrial activity and a stronger dependence on aerobic glycolysis. Here, we aimed to comparatively analyze bioenergetics features of the human osteosarcoma 3AB-OS CSC-like line, and the parental osteosarcoma MG63 cells, from which previously 3AB-OS cells have been selected.

We used different cultural approaches to investigate and primarily characterize the metabolic feature of 3AB-OS as compared to MG63. In particular, as previously described, glucose deprivation conditions can unmask peculiar metabolic mechanisms and weaknesses of a specific cell lines. Moreover, although 3AB-OS CSCs, as well as osteosarcoma parental cells MG63, do not present oncogenic mutations of *KRAS*, it has been observed that 3AB-OS present enhanced expression of MAPK pathway components and of HIF-1α (Di Fiore *et al.*, 2012a; Di Fiore *et al.*, 2009), suggesting that they could be very similar to "glucose addicted" *K-ras*-transformed cells. In this scenario, investigation of their metabolism could result of high interest.

Results

3AB-OS cancer stem cells are strongly dependent on glucose but not glutamine availability for cell proliferation and survival

Cancer cells are more susceptible, in terms of proliferation and cell death, to glucose (Glc) or glutamine (Gln) withdrawal as compared to normal counterparts (Chiaradonna *et al.*, 2006a; Yuneva *et al.*, 2007). Thus, we decided to analyze cell proliferation of the MG63 and 3AB-OS cell lines in different initial glucose and glutamine concentrations: normal glucose and glutamine condition (25 mM Glc plus 4 mM Gln); low glucose condition (1 or 0.25 mM Glc plus 4 mM Gln); low glutamine condition (25 mM Glc plus 0.5 mM Gln). Although glucose withdrawal halted proliferation in both cell lines, as shown by cell counting (**figures 1A and 1B**), it induced specifically cell death in 3AB-OS cells. In fact, microscopy observation showed floating rounded 3AB-OS cells upon glucose depletion (**figure 1C**); this observation was confirmed by Trypan Blue vital stain (**figures 1D and 1E**) and Annexin-V/PI staining followed by FACS analysis (**figures 1F and 1G**). In particular, the latter analysis, performed at 72 hours of culture in low glucose, indicated an about 3-fold increase of percentage of cell death in 3AB-OS cells as compared to MG63 (42.3% *vs.* 13.5% of cells both PI and Annexin V positive). In addition, such an increase was glucose-dependent only in 3AB-OS cells, since the percentage measured at normal glucose was 11.1% in 3AB-OS cells and 6.1% in MG63 cells.

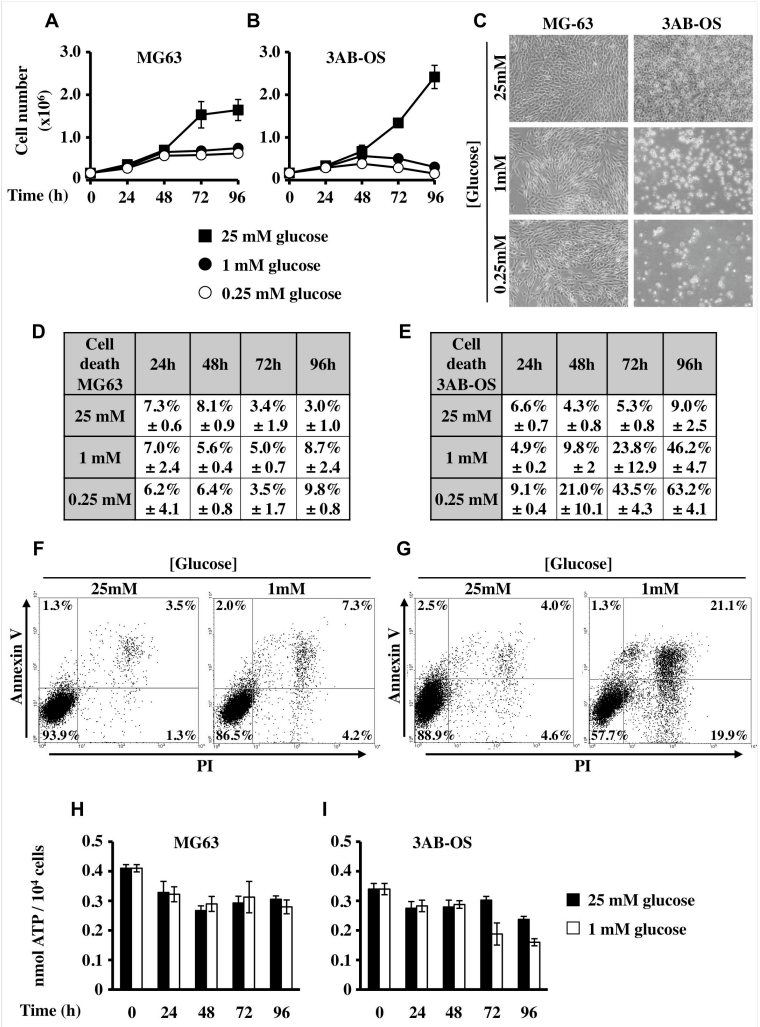

Cell death MG63	24h	48h	72h	96h
25 mM	7.3% ± 0.6	8.1% ± 0.9	3.4% ± 1.9	3.0% ± 1.0
1 mM	7.0% ± 2.4	5.6% ± 0.4	5.0% ± 0.7	8.7% ± 2.4
0.25 mM	6.2% ± 4.1	6.4% ± 0.8	3.5% ± 1.7	9.8% ± 0.8

Cell death 3AB-OS	24h	48h	72h	96h
25 mM	6.6% ± 0.7	4.3% ± 0.8	5.3% ± 0.8	9.0% ± 2.5
1 mM	4.9% ± 0.2	9.8% ± 2	23.8% ± 12.9	46.2% ± 4.7
0.25 mM	9.1% ± 0.4	21.0% ± 10.1	43.5% ± 4.3	63.2% ± 4.1

Figure 1. Glucose deprivation leads to 3AB-OS cell death. Proliferation curves of MG63 **(A)** and 3AB-OS **(B)** cells cultured at 25, 1 or 0.25 mM glucose (Glc) were determined counting cells at indicated time points. **(C)** Phase contrast microscopy images were then collected for MG63 and 3AB-OS cells at 72 hours of cell culture. **(D, E)** Percentage of MG63 (**D**) and 3AB-OS (**E**) cell death at the different culturing conditions was evaluated by using Trypan Blue Stain. **(F, G)** Apoptosis was also evaluated by staining MG63 (**F**) and 3AB-OS (**G**) cells with Annexin V-FITC and Propidium Iodide (PI). Representative dot plots are shown. **(H, I)** Total intracellular ATP was measured in MG63 (**H**) and 3AB-OS (**I**) cells. All data represent the average of at least three independent experiments (± s.d.).

Several studies have reported that glucose deprivation can lead to ATP depletion-inducing cell death (Chiaradonna *et al.*, 2006b; Kim *et al.*, 2007a; Sandulache *et al.*, 2011; see also **chapter 3**). Therefore we determined the levels of ATP in both cell lines grown in high and low glucose along a time-course of 96 hours. Overall, ATP levels were slightly higher in MG63 cells as compared to 3AB-OS cells (**figures 1H and 1I**). In particular, at the later time points of low glucose growth (72 and 96 hours), in correlation with the appearance of cell death, 3AB-OS cells showed a significant decrease in ATP levels as compared to the high glucose condition (**figure 1I**). Differently, such a decrease was not observed in MG63 cells in the same glucose availability (**figure 1H**).

These findings suggest that 3AB-OS cells are strongly dependent for their proliferation and survival on glucose availability as compared to MG63 cells.

Conversely, glutamine withdrawal induced only a slight decrease of proliferation in both cell lines, in particular in MG63 cells (**figure 2**).

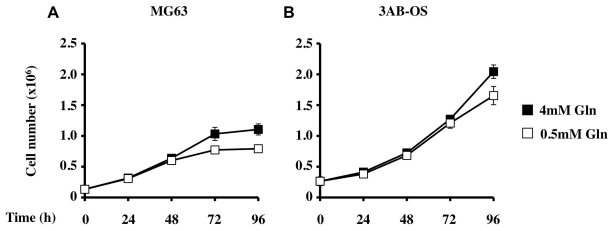

Figure 2. Glutamine induces sligth proliferation arrest in both cell lines. Proliferation curves of MG63 **(A)** and 3AB-OS **(B)** cells cultured at 4 or 0.5 mM glutamine (Gln) were determined counting cells at indicated time points. All data represent the average of three independent experiments (± s.d.).

Despite comparable or lower levels of glucose utilization, 3AB-OS are more sensitive to glycolysis inhibition as compared to MG63

In order to investigate whether the 3AB-OS cell dependence to glucose availability could be a consequence of an altered transport and utilization of

glucose, glucose utilization as well as lactate production of both cell lines grown in 1 mM glucose condition were assayed (**figure 3**).

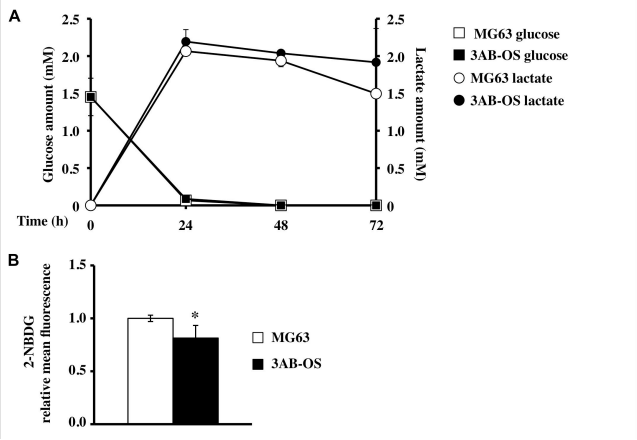

Figure 3. Measure of glucose consumption and uptake and of lactate secretion. (A) Residual glucose and secreted lactate in the culture medium of MG63 and 3AB-OS cells, grown at 1 mM initial glucose concentration, were measured by using specific enzymatic kits. **(B)** Glucose uptake rate was determined by using the fluorescent glucose analogue 2-NBDG at 24 hours of culture. All data represent the average of three independent experiments (± s.d.); *p<0.05 (Student's *t*-test).

As shown in **figure 3A**, the amounts of consumed glucose and of secreted lactate, as measured in the culture medium along the time-course, were substantially identical between the two cell lines. These findings were confirmed also by measuring both glucose and lactate on a per cell basis (**data not shown**). In addition, measurement of the rate of glucose transport into the cells, by using the fluorescent derivative of glucose 2-NBDG, indicated a slightly faster glucose uptake in MG63 cells as compared to 3AB-OS during the 30 minutes of the incorporation experiment (**figure 3B**).

Considering the data on glucose consumption and uptake and lactate secretion, we decided to better define the dependence on glucose availability of 3AB-OS as compared to MG63 cells by assessing their proliferation ability upon

treatment with the glycolytic inhibitor oxamate in normal glucose availability. Oxamate is a structural analog of pyruvate and a competitive inhibitor of LDH (Wilkinson and Walter, 1972). As shown in **figures 4A and 4B**, oxamate addition to the culture medium induced in 3AB-OS cell line a time- and dose-dependent cell death process that was not observed in MG63 cell line.

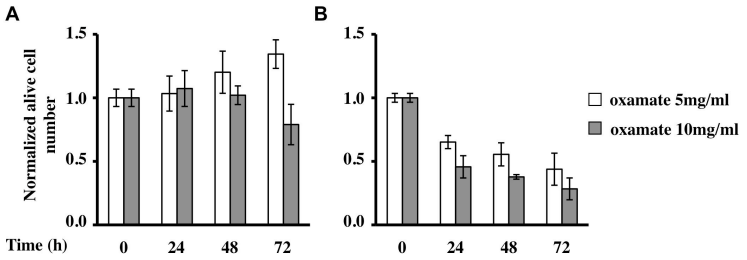

Figure 4. 3AB-OS are more sensitive to glycolysis inhibition than MG63. (A, B) MG63 **(A)** and 3AB-OS **(B)** cells were cultured at 25 mM glucose in presence of the glycolysis inhibitor oxamate and counted at the indicated time points using Trypan Blue Stain. Cell number at the different time points is normalized on the value at time 0. All data represent the average of three independent experiments (± s.d.)

Thus, these data showed that in 3AB-OS cells, despite a comparable or slightly lower rate of glucose consumption and uptake compared to MG63 cells, glycolysis is fundamental for their proliferation and survival. In MG63 cells other metabolic processes, i.e., oxidative phosphorylation, could guarantee their survival when glucose metabolism is inhibited.

Experimental evidence of the deficient mitochondrial activity of 3AB-OS cells

To test whether high sensitivity to aerobic glycolysis inhibition of 3AB-OS cells was a consequence of reduced mitochondrial activity, we assessed the ability of both cell lines to grow in media containing galactose (25 mM) or methyl-pyruvate (10 mM). In fact, both substrates, in a glucose-free medium favor mitochondrial oxidative respiration over glycolysis. MG63 cells, grown in media

containing 1 mM glucose, 25 mM galactose or 10 mM pyruvate, exhibited a similar rate of proliferation with a partial reduction in OXPHOS-inducer substrates only at late time points as compared to culture in high glucose (**figures 5A, 5C and 5D**). Conversely, galactose and pyruvate enriched growth media further decreased 3AB-OS proliferation as compared to low glucose, since an early decrease in the slope of the growth curve (24 hours) was observed (**figures 5B, 5C and 5D**).

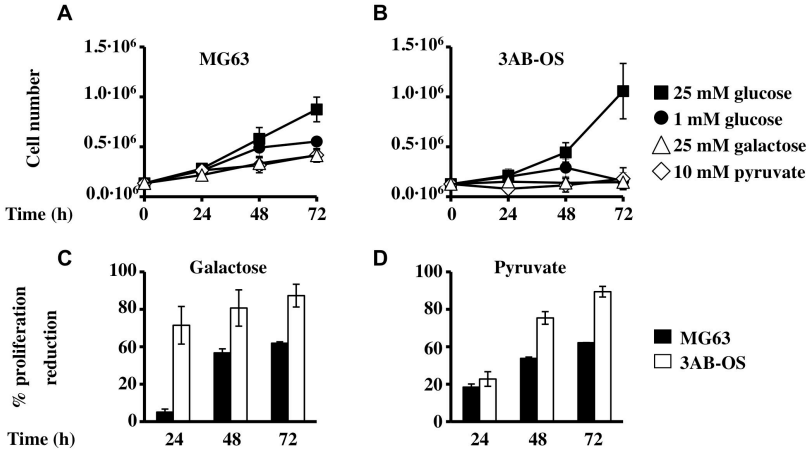

Figure 5. 3AB-OS cells are unable to proliferate in presence of respiratory substrates. Proliferation curves of MG63 **(A)** and 3AB-OS **(B)** cells cultured at 25 mM glucose (Glc), at 1 mM Glc, at 25 mM galactose (Gal) or 10 mM methyl-pyruvate (Pyr) were determined counting cells at the indicated time points. **(C, D)** Percentages of proliferation reduction in 25 mM Gal **(C)** and 10 mM Pyr **(D)** as compared with 25 mM Glc at each time point for both cell lines. All data represent the average of at least three independent experiments (± s.d.)

To measure the fraction of total ATP generated by mitochondrial oxidative phosphorylation, under the prevailing cultivation conditions, the cells were treated with oligomycin and rotenone. Addition to a normal culture medium of oligomycin, a specific inhibitor of the mitochondrial F_oF_1 ATP synthase (Papa *et al.*, 1996), or rotenone, a mitochondrial Complex I inhibitor (Benard *et al.*,

2007), reduced the intracellular ATP levels of MG63 cells by around 26% and 20% respectively (**figure 6A**).

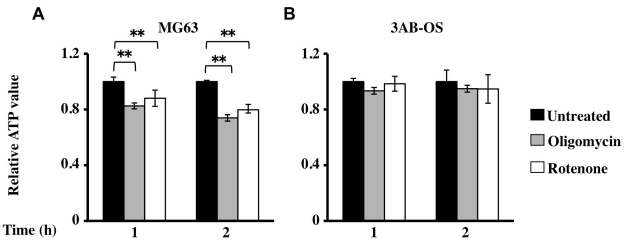

Figure 6. 3AB-OS cells are less sensitive to respiratory inhibitors as compared to MG63. Total intracellular ATP levels were measured in MG63 **(A)** and 3AB-OS **(B)** cells grown for 24 hours at 25 mM glucose, treated or not with 5 μM oligomycin or 3 nM Rotenone for 1 or 2 hours. Values are relative to untreated samples. All data represent the average of at least three independent experiments (± s.d.); **p<0.001 (Student's *t*-test).

In 3AB-OS cells, cultivated in the same condition, oligomycin and rotenone addition did not exert a major inhibitory effect on cellular ATP levels (around 5% for both molecules) as compared to MG63 cells (**Figure 6B**) and as compared to oxamate effect (**data not shown**). These findings showed that in 3AB-OS cells the mitochondrial oxidative phosphorylation contributes only marginally to cellular ATP production, which is essentially contributed by glycolysis.

Altogether these observations confirmed the low functioning of 3AB-OS mitochondria, resulting in the stronger inability to grow on specific respiratory substrates as compared to MG63 cells.

3AB-OS cells show high levels of mRNA encoding respiratory chain subunits but they undergo mitochondria fragmentation in glucose shortage

In order to determine whether 3AB-OS cells showed a reduced mitochondrial

activity as a consequence of a reduced expression of genes encoding OXPHOS proteins, both nuclear and mitochondrial genes expression levels were measured by semi-quantitative RT-PCR in the two cell lines grown in 25 mM glucose medium (**figure 7**).

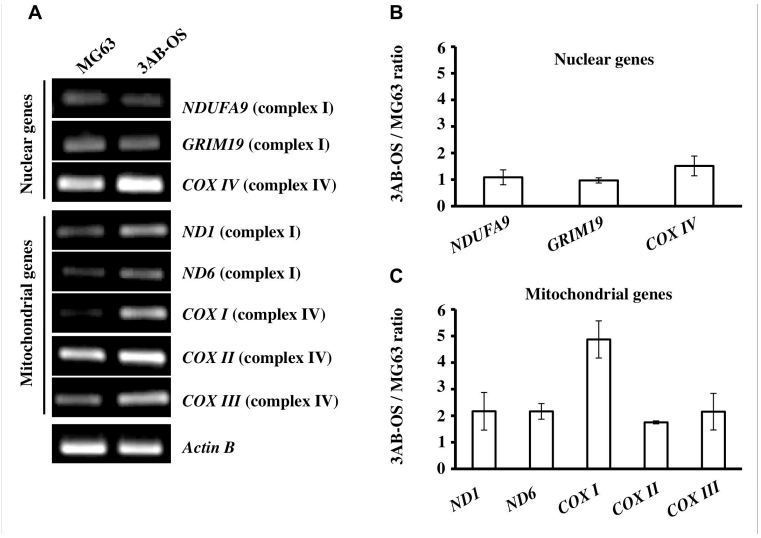

Figure 7. 3AB-OS cells present higher expression of respiratory chain subunits encoded by mtDNA. (A) Agarose gel results of RT-PCR amplification of nuclear genes encoding for mitochondrial proteins (upper panels) and mtDNA genes (lower panels) in MG63 and 3AB-OS cells. **(B, C)** Each amplified gene sequence has been quantified by ImageJ densitometric analysis and used to calculate the ratio between 3AB-OS cells and MG63 cells after normalization with *actin B* gene.

In particular the level of expression of five mitochondrial genes, *ND1*, *ND6*, *COX I*, *COX II* and *COX III* and three nuclear genes, *NDUFA9, GRIM19* and *COX IV*, encoding for mitochondrial proteins, were simultaneously assessed. As shown in **figures 7A and 7C**, a significant increase of mitochondrial genes expression in 3AB-OS cells as compared to MG63 cells was observed. At least, this observation could be considered also an indication that 3AB-OS presented higher amount of mtDNA as compared to MG63. Notable, no significant

difference in nuclear mRNAs levels between the two cells was observed (**figures 7A and 7B**).

Mitochondria are dynamic organelles that mediate several cell functions. Depending on the cellular context, mitochondria shift between fragmented and network structure by means of coordinated fission and fusion (Westermann, 2010). Given that, it has been shown that interconnected mitochondria are functionally more active than fragmented mitochondria (Gomes *et al.*, 2011; Mitra *et al.*, 2009). Therefore we decided to determine mitochondrial morphology of both cell lines, along a time-course in normal growth conditions and in low glucose, that is known to induce mitochondrial elongation (Rambold *et al.*, 2011a; Rambold *et al.*, 2011b; see also **chapter 3**).

Mitochondrial morphology was analyzed by means of stable clones of both cell lines expressing a mitochondrially targeted EYFP-Mito protein (**figure 8**). Three types of mitochondrial morphologies were classified as fragmented, intermediate and networked (**figure 8A**).

At an early growth time (0-24 hours), MG63 cells displayed especially networked and intermediate mitochondria regardless of initial glucose concentrations (**figure 8B**). At a later growth time (72 hours), mitochondrial morphology was strictly associated with glucose availability. In fact, in glucose rich medium, MG63 cells showed a slight reduction of networked mitochondria, while, in low glucose medium, they showed a completely disappearance of fragmented mitochondria in favor of more interconnected mitochondria (**figure 8B**). Similar analyses in 3AB-OS cells indicated a completely opposite behavior. In fact, at an early growth time (0-24 hours), 3AB-OS displayed especially fragmented mitochondria regardless of initial glucose concentrations (**figure 8C**). At the later growth time (72 hours), in glucose rich medium intermediate

and networked mitochondria increased, while in low glucose these structures were almost lost with a parallel increase of fragmented mitochondria (**figure 8C**).

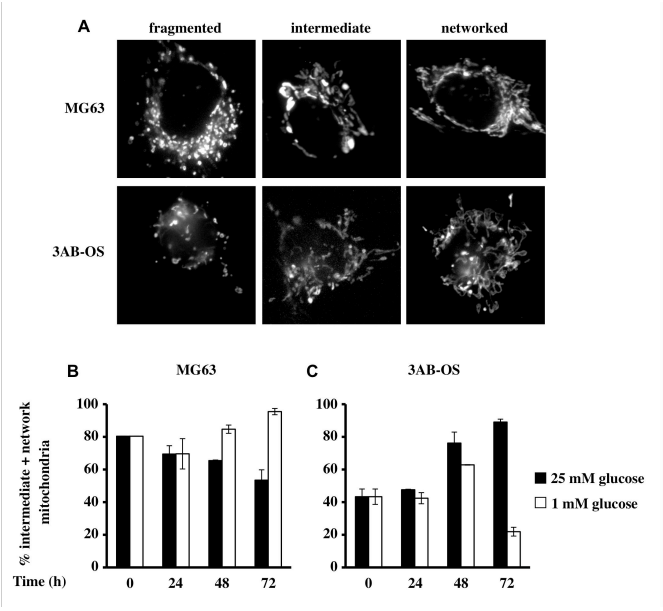

Figure 8. 3AB-OS cells upon glucose depletion are unable to network mitochondria. (A) Examples of fragmented, intermediate and networked mitochondria in stable EYFP-Mito expressing MG63 (upper panels) and 3AB-OS cells (lower panels). **(B, C)** Analysis of mitochondrial morphology in MG63 **(B)** and 3AB-OS **(C)** cells grown at 25 and 1 mM glucose for 72 hours. For each determination, at least 100 cells were counted and classified depending their mitochondrial morphology. Data represent the average of at least three independent experiments (± s.d.)

Taken together, these results further confirmed the differences between these two cell lines regarding mitochondrial function, and highlighted the inability of 3AB-OS cell mitochondria to elongate under glucose starvation.

Chapter 7

Discussion

CHAPTER 7. DISCUSSION

Several cancer cells, in order to generate ATP and sustain different anabolic processes, rely mainly on glycolysis instead of OXPHOS (Warburg effect) (Chiaradonna *et al.*, 2012; Tennant *et al.*, 2010). Thus, glucose metabolism assumes an essential role in cancer cells. Such a metabolic switch observed in different cancer cells can be consequence of different mechanisms such as environment changes (for example, hypoxia), mutations of oncogenes and tumor suppressors and mitochondria impairment (Levine and Puzio-Kuter, 2010; Lopez-Rios *et al.*, 2007; Semenza, 2010b). All these causes can be interconnected and together can promote Warburg effect and tumorigenesis.

Oncogenic *K-ras* mutations have been described to be involved in promoting enhanced glycolysis and mitochondria dysfunctions (Chiaradonna *et al.*, 2006a; Yang *et al.*, 2010; Yun *et al.*, 2009).

In this regard, in different cellular models it has been reported that oncogenic *K-ras* can also lead to the derangement of the cAMP/PKA signal pathway (Balestrieri *et al.*, 2009; Borlikova and Endo, 2009), that normally is able to regulate both glycolysis and mitochondria function. In this thesis work has been addressed the role of oncogenic *K-ras* in influencing cancer cell metabolism through interference with cAMP/PKA pathway. *K-ras*-transformed cells analyzed in the present study exhibit a strict dependence on high glucose concentration for growth (see **chapter 3, figures 1, 2 and 14** and Chiaradonna *et al.*, 2006b). It is shown that the shift from aerobic to fermentative ATP supply is associated with a derangement in the cAMP/PKA system resulting in structural and functional alterations of mitochondria (**chapter 3**). *K-ras*-transformed mouse fibroblasts, in fact, showed a reduced enzymatic activity of PKA (**chapter 3, figure 3**) that was also reflected in the reduced phosphorylation of

its main substrate CREB (**chapter 3, figure 4**) as compared to control fibroblasts (**chapter 3, figures 3 and 4**). Reduced levels of CREB phosphorylation were observed also in human *K-ras*-transformed MDA-MB-231 cells (**chapter 3, figure 17**), confirming a *K-ras*-dependent repression of PKA activity. Accordingly, Reverted cell line, expressing a GEF-DN able to down regulate *K-ras* activation, recovered the PKA capability to phosphorylate CREB to levels comparable to Normal cells (**chapter 3, figure 5**). The differences in the functional capacity of PKA between Normal and Transformed cells were not due to changes in the enzyme content (data not shown) but presumably reflected an altered responsiveness of PKA to cellular activators/inhibitors. Despite the lower PKA activity, Transformed cells presented higher levels of intracellular cAMP (**chapter 3, figure 3**), indicating that the deregulation of the cAMP/PKA pathway in these cells could possibly be represented as a feedback compensatory response of the adenylyl cyclase to the depression of PKA activity. Forskolin (FSK) treatment recovered such a reduced PKA activity both in mouse and human *K-ras*-transformed cell lines, resulting also in the increase of CREB phosphorylation levels upon stimulation (**chapter 3, figures 3, 4 and 17**). Notably, PKA activity enhancement prevented the death of transformed fibroblasts (**chapter 3, figure 6**) and of some human *K-ras*-transformed cells like MDA-MB-231, MIA PaCa-2 and A549 (**chapter 3, figures 14 and 15**), under glucose depletion. FSK effect was almost inhibited by the specific PKA inhibitor H89 (**chapter 3, figure 7**).

K-ras-transformed fibroblasts showed depression of Complex I activity and increase of ROS level as compared to normal fibroblasts (**chapter 3, figure 12**). As previously observed in various cellular pathophysiological conditions (Papa *et al.*, 2008; Piccoli *et al.*, 2006) elevation of the cAMP levels, induced by FSK in mouse and human *K-ras*-transformed cells, promoted the activity of Complex

I and decreased the ROS levels (**chapter 3, figures 12 and 16**). Depression of Complex I, which is by itself a major producer of ROS and is particularly vulnerable to oxidative stress (Lenaz *et al.*, 2010), can set up a "vicious" cycle, detrimental for cell growth. The decrease of ROS levels, obtained by the addition of the antioxidant N-acetyl-cysteine in the medium, partially protected *K-ras*-transformed cells from death in glucose depletion (**chapter 3, figure 13**), confirming the implication of ROS in glucose-dependent death. It is worth noting that, although the influence of cAMP/PKA pathway on Complex IV has been also demonstrated (Acin-Perez *et al.*, 2009), in the cell lines and the prevailing experimental conditions of the present work the activity of Complex IV was stable and unaffected by PKA activation (**chapter 3, figure 12**).

The cAMP/PKA system is also involved in regulation of the dynamics of mitochondrial fusion and fission (Chang and Blackstone, 2007; Cribbs and Strack, 2007). In *K-ras*-transformed cells, mitochondria were mainly in the fragmented state (**chapter 3, figures 10 and 16**). FSK largely reverted mitochondrial fragmentation promoting mitochondria fusion, an effect that was prevented by the PKA inhibitor H89 (**chapter 3, figures 10 and 16**). The relationship between the dynamic equilibrium between fusion and fission of mitochondria and their respiratory activity is a matter of current investigation (Grandemange *et al.*, 2009; Sauvanet *et al.*, 2010). Experimental observations support the link between respiratory chain complexes activity, in particular Complex I, and the mitochondrial fusion/fission process (Koopman *et al.*, 2007). A set of G proteins has been found to regulate mitochondrial dynamics (Palmer *et al.*, 2011). Among these the Drp1 protein promotes mitochondrial fission. Inactivation of Drp1, effected by its phosphorylation by PKA, can result in promotion of fusion and hence in protection from autophagy (Gomes *et al.*, 2011). Western blot assays showed that in MDA-MB-231 cells, whose

mitochondria were prevalently in the fragmented state, Drp1 protein was essentially in the dephosphorylated state (**chapter 3, figure 18**). Addition of FSK promoted phosphorylation of Drp1, associated with an increase of mitochondrial interconnection and a decrease of ROS levels (**chapter 3, figure 18**). Accordingly, suppression of the activity of Drp1 by its inhibitor Mdivi-1 promoted mitochondrial fusion and prevented ROS generation in MDA-MB-231 cells (**chapter 3, figure 18**). These findings indicated a close relationship between mitochondria morphology and activity and the role of PKA in regulating both of them. Importantly the positive effects of FSK treatment on the mitochondrial morphology and activity were observed both in high and low glucose availabilities (**chapter 3, figure 11** and data not shown), implying that PKA pathway regulated mitochondrial function, at least in our experimental conditions, independently from glucose deprivation.

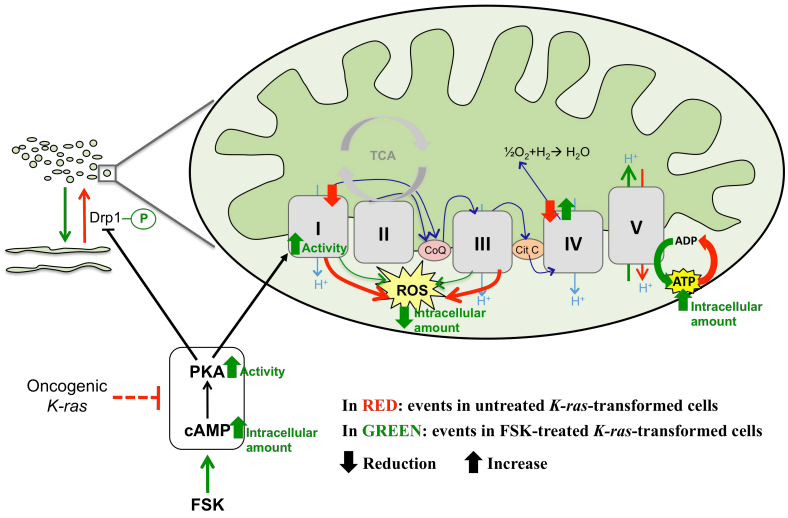

Figure 1. Exogenous stimulation of the cAMP/PKA pathway induces positive effects on mitochondria function, protecting *K-ras*-transformed cells from death in glucose depletion. In transformed cells, oncogenic *K-ras* leads to a general inhibition of the cAMP/PKA pathway, in turn causing reduction of mitochondrial OXPHOS activity and derangement of fusion process. In fact, in these cells the low activity of Complex I

strongly impairs respiratory chain activity, leading to an overproduction of ROS and a decreased production of ATP. Moreover, mitochondria of *K-ras*-transformed cells are mainly fragmented and are unable to form network especially under glucose starvation. In this scenario, to avoid the loss of mitochondrial potential, residual ATP is partially used by Complex V in reverse mode. However, the high level of ROS and the drop of intracellular ATP lead to transformed cell death in glucose deprivation. In accordance, the exogenous stimulation of the cAMP/PKA pathway by FSK improves mitochondrial function of *K-ras*-transformed cells, protecting them from apoptosis in glucose deprivation. In fact, PKA stimulates the Complex I activity leading to an increase of oxygen consumption and intracellular ATP level and to a decrease of ROS. Moreover, FSK also favors mitochondria fusion by inhibiting the pro-fission protein Drp1.

Altogether these results show that the derangement of cAMP/PKA pathway in *K-ras*-transformed cells results in the alteration of mitochondrial structure (impairment of mitochondrial fusion) and respiration (decreased activity of Complex I). Such an alteration, making *K-ras*-transformed cells dependent on glucose concentration, leads to increased ROS production and apoptosis in the condition of low glucose availability (see above, **figure 1**).

These data also indicate that mitochondria dysfunction in cancer cells may be a reversible condition modulated by oncogenes expression, such as *K-ras,* and related perturbations of cellular pathways. Therefore, the reversible mechanisms can be exploited to project new anticancer therapies, for example inducing OXPHOS activity and reverting the Warburg effect. In fact, the promotion of OXPHOS activity in cancer cells has been shown *per se* a possible strategy to kill them (Bonnet *et al.*, 2007; Fantin *et al.*, 2006; see also introduction and below). Moreover, mitochondria maintain an important role also in cancer cells, not only as producers of energy but in particular for their role in mediating anti-apoptotic processes and maintaining oxidative equilibrium. Recently, different therapeutic approaches based on targeting tumor mitochondria have been proposed (Biasutto *et al.*, 2010). In particular, the use of strategies that fuel

mitochondria metabolism and activity could make them more sensitive to mitochondria-targeting drugs and could be possible and promising anticancer approaches.

We decided to utilize the main metabolic alterations of cancer cells, namely hyperglycolytic phenotype (Warburg effect), and mitochondria dysfunctions, as targets for combined treatments aimed to specifically kill cancer cells (**chapter 4**). In particular, by using a glycolytic human breast cancer cell line, namely MDA-MB-231, grown in limiting glucose availability, and some natural inhibitors of mitochondria activity, we showed that Complex I inhibition associated with an acute stimulation of respiration, due to glucose depletion, induced specifically cancer cell death (**chapter 4, figures 2 and 6**). Notably, this effect was observed by using three different mitochondrial Complex I inhibitors (Okun *et al.*, 1999) that strongly support our results (**chapter 4, figures 2 and 6**). In addition, our and previously published data indicated that, at the used concentrations, rotenone (3 nM), capsaicin (100 μM) and piericidin A (5 nM) have no effect on normal cells, specifically immortalized fibroblasts (**chapter 4, figure 5**), normal pancreatic cells (Pramanik *et al.*, 2011) and dopaminergic neurons (Choi *et al.*, 2011), respectively. This reduced or absent effect on normal cells is an important characteristic for exploiting these compounds for cancer therapy. Regardless the mechanism of action of the three molecules, we showed that their effectiveness increased upon glucose depletion reflecting the dependency of the cancer cells on glycolysis (**chapter 4, figures 2 and 6B** *vs*. **figures 4 and 6A**). In fact, less glycolytic cells, like the mouse immortalized fibroblasts, were also less sensitive to these treatments (**chapter 4, figure 5C**). Regarding the synergistic effect on cell survival we think that it is caused by the ATP depletion more than a rapid decrease of mitochondrial potential, although both parameters were influenced by combined approach. However we cannot

exclude an increase of ROS levels, as shown by other authors as a consequence of Complex I inhibition (Deng *et al.*, 2010; Fath *et al.*, 2009). Further experiments exploring this point would be addressed in the future.

Using FSK in our experiments, we clearly observed that the stimulation of mitochondrial activity, characteristic of non-malignant cells, might be an efficient tool in anticancer strategy. In this regard, inhibition of PDK or LDH has been shown to shift metabolism from glycolysis to glucose oxidation and hence to a reduction of cancer cell viability and tumor growth (Bonnet *et al.*, 2007; Fantin *et al.*, 2006). Our results with FSK suggest a similar mechanism in which reactivation of the mitochondrial function associated with glucose depletion and Complex I mitochondria inhibition strongly affect cancer cell survival (**chapter 4, figures 4, 5 and 6**). Taken together these results provide a rationale for the use of mitochondrial inhibitors in cancer cells exploiting cancer cell fragility versus glucose depletion. In addition they point out to an energetic switch from glycolysis to OXPHOS as an important therapeutic approach, since normal cells appear resistant to such combined treatments.

Previous reports (Baracca *et al.*, 2010; Chiaradonna *et al.*, 2006a; Gaglio *et al.*, 2011) and above presented data (**chapter 3**) indicate that *K-ras*-transformed mouse and human cells upon glucose depletion undergo intracellular ATP levels decrease and, as a consequence of Complex I mitochondrial dysfunction, accumulation of intracellular ROS and eventually cell death. Importantly, low glucose-cell death in both cancer cell lines is partly avoided by ROS levels reduction or by enhancement of mitochondrial activity (**chapter 3**).

Therefore, glucose-dependent cell death can be associated to a few molecular events including ATP level fall, ROS accumulation, and mitochondrial dysfunction (**chapter 3**).

Nevertheless the complete mechanism by which glucose depletion induces cancer cell death is not yet fully understood. In order to determine the processes involved in transformed cell death, we decided to identify changes in gene and protein expression induced by glucose deprivation. The results of transcriptomic and proteomic analyses indicated that glucose deprivation induces ER stress and hence Unfolded Protein Response (UPR) activation (**chapter 5**). Moreover, experimental evidence showed that such activation was due to a reduction of glucose entry into the Hexosamine Biosynthesis Pathway (HBP), that reduced protein glycosylation levels, as shown by alteration of O-glycosylation (**chapter 5, figure 7**), and hence brought to a sustained UPR stimulation and to transformed cell death (**chapter 5**).

Although the role of UPR is to reduce ER stress and to induce survival, persistent ER stress is known to induce cell death (Marciniak *et al.*, 2004; Ron and Walter, 2007). Interestingly, our data showed that UPR was activated both in Normal and in Transformed cells in condition of glucose shortage (**chapter 5, figure 2** *vs.* **figure 3**), but only Normal cells were able to cope with this stress, avoiding glucose-dependent massive cell death. We made the hypothesis that the concomitant presence in Normal cells of low ROS levels, sustained ATP levels, mitochondria functionality (Chiaradonna *et al.*, 2006a and **chapter 3**) and a tunable UPR, may provide conditions necessary to re-establish cellular homeostasis (see below, **figure 2**). On the other hand, our transcriptional data indicated a more sustained UPR activation in Transformed cells as compared to Normal ones, since several UPR-related genes and relative targets, particularly that involved in inducing cell death processes, were more actively expressed in these cells (**chapter 5, figure 1**). Moreover, XBP1 splicing and JNK activation, known as Bcl-2 antiapoptotic protein inhibitors (Wei *et al.*, 2008), were specifically observed in Transformed cells (**chapter 5, figures 2 and 6**). Taken

together these findings strongly support the notion that transformed cells growing in normoxia, upon glucose deprivation undergo cell death mainly through prolonged UPR activation (see below, **figure 2**).

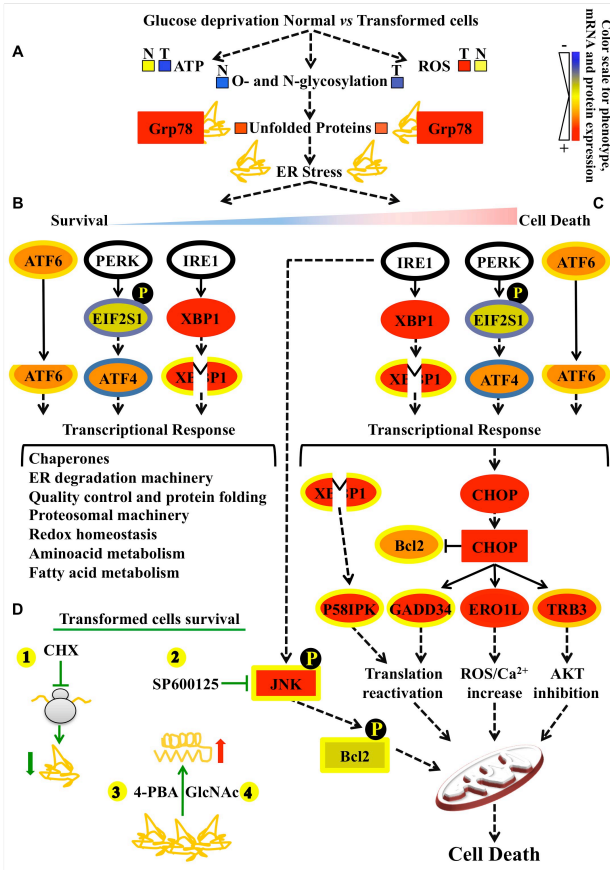

Figure 2. Glucose deprivation in cancer cells activates UPR following HBP flux reduction. Proteins are represented by a colored rectangle; in particular, the external rectangle represents Normal cell data and the internal rectangle Transformed cell data. Similarly, each mRNA has been represented by a colored ellipse, in which the external ellipse represents Normal cell data and the internal ellipse Transformed cell data. Changes in protein and gene expression levels are represented by a color scale between red (high expression) and blue (low expression); yellow indicates unchanged expression. (**A**) Events that characterize cells in glucose deprivation and ER stress. Levels of ATP, ROS and unfolded proteins in Normal (N) and Transformed (T) cells are represented by colored boxes. The double colors triangle indicates the relation between time and

intensity of ER-stress and effect on cell homeostasis (blue: survival, red: death). (**B**) Survival processes activated by UPR have been represented as a cascade of events starting from UPR sensors activation (ATF6 cleavage, eIF2a phosphorylation -EIF2S1 gene- by PERK, ATF4 expression and XBP1 splicing form expression upon IRE1 activation) and ending with a list of downstream regulated processes (transcriptional response). (**C**) Cell death processes activated by UPR have been presented as a cascade of events starting from UPR sensors activation (as above) and ending either with a transcriptional response (CHOP, P58IPK, GADD34, ERO1L, TRB3) or a post-translational mechanism (phosphorylation) controlling positively JNK and negatively Bcl-2 proteins. (D) Schematic representation of the survival mechanisms of *K-ras*-transformed cells identified in our work. In particular the protective effects of CHX (1, translation inhibition), SP600125 (2, JNK inhibitor), 4-PBA (3, chemical chaperone) and GlcNAc (4, HBP substrate) are shown.

In accordance, attenuation of UPR, obtained by decreasing unfolded proteins accumulation through the translation inhibitor CHX, increasing cell folding ability through the chemical chaperon 4-PBA or inhibiting JNK, as a downstream pro-apoptotic signaling, through SP600125, protected transformed cells from glucose-dependent death (**chapter 5, figures 4, 5 and 6;** see also above **figure 2**). Besides, our results showed that HBP fuelling by addition of N-Acetyl-D-glucosamine (GlcNAc), a sugar essential for O- and N-glycosylation, induced prolonged survival of glucose-starved *K-ras*-transformed cells by inhibiting UPR activation (**chapter 5, figure 8, 9 and 12**; see also above **figure 2**). Such an ability of GlcNAc to completely restore transformed cell survival in absence of glucose provides strong evidence that HBP, regulating protein folding and localization through the synthesis of UDP-GlcNAc, represents an important pathway sensitive to glucose deficiency. Importantly, our data, obtained by using the glycolytic inhibitor oxamate together with GlcNAc, indicated that such a positive effect is glycolysis-independent (**chapter 5, figure 10**). Taken together our findings are also supported by literature data showing that oncogenic *K-ras* signaling plays a prominent role in the flux of glucose into the HBP sustaining protein N- and O-glycosylation during tumor maintenance

(Wojciechowicz *et al.*, 1995; Ying *et al.*, 2012), and that GlcNAc addition may induce cell survival, in complete absence of glucose, by increasing membrane receptor localization, glutamine uptake and mitochondrial function (Wellen *et al.*, 2010). Results presented in **chapter 5** do not exclude that other processes, known to be either pro-survival and pro-apoptotic, i.e., autophagy and mitochondrial dysfunction (see **chapter 3**), could participate, together with HBP flux reduction and UPR activation, to detrimental effect of glucose depletion in cancer cells. Rather, further investigation in cancer cells on the cell death mechanism activated downstream of UPR as well as the HBP regulatory mechanisms and the relation of such pathways with the other ones involved in metabolic reprogramming (glucose addiction and mitochondrial impairment) will be required.

Altogether these findings confirm the essential role of glucose in cancer cells and suggest that glucose metabolism remain an important possible target for anticancer therapy. More specifically, we have elucidated new mechanisms that make cancer cells dependent to glucose availability, i.e., *K-ras*-dependent deregulation of cAMP/PKA pathway that contributes to mitochondria dysfunction, and HBP, that is up-regulated in cancer cells and can induce lethal stress when it is not properly fuelled. These observations, adding new information to the complex scenario of cancer metabolic reprogramming, suggest also possible approaches and targets for therapies aimed to block particularly *K-ras* cancers.

Worth noting, tumors are no longer viewed as homogenous masses of proliferating cells, each with identical genetic alterations, but more as a heterogeneous tissue that contains a hierarchy of cells, perhaps originating from

a single cancer stem cell (CSC) (Hanahan and Weinberg, 2011). Therefore, now the investigation of CSC population features is really fundamental for projecting new anticancer therapies. Considering the important role of metabolism and metabolic reprogramming in cancer development, also the definition of CSCs metabolism can be considered an important tool for future strategies targeting these cells. Given that, we sought to define the energetic metabolism of a novel CSC-like line, 3AB-OS, as compared to its osteosarcoma cancer cell line of origin, MG63 (Di Fiore *et al.*, 2009) (**chapter 6**). It has been observed that 3AB-OS present enhanced expression of MAPK pathway components and of HIF-1α (Di Fiore *et al.*, 2012a; Di Fiore *et al.*, 2009), suggesting that these cells could be very similar to "glucose addicted" *K-ras*-transformed cells. In addition, recent reports have shown that human pluripotent stem cells rely mostly on glycolysis to meet their energy demands (Chen *et al.*, 2010b). Our data clearly confirm that 3AB-OS cells have a hyperglycolitic metabolism, similar to cancer cells and pluripotent stem cells and different to the osteosarcoma cancer cells of origin. In fact, when they were subjected to glucose deprivation 3AB-OS underwent cell death, differently to MG63 that showed only proliferation arrest (**chapter 6, figure 1**). No effect on proliferation and survival, as shown also for other glucose-addicted cancer cells, was observed upon glutamine shortage (**chapter 6, figure 2**). Since both cell lines cultured in 1 mM glucose consumed the total amount of glucose in 24 hours of culture (**chapter 6, figure 3**), MG63 cells may use different substrates, i.e., amino acids and fatty acids, for energy or anabolic purposes. Conversely, 3AB-OS cells appear completely dependent on glucose availability and glycolysis (see their proliferation in presence of oxamate in **chapter 6, figure 4**). Such dependence seems fundamental especially for anabolism, since significant ATP depletion was observed only after 72 hours of growth in glucose shortage (**chapter 6, figure 1**). Notably, despite a stronger

dependence of 3AB-OS cells from glucose availability, the rate of glucose uptake in this cell line was slightly lower as compared to MG63 cells (**chapter 6, figure 3**). This result was in part expected because cancer cells often present increased expression of glucose transporters and glucose uptake (Chiaradonna *et al.*, 2012). Moreover, a reduced glucose consumption and FDG uptake in CSCs as compared to cancer cells have been also observed, as consequence of a reduced energy requirement and of a more undifferentiated state (Martins-Neves *et al.*, 2012; Ye *et al.*, 2011). In addition, transcriptional profiling showed that the glucose transporters SLC2A10 and SLC2A12 were downregulated in 3AB-OS cells as compared to MG63 (Di Fiore *et al.*, 2012a). On the other hand, repression and activation of the mitochondrial function are critical for self-renewal and differentiation of human embryonic stem cells (hESCs), respectively (see also chapter 1 – introduction). Indeed, various authors have shown that SCs, before spontaneous differentiation or compared to differentiated cells, show lower mitochondrial mass, lower mtDNA copy number, lower ATP content and lower OXPHOS activity (Chen *et al.*, 2008; Facucho-Oliveira and St John, 2009; Hom *et al.*, 2011; Piccoli *et al.*, 2005). Our findings are in agreement with these observations. In fact, 3AB-OS, differently to MG63, were unable to grow on OXPHOS substrates like galactose and pyruvate (**chapter 6, figure 5**) and did not show decrease of intracellular ATP levels when treated with the mitochondrial inhibitors oligomycin and rotenone (**chapter 6, figure 6**). The ability in keeping a low energetic mitochondrial metabolism may also favor undifferentiated state and the ability to renew, fundamental characteristics associated with high tumorigenic potential of CSCs (Kelly *et al.*, 2007). Despite the reduced dependence on mitochondrial respiration, 3AB-OS cells showed a larger expression of mitochondrial genes encoding for Complex I and IV subunits (**chapter 6, figure 7**). This result was in part unexpected since previous

data obtained in ESCs as well as in lung CSCs-like have shown a reduced amount of mtDNA as compared to differentiated cells (Cho *et al.*, 2006; Ye *et al.*, 2011). However, Varum *et al.* (2011) have observed that pluripotent cells present higher protein levels of mitochondrial complexes than differentiated cells, although they show a lower OXPHOS activity and rely mostly on glycolysis to meet their energy demands (Varum *et al.*, 2011). Given this result, further studies, such as the analysis also of protein levels, are needed. Morphological analysis of 3AB-OS mitochondria indicated that they were more fragmented and perinuclear distributed as compared to MG63 cells, in particular at early time of culture in both glucose concentrations (**chapter 6, figure 8**). Moreover, they underwent total mitochondria fragmentation at 72 hours of culture in low glucose (**chapter 6, figure 8**), in association with ATP drop and cell death. This result further supported a reduced mitochondrial activity in CSCs since such a morphology has been observed in ESCs, iPSCs, CSCs and in several glucose-addicted cancer cells, which are all characterized by OXPHOS impairment (see **chapter 3, figures 10, 11 and 16**; Chiaradonna *et al.*, 2006a; Mandal *et al.*, 2011; Ye *et al.*, 2011). On the other hand, our data indicated that 3AB-OS cells changed spontaneously mitochondrial morphology, increasing the percentage of more interconnected mitochondria, when grown in optimal conditions for at least 72 hours (**chapter 6, figure 8**). Notably, the immature morphology evolves into filamentous networks of elongated and branched mitochondria when stem cells undergo differentiation (Mandal *et al.*, 2011). This observation could suggest a partial spontaneous differentiation of CSCs as well as a partial use of mitochondrial function, perhaps for an anabolic more than an energetic purpose, to maintain their proliferation capacity in high glucose (Mandal *et al.*, 2011).

In conclusion our data indicated that 3AB-OS cells rely mostly on glycolysis for

their proliferation, survival and ATP production. In addition we clearly showed that these cells have a reduced mitochondrial function and different mitochondrial morphology, despite a higher expression of genes encoding for mitochondrial complexes subunits, as compared to MG63 cells. Altogether these data confirm that CSCs have an energetic metabolism similar to either normal tissue stem cells (Varum *et al.*, 2011) or to high glycolytic cancer cells (Chiaradonna *et al.*, 2012).

In conclusion, considering altogether these observations, oncogenic *K-ras* appears to make cancer cells totally addicted to glucose availability, regulating different processes, such as cAMP/PKA pathway, and, as consequence, mitochondrial function, and HBP. Elucidation of these processes should permit the development of novel therapeutic strategies. As example, the exploitation of FSK stimulatory effect on OXPHOS combined with OXPHOS-targeting drugs has been resulted an efficacious approach to kill *K-ras*-cancer cells. On the other hand, today the new challenge of anticancer research and therapy is the total eradication of the cancer, targeting CSCs. Here we have observed that CSCs appear completely glucose-dependent, resulting similar to normal stem cells and to most glycolytic cancer cells. Interestingly, the transcriptional profile of CSCs is similar to that of *K-ras* transformed cells, indicating that it could be used as a possible metabolic marker and that some strategies developed for glucose addicted cancer cells could be used also to treat specific CSCs. At the same time, a better definition of the differences between CSCs and the associated cancer cells will be useful for development of novel therapies aimed to completely eradicate the tumors.

Chapter 8

References

CHAPTER 8. REFERENCES

Acin-Perez R, Salazar E, Kamenetsky M, Buck J, Levin LR, Manfredi G (2009). Cyclic AMP produced inside mitochondria regulates oxidative phosphorylation. *Cell Metab* **9:** 265-76.

Ahmad IM, Aykin-Burns N, Sim JE, Walsh SA, Higashikubo R, Buettner GR *et al* (2005). Mitochondrial O2*- and H2O2 mediate glucose deprivation-induced stress in human cancer cells. *J Biol Chem* **280:** 4254-63.

Ahuja P, Zhao P, Angelis E, Ruan H, Korge P, Olson A *et al* (2010). Myc controls transcriptional regulation of cardiac metabolism and mitochondrial biogenesis in response to pathological stress in mice. *J Clin Invest* **120:** 1494-505.

Al-Hajj M, Wicha MS, Benito-Hernandez A, Morrison SJ, Clarke MF (2003). Prospective identification of tumorigenic breast cancer cells. *Proc Natl Acad Sci U S A* **100:** 3983-8.

Atsumi T, Chesney J, Metz C, Leng L, Donnelly S, Makita Z *et al* (2002). High expression of inducible 6-phosphofructo-2-kinase/fructose-2,6-bisphosphatase (iPFK-2; PFKFB3) in human cancers. *Cancer Res* **62:** 5881-7.

Aykin-Burns N, Ahmad IM, Zhu Y, Oberley LW, Spitz DR (2009). Increased levels of superoxide and H2O2 mediate the differential susceptibility of cancer cells versus normal cells to glucose deprivation. *Biochem J* **418:** 29-37.

Balestrieri C, Alberghina L, Vanoni M, Chiaradonna F (2009). Data recovery and integration from public databases uncovers transformation-specific transcriptional downregulation of cAMP-PKA pathway-encoding genes. *BMC Bioinformatics* **10 Suppl 12:** S1.

Baracca A, Chiaradonna F, Sgarbi G, Solaini G, Alberghina L, Lenaz G (2010). Mitochondrial Complex I decrease is responsible for bioenergetic dysfunction in K-ras transformed cells. *Biochim Biophys Acta* **1797:** 314-23.

Baratta MG, Porreca I, Di Lauro R (2009). Oncogenic ras blocks the cAMP pathway and dedifferentiates thyroid cells via an impairment of pax8 transcriptional activity. *Mol Endocrinol* **23:** 838-48.

Barthel A, Okino ST, Liao J, Nakatani K, Li J, Whitlock JP, Jr. *et al* (1999). Regulation of GLUT1 gene transcription by the serine/threonine kinase Akt1. *J Biol Chem* **274:** 20281-6.

Bartrons R, Caro J (2007). Hypoxia, glucose metabolism and the Warburg's effect. *J Bioenerg Biomembr* **39:** 223-9.

Benard G, Bellance N, James D, Parrone P, Fernandez H, Letellier T *et al* (2007). Mitochondrial bioenergetics and structural network organization. *J Cell Sci* **120:** 838-48.

Bensaad K, Tsuruta A, Selak MA, Vidal MN, Nakano K, Bartrons R *et al* (2006). TIGAR, a p53-inducible regulator of glycolysis and apoptosis. *Cell* **126:** 107-20.

Berggren MI, Husbeck B, Samulitis B, Baker AF, Gallegos A, Powis G (2001). Thioredoxin peroxidase-1 (peroxiredoxin-1) is increased in thioredoxin-1 transfected cells and results in enhanced protection against apoptosis caused by hydrogen peroxide but not by other agents including dexamethasone, etoposide, and doxorubicin. *Arch Biochem Biophys* **392:** 103-9.

Beug H (2009). Breast cancer stem cells: eradication by differentiation therapy? *Cell* **138:** 623-5.

Biaglow JE, Cerniglia G, Tuttle S, Bakanauskas V, Stevens C, McKenna G (1997). Effect of oncogene transformation of rat embryo cells on cellular oxygen consumption and glycolysis. *Biochem Biophys Res Commun* **235:** 739-42.

Biasutto L, Dong LF, Zoratti M, Neuzil J (2010). Mitochondrially targeted anti-cancer agents. *Mitochondrion* **10:** 670-81.

Bolscher JG, van der Bijl MM, Neefjes JJ, Hall A, Smets LA, Ploegh HL (1988). Ras (proto)oncogene induces N-linked carbohydrate modification: temporal relationship with induction of invasive potential. *EMBO J* **7:** 3361-8.

Bonnet S, Archer SL, Allalunis-Turner J, Haromy A, Beaulieu C, Thompson R *et al* (2007). A mitochondria-K+ channel axis is suppressed in cancer and its normalization promotes apoptosis and inhibits cancer growth. *Cancer Cell* **11:** 37-51.

Bonora E, Porcelli AM, Gasparre G, Biondi A, Ghelli A, Carelli V *et al* (2006). Defective oxidative phosphorylation in thyroid oncocytic carcinoma is associated with pathogenic mitochondrial DNA mutations affecting complexes I and III. *Cancer Res* **66:** 6087-96.

Borlikova G, Endo S (2009). Inducible cAMP early repressor (ICER) and brain functions. *Mol Neurobiol* **40:** 73-86.

Bossu P, Vanoni M, Wanke V, Cesaroni MP, Tropea F, Melillo G *et al* (2000). A dominant negative RAS-specific guanine nucleotide exchange factor reverses neoplastic phenotype in K-ras transformed mouse fibroblasts. *Oncogene* **19:** 2147-54.

Brown J (1962). Effects of 2-deoxyglucose on carbohydrate metablism: review of the literature and studies in the rat. *Metabolism* **11:** 1098-112.

Brown RS, Wahl RL (1993). Overexpression of Glut-1 glucose transporter in human breast cancer. An immunohistochemical study. *Cancer* **72:** 2979-85.

Campanella M, Parker N, Tan CH, Hall AM, Duchen MR (2009). IF(1): setting the pace of the F(1)F(o)-ATP synthase. *Trends Biochem Sci* **34:** 343-50.

Carlucci A, Lignitto L, Feliciello A (2008). Control of mitochondria dynamics and oxidative metabolism by cAMP, AKAPs and the proteasome. *Trends Cell Biol* **18:** 604-13.

Chan KK, Chan JY, Chung KK, Fung KP (2004). Inhibition of cell proliferation in human breast tumor cells by antisense oligonucleotides against facilitative glucose transporter 5. *J Cell Biochem* **93:** 1134-42.

Chang CR, Blackstone C (2007). Cyclic AMP-dependent protein kinase phosphorylation of Drp1 regulates its GTPase activity and mitochondrial morphology. *J Biol Chem* **282:** 21583-7.

Chen CT, Hsu SH, Wei YH (2010a). Upregulation of mitochondrial function and antioxidant defense in the differentiation of stem cells. *Biochim Biophys Acta* **1800:** 257-63.

Chen CT, Shih YR, Kuo TK, Lee OK, Wei YH (2008). Coordinated changes of mitochondrial biogenesis and antioxidant enzymes during osteogenic differentiation of human mesenchymal stem cells. *Stem Cells* **26:** 960-8.

Chen H, Chomyn A, Chan DC (2005). Disruption of fusion results in mitochondrial heterogeneity and dysfunction. *J Biol Chem* **280:** 26185-92.

Chen H, Vermulst M, Wang YE, Chomyn A, Prolla TA, McCaffery JM *et al* (2010b). Mitochondrial fusion is required for mtDNA stability in skeletal muscle and tolerance of mtDNA mutations. *Cell* **141:** 280-9.

Cheng L, Alexander R, Zhang S, Pan CX, MacLennan GT, Lopez-Beltran A *et al* (2011). The clinical and therapeutic implications of cancer stem cell biology. *Expert Rev Anticancer Ther* **11:** 1131-43.

Cheong JH, Park ES, Liang J, Dennison JB, Tsavachidou D, Nguyen-Charles C *et al* (2011). Dual inhibition of tumor energy pathway by 2-deoxyglucose and metformin is effective against a broad spectrum of preclinical cancer models. *Mol Cancer Ther* **10:** 2350-62.

Chevrollier A, Loiseau D, Chabi B, Renier G, Douay O, Malthiery Y *et al* (2005). ANT2 isoform required for cancer cell glycolysis. *J Bioenerg Biomembr* **37:** 307-16.

Chiaradonna F, Balestrieri C, Gaglio D, Vanoni M (2008). RAS and PKA pathways in cancer: new insight from transcriptional analysis. *Front Biosci* **13:** 5257-78.

Chiaradonna F, Gaglio D, Vanoni M, Alberghina L (2006a). Expression of transforming K-Ras oncogene affects mitochondrial function and morphology in mouse fibroblasts. *Biochim Biophys Acta* **1757:** 1338-56.

Chiaradonna F, Moresco RM, Airoldi C, Gaglio D, Palorini R, Nicotra F *et al* (2012). From cancer metabolism to new biomarkers and drug targets. *Biotechnol Adv* **30:** 30-51.

Chiaradonna F, Sacco E, Manzoni R, Giorgio M, Vanoni M, Alberghina L (2006b). Ras-dependent carbon metabolism and transformation in mouse fibroblasts. *Oncogene* **25:** 5391-404.

Chijiwa T, Mishima A, Hagiwara M, Sano M, Hayashi K, Inoue T *et al* (1990). Inhibition of forskolin-induced neurite outgrowth and protein phosphorylation by a newly synthesized selective inhibitor of cyclic AMP-dependent protein kinase, N-[2-(p-bromocinnamylamino)ethyl]-5-isoquinolinesulfonamide (H-89), of PC12D pheochromocytoma cells. *J Biol Chem* **265:** 5267-72.

Cho RW, Clarke MF (2008). Recent advances in cancer stem cells. *Curr Opin Genet Dev* **18:** 48-53.

Cho YM, Kwon S, Pak YK, Seol HW, Choi YM, Park do J *et al* (2006). Dynamic changes in mitochondrial biogenesis and antioxidant enzymes during the spontaneous differentiation of human embryonic stem cells. *Biochem Biophys Res Commun* **348:** 1472-8.

Choi WS, Palmiter RD, Xia Z (2011). Loss of mitochondrial complex I activity potentiates dopamine neuron death induced by microtubule dysfunction in a Parkinson's disease model. *J Cell Biol* **192:** 873-82.

Choi Y, Lee JH (2011). The combination of tephrosin with 2-deoxy-D-glucose enhances the cytotoxicity via accelerating ATP depletion and blunting autophagy in human cancer cells. *Cancer Biol Ther* **12:** 989-96.

Christofk HR, Vander Heiden MG, Harris MH, Ramanathan A, Gerszten RE, Wei R *et al* (2008). The M2 splice isoform of pyruvate kinase is important for cancer metabolism and tumour growth. *Nature* **452:** 230-3.

Clarke MF, Dick JE, Dirks PB, Eaves CJ, Jamieson CH, Jones DL *et al* (2006). Cancer stem cells--perspectives on current status and future directions: AACR Workshop on cancer stem cells. *Cancer Res* **66:** 9339-44.

Cribbs JT, Strack S (2007). Reversible phosphorylation of Drp1 by cyclic AMP-dependent protein kinase and calcineurin regulates mitochondrial fission and cell death. *EMBO Rep* **8:** 939-44.

Cuezva JM, Krajewska M, de Heredia ML, Krajewski S, Santamaria G, Kim H *et al* (2002). The bioenergetic signature of cancer: a marker of tumor progression. *Cancer Res* **62:** 6674-81.

Das UN (2006). Pyruvate is an endogenous anti-inflammatory and anti-oxidant molecule. *Med Sci Monit* **12:** RA79-84.

De Rasmo D, Gattoni G, Papa F, Santeramo A, Pacelli C, Cocco T *et al* (2011). The beta-adrenoceptor agonist isoproterenol promotes the activity of respiratory chain complex I and lowers cellular reactive oxygen species in fibroblasts and heart myoblasts. *Eur J Pharmacol* **652:** 15-22.

De Rasmo D, Panelli D, Sardanelli AM, Papa S (2008). cAMP-dependent protein kinase regulates the mitochondrial import of the nuclear encoded NDUFS4 subunit of complex I. *Cell Signal* **20:** 989-97.

De Rasmo D, Signorile A, Papa F, Roca E, Papa S (2010). cAMP/Ca2+ response element-binding protein plays a central role in the biogenesis of respiratory chain proteins in mammalian cells. *IUBMB Life* **62:** 447-52.

DeBerardinis RJ, Cheng T (2010). Q's next: the diverse functions of glutamine in metabolism, cell biology and cancer. *Oncogene* **29:** 313-24.

DeBerardinis RJ, Mancuso A, Daikhin E, Nissim I, Yudkoff M, Wehrli S *et al* (2007). Beyond aerobic glycolysis: transformed cells can engage in glutamine metabolism that exceeds the requirement for protein and nucleotide synthesis. *Proc Natl Acad Sci U S A* **104:** 19345-50.

Deberardinis RJ, Sayed N, Ditsworth D, Thompson CB (2008). Brick by brick: metabolism and tumor cell growth. *Curr Opin Genet Dev* **18:** 54-61.

Deng YT, Huang HC, Lin JK (2010). Rotenone induces apoptosis in MCF-7 human breast cancer cell-mediated ROS through JNK and p38 signaling. *Mol Carcinog* **49:** 141-51.

Dennis JW, Kosh K, Bryce DM, Breitman ML (1989). Oncogenes conferring metastatic potential induce increased branching of Asn-linked oligosaccharides in rat2 fibroblasts. *Oncogene* **4:** 853-60.

Dewhirst MW, Cao Y, Moeller B (2008). Cycling hypoxia and free radicals regulate angiogenesis and radiotherapy response. *Nat Rev Cancer* **8:** 425-37.

Di Fiore R, Fanale D, Drago-Ferrante R, Chiaradonna F, Giuliano M, De Blasio A *et al* (2012a). Genetic and molecular characterization of the human osteosarcoma 3AB-OS cancer stem cell line: A possible model for studying osteosarcoma origin and stemness. *J Cell Physiol*.

Di Fiore R, Guercio A, Puleio R, Di Marco P, Drago-Ferrante R, D'Anneo A *et al* (2012b). Modeling human osteosarcoma in mice through 3AB-OS cancer stem cell xenografts. *J Cell Biochem* **113:** 3380-92.

Di Fiore R, Santulli A, Ferrante RD, Giuliano M, De Blasio A, Messina C *et al* (2009). Identification and expansion of human osteosarcoma-cancer-stem cells by long-term 3-aminobenzamide treatment. *J Cell Physiol* **219:** 301-13.

Diehn M, Clarke MF (2006). Cancer stem cells and radiotherapy: new insights into tumor radioresistance. *J Natl Cancer Inst* **98:** 1755-7.

Duvel K, Yecies JL, Menon S, Raman P, Lipovsky AI, Souza AL *et al* (2010). Activation of a metabolic gene regulatory network downstream of mTOR complex 1. *Mol Cell* **39:** 171-83.

Facucho-Oliveira JM, St John JC (2009). The relationship between pluripotency and mitochondrial DNA proliferation during early embryo development and embryonic stem cell differentiation. *Stem Cell Rev* **5:** 140-58.

Fan J, Hitosugi T, Chung TW, Xie J, Ge Q, Gu TL *et al* (2011). Tyrosine phosphorylation of lactate dehydrogenase A is important for NADH/NAD(+) redox homeostasis in cancer cells. *Mol Cell Biol* **31:** 4938-50.

Fang M, Shen Z, Huang S, Zhao L, Chen S, Mak TW *et al* (2010). The ER UDPase ENTPD5 promotes protein N-glycosylation, the Warburg effect, and proliferation in the PTEN pathway. *Cell* **143:** 711-24.

Fang X, Yu SX, Lu Y, Bast RC, Jr., Woodgett JR, Mills GB (2000). Phosphorylation and inactivation of glycogen synthase kinase 3 by protein kinase A. *Proc Natl Acad Sci U S A* **97:** 11960-5.

Fantin VR, Leder P (2006). Mitochondriotoxic compounds for cancer therapy. *Oncogene* **25:** 4787-97.

Fantin VR, St-Pierre J, Leder P (2006). Attenuation of LDH-A expression uncovers a link between glycolysis, mitochondrial physiology, and tumor maintenance. *Cancer Cell* **9:** 425-34.

Fath MA, Diers AR, Aykin-Burns N, Simons AL, Hua L, Spitz DR (2009). Mitochondrial electron transport chain blockers enhance 2-deoxy-D-glucose induced oxidative stress and cell killing in human colon carcinoma cells. *Cancer Biol Ther* **8:** 1228-36.

Favaro E, Bensaad K, Chong MG, Tennant DA, Ferguson DJ, Snell C *et al* (2012). Glucose Utilization via Glycogen Phosphorylase Sustains Proliferation and Prevents Premature Senescence in Cancer Cells. *Cell Metab* **16:** 751-64.

Feliciello A, Giuliano P, Porcellini A, Garbi C, Obici S, Mele E *et al* (1996). The v-Ki-Ras oncogene alters cAMP nuclear signaling by regulating the location and the expression of cAMP-dependent protein kinase IIbeta. *J Biol Chem* **271:** 25350-9.

Fillmore CM, Kuperwasser C (2008). Human breast cancer cell lines contain stem-like cells that self-renew, give rise to phenotypically diverse progeny and survive chemotherapy. *Breast Cancer Res* **10:** R25.

Fuster MM, Esko JD (2005). The sweet and sour of cancer: glycans as novel therapeutic targets. *Nat Rev Cancer* **5:** 526-42.

Gaglio D, Metallo CM, Gameiro PA, Hiller K, Danna LS, Balestrieri C *et al* (2011). Oncogenic K-Ras decouples glucose and glutamine metabolism to support cancer cell growth. *Mol Syst Biol* **7:** 523.

Gaglio D, Soldati C, Vanoni M, Alberghina L, Chiaradonna F (2009). Glutamine deprivation induces abortive s-phase rescued by deoxyribonucleotides in k-ras transformed fibroblasts. *PLoS One* **4:** e4715.

Gallo A, Feliciello A, Varrone A, Cerillo R, Gottesman ME, Avvedimento VE (1995). Ki-ras oncogene interferes with the expression of cyclic AMP-dependent promoters. *Cell Growth Differ* **6:** 91-5.

Gao P, Tchernyshyov I, Chang TC, Lee YS, Kita K, Ochi T *et al* (2009). c-Myc suppression of miR-23a/b enhances mitochondrial glutaminase expression and glutamine metabolism. *Nature* **458:** 762-5.

Gatenby RA, Gillies RJ (2004). Why do cancers have high aerobic glycolysis? *Nat Rev Cancer* **4:** 891-9.

Gerits N, Kostenko S, Shiryaev A, Johannessen M, Moens U (2008). Relations between the mitogen-activated protein kinase and the cAMP-dependent protein kinase pathways: comradeship and hostility. *Cell Signal* **20:** 1592-607.

Gillies RJ, Robey I, Gatenby RA (2008). Causes and consequences of increased glucose metabolism of cancers. *J Nucl Med* **49 Suppl 2:** 24S-42S.

Gogvadze V, Orrenius S, Zhivotovsky B (2008). Mitochondria in cancer cells: what is so special about them? *Trends Cell Biol* **18:** 165-73.

Gomes LC, Di Benedetto G, Scorrano L (2011). During autophagy mitochondria elongate, are spared from degradation and sustain cell viability. *Nat Cell Biol* **13:** 589-98.

Gorman AM, Healy SJ, Jager R, Samali A (2012). Stress management at the ER: regulators of ER stress-induced apoptosis. *Pharmacol Ther* **134:** 306-16.

Gottlob K, Majewski N, Kennedy S, Kandel E, Robey RB, Hay N (2001). Inhibition of early apoptotic events by Akt/PKB is dependent on the first committed step of glycolysis and mitochondrial hexokinase. *Genes Dev* **15:** 1406-18.

Graham NA, Tahmasian M, Kohli B, Komisopoulou E, Zhu M, Vivanco I *et al* (2012). Glucose deprivation activates a metabolic and signaling amplification loop leading to cell death. *Mol Syst Biol* **8:** 589.

Grandemange S, Herzig S, Martinou JC (2009). Mitochondrial dynamics and cancer. *Semin Cancer Biol* **19:** 50-6.

Guppy M, Greiner E, Brand K (1993). The role of the Crabtree effect and an endogenous fuel in the energy metabolism of resting and proliferating thymocytes. *Eur J Biochem* **212:** 95-9.

Gysin S, Salt M, Young A, McCormick F (2011). Therapeutic strategies for targeting ras proteins. *Genes Cancer* **2:** 359-72.

Hanahan D, Weinberg RA (2011). Hallmarks of cancer: the next generation. *Cell* **144:** 646-74.

Harris AL (2002). Hypoxia--a key regulatory factor in tumour growth. *Nat Rev Cancer* **2:** 38-47.

Hart GW, Copeland RJ (2010). Glycomics hits the big time. *Cell* **143:** 672-6.

He X, Cao X (2010). Identification of alternatively spliced GRIM-19 mRNA in kidney cancer tissues. *J Hum Genet* **55:** 507-11.

Hervouet E, Demont J, Pecina P, Vojtiskova A, Houstek J, Simonnet H *et al* (2005). A new role for the von Hippel-Lindau tumor suppressor protein: stimulation of mitochondrial oxidative phosphorylation complex biogenesis. *Carcinogenesis* **26:** 531-9.

Hetz C (2012). The unfolded protein response: controlling cell fate decisions under ER stress and beyond. *Nat Rev Mol Cell Biol* **13:** 89-102.

Higuchi M (2007). Regulation of mitochondrial DNA content and cancer. *Mitochondrion* **7:** 53-7.

Hitosugi T, Fan J, Chung TW, Lythgoe K, Wang X, Xie J *et al* (2011). Tyrosine phosphorylation of mitochondrial pyruvate dehydrogenase kinase 1 is important for cancer metabolism. *Mol Cell* **44:** 864-77.

Ho MM, Ng AV, Lam S, Hung JY (2007). Side population in human lung cancer cell lines and tumors is enriched with stem-like cancer cells. *Cancer Res* **67:** 4827-33.

Hom JR, Quintanilla RA, Hoffman DL, de Mesy Bentley KL, Molkentin JD, Sheu SS *et al* (2011). The permeability transition pore controls cardiac mitochondrial maturation and myocyte differentiation. *Dev Cell* **21:** 469-78.

Hopper RK, Carroll S, Aponte AM, Johnson DT, French S, Shen RF *et al* (2006). Mitochondrial matrix phosphoproteome: effect of extra mitochondrial calcium. *Biochemistry* **45:** 2524-36.

Hu Y, Suarez J, Fricovsky E, Wang H, Scott BT, Trauger SA *et al* (2009). Increased enzymatic O-GlcNAcylation of mitochondrial proteins impairs mitochondrial function in cardiac myocytes exposed to high glucose. *J Biol Chem* **284:** 547-55.

Huang D, Gao Q, Guo L, Zhang C, Jiang W, Li H *et al* (2009). Isolation and identification of cancer stem-like cells in esophageal carcinoma cell lines. *Stem Cells Dev* **18:** 465-73.

Ibsen KH (1961). The Crabtree effect: a review. *Cancer Res* **21:** 829-41.

Indo HP, Davidson M, Yen HC, Suenaga S, Tomita K, Nishii T *et al* (2007). Evidence of ROS generation by mitochondria in cells with impaired electron transport chain and mitochondrial DNA damage. *Mitochondrion* **7:** 106-18.

Ishikawa K, Takenaga K, Akimoto M, Koshikawa N, Yamaguchi A, Imanishi H *et al* (2008). ROS-generating mitochondrial DNA mutations can regulate tumor cell metastasis. *Science* **320:** 661-4.

Isidoro A, Martinez M, Fernandez PL, Ortega AD, Santamaria G, Chamorro M *et al* (2004). Alteration of the bioenergetic phenotype of mitochondria is a hallmark of breast, gastric, lung and oesophageal cancer. *Biochem J* **378:** 17-20.

Jager R, Bertrand MJ, Gorman AM, Vandenabeele P, Samali A (2012). The unfolded protein response at the crossroads of cellular life and death during endoplasmic reticulum stress. *Biol Cell* **104:** 259-70.

Jones RG, Thompson CB (2009). Tumor suppressors and cell metabolism: a recipe for cancer growth. *Genes Dev* **23:** 537-48.

Kaufman RJ, Scheuner D, Schroder M, Shen X, Lee K, Liu CY *et al* (2002). The unfolded protein response in nutrient sensing and differentiation. *Nat Rev Mol Cell Biol* **3:** 411-21.

Kelly PN, Dakic A, Adams JM, Nutt SL, Strasser A (2007). Tumor growth need not be driven by rare cancer stem cells. *Science* **317:** 337.

Kim CH, Han SI, Lee SY, Youk HS, Moon JY, Duong HQ *et al* (2007a). Protein kinase C-ERK1/2 signal pathway switches glucose depletion-induced necrosis to apoptosis by regulating superoxide dismutases and suppressing reactive oxygen species production in A549 lung cancer cells. *J Cell Physiol* **211:** 371-85.

Kim HK, Park WS, Kang SH, Warda M, Kim N, Ko JH *et al* (2007b). Mitochondrial alterations in human gastric carcinoma cell line. *Am J Physiol Cell Physiol* **293:** C761-71.

Kim JW, Tchernyshyov I, Semenza GL, Dang CV (2006). HIF-1-mediated expression of pyruvate dehydrogenase kinase: a metabolic switch required for cellular adaptation to hypoxia. *Cell Metab* **3:** 177-85.

Kondoh H, Lleonart ME, Gil J, Wang J, Degan P, Peters G *et al* (2005). Glycolytic enzymes can modulate cellular life span. *Cancer Res* **65:** 177-85.

Koopman WJ, Verkaart S, Visch HJ, van Emst-de Vries S, Nijtmans LG, Smeitink JA *et al* (2007). Human NADH:ubiquinone oxidoreductase deficiency: radical changes in mitochondrial morphology? *Am J Physiol Cell Physiol* **293:** C22-9.

Krieg RC, Knuechel R, Schiffmann E, Liotta LA, Petricoin EF, 3rd, Herrmann PC (2004). Mitochondrial proteome: cancer-altered metabolism associated with cytochrome c oxidase subunit level variation. *Proteomics* **4:** 2789-95.

Kroemer G, Pouyssegur J (2008). Tumor cell metabolism: cancer's Achilles' heel. *Cancer Cell* **13:** 472-82.

Lee HC, Wei YH (2009). Mitochondrial DNA instability and metabolic shift in human cancers. *Int J Mol Sci* **10:** 674-701.

Lenaz G, Baracca A, Barbero G, Bergamini C, Dalmonte ME, Del Sole M *et al* (2010). Mitochondrial respiratory chain super-complex I-III in physiology and pathology. *Biochim Biophys Acta* **1797:** 633-40.

Levine AJ, Puzio-Kuter AM (2010). The control of the metabolic switch in cancers by oncogenes and tumor suppressor genes. *Science* **330:** 1340-4.

Lieberthal W, Menza SA, Levine JS (1998). Graded ATP depletion can cause necrosis or apoptosis of cultured mouse proximal tubular cells. *Am J Physiol* **274:** F315-27.

Linker W, Loffler M, Schneider F (1985). Uridine, but not cytidine can sustain growth of Ehrlich ascites tumor cells in glucose-deprived medium with altered proliferation kinetics. *Eur J Cell Biol* **36:** 176-81.

Lopez-Rios F, Sanchez-Arago M, Garcia-Garcia E, Ortega AD, Berrendero JR, Pozo-Rodriguez F *et al* (2007). Loss of the mitochondrial bioenergetic capacity underlies the glucose avidity of carcinomas. *Cancer Res* **67:** 9013-7.

Lunt SY, Vander Heiden MG (2011). Aerobic glycolysis: meeting the metabolic requirements of cell proliferation. *Annu Rev Cell Dev Biol* **27:** 441-64.

Maher JC, Krishan A, Lampidis TJ (2004). Greater cell cycle inhibition and cytotoxicity induced by 2-deoxy-D-glucose in tumor cells treated under hypoxic vs aerobic conditions. *Cancer Chemother Pharmacol* **53:** 116-22.

Mandal S, Lindgren AG, Srivastava AS, Clark AT, Banerjee U (2011). Mitochondrial function controls proliferation and early differentiation potential of embryonic stem cells. *Stem Cells* **29:** 486-95.

Marciniak SJ, Yun CY, Oyadomari S, Novoa I, Zhang Y, Jungreis R *et al* (2004). CHOP induces death by promoting protein synthesis and oxidation in the stressed endoplasmic reticulum. *Genes Dev* **18:** 3066-77.

Martins-Neves SR, Lopes AO, do Carmo A, Paiva AA, Simoes PC, Abrunhosa AJ *et al* (2012). Therapeutic implications of an enriched cancer stem-like cell population in a human osteosarcoma cell line. *BMC Cancer* **12:** 139.

Maschek G, Savaraj N, Priebe W, Braunschweiger P, Hamilton K, Tidmarsh GF *et al* (2004). 2-deoxy-D-glucose increases the efficacy of adriamycin and paclitaxel in human osteosarcoma and non-small cell lung cancers in vivo. *Cancer Res* **64:** 31-4.

Mathupala SP, Ko YH, Pedersen PL (2006). Hexokinase II: cancer's double-edged sword acting as both facilitator and gatekeeper of malignancy when bound to mitochondria. *Oncogene* **25:** 4777-86.

Matoba S, Kang JG, Patino WD, Wragg A, Boehm M, Gavrilova O *et al* (2006). p53 regulates mitochondrial respiration. *Science* **312:** 1650-3.

Mazurek S, Boschek CB, Hugo F, Eigenbrodt E (2005). Pyruvate kinase type M2 and its role in tumor growth and spreading. *Semin Cancer Biol* **15:** 300-8.

McClain DA (2002). Hexosamines as mediators of nutrient sensing and regulation in diabetes. *J Diabetes Complications* **16:** 72-80.

McFate T, Mohyeldin A, Lu H, Thakar J, Henriques J, Halim ND *et al* (2008). Pyruvate dehydrogenase complex activity controls metabolic and malignant phenotype in cancer cells. *J Biol Chem* **283:** 22700-8.

Meldolesi MF, Macchia V, Laccetti P (1976). Differences in phosphofructokinase regulation in normal and tumor rat thyroid cells. *J Biol Chem* **251:** 6244-51.

Mellanen P, Minn H, Grenman R, Harkonen P (1994). Expression of glucose transporters in head-and-neck tumors. *Int J Cancer* **56:** 622-9.

Metallo CM, Gameiro PA, Bell EL, Mattaini KR, Yang J, Hiller K *et al* (2011). Reductive glutamine metabolism by IDH1 mediates lipogenesis under hypoxia. *Nature* **481:** 380-4.

Mitra K, Wunder C, Roysam B, Lin G, Lippincott-Schwartz J (2009). A hyperfused mitochondrial state achieved at G1-S regulates cyclin E buildup and entry into S phase. *Proc Natl Acad Sci U S A* **106:** 11960-5.

Mitra N, Sinha S, Ramya TN, Surolia A (2006). N-linked oligosaccharides as outfitters for glycoprotein folding, form and function. *Trends Biochem Sci* **31:** 156-63.

Moiseeva O, Bourdeau V, Roux A, Deschenes-Simard X, Ferbeyre G (2009). Mitochondrial dysfunction contributes to oncogene-induced senescence. *Mol Cell Biol* **29:** 4495-507.

Nagase Y, Takata K, Moriyama N, Aso Y, Murakami T, Hirano H (1995). Immunohistochemical localization of glucose transporters in human renal cell carcinoma. *J Urol* **153:** 798-801.

Nam SY, Amoscato AA, Lee YJ (2002). Low glucose-enhanced TRAIL cytotoxicity is mediated through the ceramide-Akt-FLIP pathway. *Oncogene* **21:** 337-46.

Nath KA, Ngo EO, Hebbel RP, Croatt AJ, Zhou B, Nutter LM (1995). alpha-Ketoacids scavenge H2O2 in vitro and in vivo and reduce menadione-induced DNA injury and cytotoxicity. *Am J Physiol* **268:** C227-36.

Neuzil J, Dyason JC, Freeman R, Dong LF, Prochazka L, Wang XF *et al* (2007). Mitocans as anti-cancer agents targeting mitochondria: lessons from studies with vitamin E analogues, inhibitors of complex II. *J Bioenerg Biomembr* **39:** 65-72.

Nomura K, Imai H, Koumura T, Arai M, Nakagawa Y (1999). Mitochondrial phospholipid hydroperoxide glutathione peroxidase suppresses apoptosis mediated by a mitochondrial death pathway. *J Biol Chem* **274:** 29294-302.

O'Brien CA, Kreso A, Jamieson CH (2010). Cancer stem cells and self-renewal. *Clin Cancer Res* **16:** 3113-20.

Okar DA, Lange AJ (1999). Fructose-2,6-bisphosphate and control of carbohydrate metabolism in eukaryotes. *Biofactors* **10:** 1-14.

Okar DA, Manzano A, Navarro-Sabate A, Riera L, Bartrons R, Lange AJ (2001). PFK-2/FBPase-2: maker and breaker of the essential biofactor fructose-2,6-bisphosphate. *Trends Biochem Sci* **26:** 30-5.

Okun JG, Lummen P, Brandt U (1999). Three classes of inhibitors share a common binding domain in mitochondrial complex I (NADH:ubiquinone oxidoreductase). *J Biol Chem* **274:** 2625-30.

Oskam R, Rijksen G, Staal GE, Vora S (1985). Isozymic composition and regulatory properties of phosphofructokinase from well-differentiated and anaplastic medullary thyroid carcinomas of the rat. *Cancer Res* **45:** 135-42.

Osthus RC, Shim H, Kim S, Li Q, Reddy R, Mukherjee M *et al* (2000). Deregulation of glucose transporter 1 and glycolytic gene expression by c-Myc. *J Biol Chem* **275:** 21797-800.

Pagliarini DJ, Dixon JE (2006). Mitochondrial modulation: reversible phosphorylation takes center stage? *Trends Biochem Sci* **31:** 26-34.

Palmer CS, Osellame LD, Stojanovski D, Ryan MT (2011). The regulation of mitochondrial morphology: intricate mechanisms and dynamic machinery. *Cell Signal* **23:** 1534-45.

Papa S, De Rasmo D, Scacco S, Signorile A, Technikova-Dobrova Z, Palmisano G *et al* (2008). Mammalian complex I: a regulable and vulnerable pacemaker in mitochondrial respiratory function. *Biochim Biophys Acta* **1777:** 719-28.

Papa S, Zanotti F, Cocco T, Perrucci C, Candita C, Minuto M (1996). Identification of functional domains and critical residues in the adenosinetriphosphatase inhibitor protein of mitochondrial F0F1 ATP synthase. *Eur J Biochem* **240:** 461-7.

Parsons SJ, Parsons JT (2004). Src family kinases, key regulators of signal transduction. *Oncogene* **23:** 7906-9.

Pathania D, Millard M, Neamati N (2009). Opportunities in discovery and delivery of anticancer drugs targeting mitochondria and cancer cell metabolism. *Adv Drug Deliv Rev* **61:** 1250-75.

Pelicano H, Martin DS, Xu RH, Huang P (2006). Glycolysis inhibition for anticancer treatment. *Oncogene* **25:** 4633-46.

Penta JS, Johnson FM, Wachsman JT, Copeland WC (2001). Mitochondrial DNA in human malignancy. *Mutat Res* **488:** 119-33.

Piccoli C, Ria R, Scrima R, Cela O, D'Aprile A, Boffoli D *et al* (2005). Characterization of mitochondrial and extra-mitochondrial oxygen consuming reactions in human hematopoietic stem cells. Novel evidence of the occurrence of NAD(P)H oxidase activity. *J Biol Chem* **280:** 26467-76.

Piccoli C, Scacco S, Bellomo F, Signorile A, Iuso A, Boffoli D *et al* (2006). cAMP controls oxygen metabolism in mammalian cells. *FEBS Lett* **580:** 4539-43.

Pramanik KC, Boreddy SR, Srivastava SK (2011). Role of mitochondrial electron transport chain complexes in capsaicin mediated oxidative stress leading to apoptosis in pancreatic cancer cells. *PLoS One* **6:** e20151.

Prigione A, Adjaye J (2010). Modulation of mitochondrial biogenesis and bioenergetic metabolism upon in vitro and in vivo differentiation of human ES and iPS cells. *Int J Dev Biol* **54:** 1729-41.

Prigione A, Fauler B, Lurz R, Lehrach H, Adjaye J (2010). The senescence-related mitochondrial/oxidative stress pathway is repressed in human induced pluripotent stem cells. *Stem Cells* **28:** 721-33.

Pulciani S, Santos E, Long LK, Sorrentino V, Barbacid M (1985). ras gene Amplification and malignant transformation. *Mol Cell Biol* **5:** 2836-41.

Qiang L, Yang Y, Ma YJ, Chen FH, Zhang LB, Liu W *et al* (2009). Isolation and characterization of cancer stem like cells in human glioblastoma cell lines. *Cancer Lett* **279:** 13-21.

Rak JW, Basolo F, Elliott JW, Russo J, Miller FR (1991). Cell surface glycosylation changes accompanying immortalization and transformation of normal human mammary epithelial cells. *Cancer Lett* **57:** 27-36.

Ralph SJ, Low P, Dong L, Lawen A, Neuzil J (2006). Mitocans: mitochondrial targeted anti-cancer drugs as improved therapies and related patent documents. *Recent Pat Anticancer Drug Discov* **1:** 327-46.

Ramanathan A, Wang C, Schreiber SL (2005). Perturbational profiling of a cell-line model of tumorigenesis by using metabolic measurements. *Proc Natl Acad Sci U S A* **102:** 5992-7.

Rambold AS, Kostelecky B, Elia N, Lippincott-Schwartz J (2011a). Tubular network formation protects mitochondria from autophagosomal degradation during nutrient starvation. *Proc Natl Acad Sci U S A* **108:** 10190-5.

Rambold AS, Kostelecky B, Lippincott-Schwartz J (2011b). Fuse or die: Shaping mitochondrial fate during starvation. *Commun Integr Biol* **4:** 752-4.

Reitzer LJ, Wice BM, Kennell D (1979). Evidence that glutamine, not sugar, is the major energy source for cultured HeLa cells. *J Biol Chem* **254:** 2669-76.

Richter C, Park JW, Ames BN (1988). Normal oxidative damage to mitochondrial and nuclear DNA is extensive. *Proc Natl Acad Sci U S A* **85:** 6465-7.

Rodenhuis S (1992). ras and human tumors. *Semin Cancer Biol* **3:** 241-7.

Romero-Fernandez W, Borroto-Escuela DO, Alea MP, Garcia-Mesa Y, Garriga P (2011). Altered trafficking and unfolded protein response induction as a result of M3 muscarinic receptor impaired N-glycosylation. *Glycobiology* **21:** 1663-72.

Ron D, Walter P (2007). Signal integration in the endoplasmic reticulum unfolded protein response. *Nat Rev Mol Cell Biol* **8:** 519-29.

Ross DT, Scherf U, Eisen MB, Perou CM, Rees C, Spellman P *et al* (2000). Systematic variation in gene expression patterns in human cancer cell lines. *Nat Genet* **24:** 227-35.

Salceda S, Caro J (1997). Hypoxia-inducible factor 1alpha (HIF-1alpha) protein is rapidly degraded by the ubiquitin-proteasome system under normoxic conditions. Its stabilization by hypoxia depends on redox-induced changes. *J Biol Chem* **272:** 22642-7.

Sandulache VC, Ow TJ, Pickering CR, Frederick MJ, Zhou G, Fokt I *et al* (2011). Glucose, not glutamine, is the dominant energy source required for

proliferation and survival of head and neck squamous carcinoma cells. *Cancer* **117:** 2926-38.

Sauvanet C, Duvezin-Caubet S, di Rago JP, Rojo M (2010). Energetic requirements and bioenergetic modulation of mitochondrial morphology and dynamics. *Semin Cell Dev Biol* **21:** 558-65.

Schulz TJ, Thierbach R, Voigt A, Drewes G, Mietzner B, Steinberg P *et al* (2006). Induction of oxidative metabolism by mitochondrial frataxin inhibits cancer growth: Otto Warburg revisited. *J Biol Chem* **281:** 977-81.

Schulze A, Downward J (2011). Flicking the Warburg switch-tyrosine phosphorylation of pyruvate dehydrogenase kinase regulates mitochondrial activity in cancer cells. *Mol Cell* **44:** 846-8.

Semenza GL (2010a). Defining the role of hypoxia-inducible factor 1 in cancer biology and therapeutics. *Oncogene* **29:** 625-34.

Semenza GL (2010b). HIF-1: upstream and downstream of cancer metabolism. *Curr Opin Genet Dev* **20:** 51-6.

Shim H, Dolde C, Lewis BC, Wu CS, Dang G, Jungmann RA *et al* (1997). c-Myc transactivation of LDH-A: implications for tumor metabolism and growth. *Proc Natl Acad Sci U S A* **94:** 6658-63.

Shoemaker RH (2006). The NCI60 human tumour cell line anticancer drug screen. *Nat Rev Cancer* **6:** 813-23.

Simons AL, Mattson DM, Dornfeld K, Spitz DR (2009). Glucose deprivation-induced metabolic oxidative stress and cancer therapy. *J Cancer Res Ther* **5 Suppl 1:** S2-6.

Slawson C, Copeland RJ, Hart GW (2010). O-GlcNAc signaling: a metabolic link between diabetes and cancer? *Trends Biochem Sci* **35:** 547-55.

Staal GE, Kalff A, Heesbeen EC, van Veelen CW, Rijksen G (1987). Subunit composition, regulatory properties, and phosphorylation of phosphofructokinase from human gliomas. *Cancer Res* **47:** 5047-51.

Tabas I, Ron D (2011). Integrating the mechanisms of apoptosis induced by endoplasmic reticulum stress. *Nat Cell Biol* **13:** 184-90.

Tang C, Ang BT, Pervaiz S (2007). Cancer stem cell: target for anti-cancer therapy. *FASEB J* **21:** 3777-85.

Telang S, Yalcin A, Clem AL, Bucala R, Lane AN, Eaton JW *et al* (2006). Ras transformation requires metabolic control by 6-phosphofructo-2-kinase. *Oncogene* **25:** 7225-34.

Tennant DA, Duran RV, Boulahbel H, Gottlieb E (2009). Metabolic transformation in cancer. *Carcinogenesis* **30:** 1269-80.

Tennant DA, Duran RV, Gottlieb E (2010). Targeting metabolic transformation for cancer therapy. *Nat Rev Cancer* **10:** 267-77.

Tibaldi E, Brunati AM, Massimino ML, Stringaro A, Colone M, Agostinelli E *et al* (2008). Src-Tyrosine kinases are major agents in mitochondrial tyrosine phosphorylation. *J Cell Biochem* **104:** 840-9.

Twig G, Elorza A, Molina AJ, Mohamed H, Wikstrom JD, Walzer G *et al* (2008). Fission and selective fusion govern mitochondrial segregation and elimination by autophagy. *EMBO J* **27:** 433-46.

Urano F, Wang X, Bertolotti A, Zhang Y, Chung P, Harding HP *et al* (2000). Coupling of stress in the ER to activation of JNK protein kinases by transmembrane protein kinase IRE1. *Science* **287:** 664-6.

Vander Heiden MG (2011). Targeting cancer metabolism: a therapeutic window opens. *Nat Rev Drug Discov* **10:** 671-84.

Vander Heiden MG, Locasale JW, Swanson KD, Sharfi H, Heffron GJ, Amador-Noguez D *et al* (2010). Evidence for an alternative glycolytic pathway in rapidly proliferating cells. *Science* **329:** 1492-9.

Varum S, Momcilovic O, Castro C, Ben-Yehudah A, Ramalho-Santos J, Navara CS (2009). Enhancement of human embryonic stem cell pluripotency through inhibition of the mitochondrial respiratory chain. *Stem Cell Res* **3:** 142-56.

Varum S, Rodrigues AS, Moura MB, Momcilovic O, Easley CAt, Ramalho-Santos J *et al* (2011). Energy metabolism in human pluripotent stem cells and their differentiated counterparts. *PLoS One* **6:** e20914.

Vigano A, Vasso M, Caretti A, Bravata V, Terraneo L, Fania C *et al* (2011). Protein modulation in mouse heart under acute and chronic hypoxia. *Proteomics* **11:** 4202-17.

Vizan P, Boros LG, Figueras A, Capella G, Mangues R, Bassilian S *et al* (2005). K-ras codon-specific mutations produce distinctive metabolic phenotypes in NIH3T3 mice [corrected] fibroblasts. *Cancer Res* **65:** 5512-5.

Vora S, Halper JP, Knowles DM (1985). Alterations in the activity and isozymic profile of human phosphofructokinase during malignant transformation in vivo and in vitro: transformation- and progression-linked discriminants of malignancy. *Cancer Res* **45:** 2993-3001.

Wang X, Perez E, Liu R, Yan LJ, Mallet RT, Yang SH (2007). Pyruvate protects mitochondria from oxidative stress in human neuroblastoma SK-N-SH cells. *Brain Res* **1132:** 1-9.

Warburg O (1956). On the origin of cancer cells. *Science* **123:** 309-14.

Wei Y, Sinha S, Levine B (2008). Dual role of JNK1-mediated phosphorylation of Bcl-2 in autophagy and apoptosis regulation. *Autophagy* **4:** 949-51.

Weinberg F, Hamanaka R, Wheaton WW, Weinberg S, Joseph J, Lopez M *et al* (2010). Mitochondrial metabolism and ROS generation are essential for Kras-mediated tumorigenicity. *Proc Natl Acad Sci U S A* **107:** 8788-93.

Wellen KE, Lu C, Mancuso A, Lemons JM, Ryczko M, Dennis JW *et al* (2010). The hexosamine biosynthetic pathway couples growth factor-induced glutamine uptake to glucose metabolism. *Genes Dev* **24:** 2784-99.

Westermann B (2010). Mitochondrial fusion and fission in cell life and death. *Nat Rev Mol Cell Biol* **11:** 872-84.

Wilkinson JH, Walter SJ (1972). Oxamate as a differential inhibitor of lactate dehydrogenase isoenzymes. *Enzyme* **13:** 170-6.

Wise DR, Thompson CB (2010). Glutamine addiction: a new therapeutic target in cancer. *Trends Biochem Sci* **35:** 427-33.

Wojciechowicz DC, Park PY, Paty PB (1995). Beta 1-6 branching of N-linked carbohydrate is associated with K-ras mutation in human colon carcinoma cell lines. *Biochem Biophys Res Commun* **212:** 758-66.

Yamamoto F, Perucho M (1984). Activation of a human c-K-ras oncogene. *Nucleic Acids Res* **12:** 8873-85.

Yamamoto T, Seino Y, Fukumoto H, Koh G, Yano H, Inagaki N *et al* (1990). Over-expression of facilitative glucose transporter genes in human cancer. *Biochem Biophys Res Commun* **170:** 223-30.

Yang D, Wang MT, Tang Y, Chen Y, Jiang H, Jones TT *et al* (2010). Impairment of mitochondrial respiration in mouse fibroblasts by oncogenic H-RAS(Q61L). *Cancer Biol Ther* **9:** 122-33.

Ye XQ, Li Q, Wang GH, Sun FF, Huang GJ, Bian XW *et al* (2011). Mitochondrial and energy metabolism-related properties as novel indicators of lung cancer stem cells. *Int J Cancer* **129:** 820-31.

Ying H, Kimmelman AC, Lyssiotis CA, Hua S, Chu GC, Fletcher-Sananikone E *et al* (2012). Oncogenic Kras maintains pancreatic tumors through regulation of anabolic glucose metabolism. *Cell* **149:** 656-70.

Younes M, Lechago LV, Somoano JR, Mosharaf M, Lechago J (1997). Immunohistochemical detection of Glut3 in human tumors and normal tissues. *Anticancer Res* **17:** 2747-50.

Yun J, Rago C, Cheong I, Pagliarini R, Angenendt P, Rajagopalan H *et al* (2009). Glucose deprivation contributes to the development of KRAS pathway mutations in tumor cells. *Science* **325:** 1555-9.

Yuneva M, Zamboni N, Oefner P, Sachidanandam R, Lazebnik Y (2007). Deficiency in glutamine but not glucose induces MYC-dependent apoptosis in human cells. *J Cell Biol* **178:** 93-105.

Zhang J, Khvorostov I, Hong JS, Oktay Y, Vergnes L, Nuebel E *et al* (2011). UCP2 regulates energy metabolism and differentiation potential of human pluripotent stem cells. *EMBO J* **30:** 4860-73.

Zhang XD, Deslandes E, Villedieu M, Poulain L, Duval M, Gauduchon P *et al* (2006). Effect of 2-deoxy-D-glucose on various malignant cell lines in vitro. *Anticancer Res* **26:** 3561-6.

Zimmermann FA, Mayr JA, Neureiter D, Feichtinger R, Alinger B, Jones ND *et al* (2009). Lack of complex I is associated with oncocytic thyroid tumours. *Br J Cancer* **100:** 1434-7.

Zu XL, Guppy M (2004). Cancer metabolism: facts, fantasy, and fiction. *Biochem Biophys Res Commun* **313:** 459-65.

LIST OF PUBLICATIONS

Ferdinando Chiaradonna, Rosa Maria Moresco, Cristina Airoldi, Daniela Gaglio, Roberta Palorini, Francesco Nicotra, Cristina Messa and Lilia Alberghina, **From cancer metabolism to new biomarkers and drug targets.** *Biotechnol Adv.* 2012 Jan; 30(1):30-51. Epub 2011 Jul 23.

Roberta Palorini, Domenico De Rasmo, Marco Gaviraghi, Lara Sala Danna, Anna Signorile, Claudia Cirulli, Ferdinando Chiaradonna, Lilia Alberghina and Sergio Papa, **Oncogenic K-ras expression is associated with derangement of the cAMP/PKA pathway and forskolin-reversible alterations of mitochondrial dynamics and respiration**. *Oncogene* 2012 Mar 12.
doi: 10.1038/onc.2012.50.

Roberta Palorini, Tiziana Simonetto, Claudia Cirulli and Ferdinando Chiaradonna, **Mitochondrial OXPHOS modulators and low glucose synergize to induce MDA-MB-231 cancer cell death.** *Paper under revision*

Roberta Palorini, Francesco Cammarata, Chiara Balestrieri, Andrea Monestiroli, Michele Vasso, Cecilia Gelfi, Lilia Alberghina and Ferdinando Chiaradonna, **Glucose starvation induces cell death in K-ras transformed cells by interfering with Hexosamine Biosynthesis Pathway and activating the Unfolded Protein Response.** *Paper submitted*

Roberta Palorini, Chiara Balestrieri, Andrea Monestiroli, Sandro Olivieri, Renza Vento and Ferdinando Chiaradonna. **Energy metabolism characterization of a novel cancer stem cell line 3AB-OS.** *Paper under revision*

RINGRAZIAMENTI

Il primo e principale ringraziamento va al mio tutor, Ferdinando Chiaradonna, per tutto ciò che mi ha insegnato e per la fiducia che ha riposto in me. Credo di essere cresciuta molto in questi tre anni e lui ha avuto un ruolo importante in questo cammino.

Grazie a tutti coloro che hanno lavorato o lavorano nel laboratorio 5048, Chiara, Marco, Lara, Daniela, Andrea, Claudia e Giusy, ciascuno di loro ha inevitabilmente lasciato un segno nel mio percorso. Vorrei ricordare anche i tesisti, Tiziana, Simao e Giulia, con loro condivido alcuni pezzetti di questa tesi. Grazie al laboratorio 5051, in particolare a Miluscia, per il reciproco costante aiuto.

Un grazie speciale va ai miei colleghi di dottorato, con alcuni dei quali, in particolare, si è instaurato un rapporto di stima e complicità. Tra questi, voglio nominare Valeria, che è prima di tutto un'Amica. Ogni tappa di questo percorso è stata speciale perché condivisa con lei; le pause al quarto piano per condividere "scleri" e gioie, per fare quattro chiacchiere o solo per un saluto, sono state per me, sempre, aria fresca.

Ringrazio la mia famiglia. I miei genitori, Federica, Michele, gli zii, per il loro sostegno. Un particolare grazie alla più piccola, Francesca, che con i suoi sorrisi e continui progressi ci ha donato gioia, vitalità e speranza.

Infine, grazie a Riccardo, che ha scelto di partecipare ad ogni decisione e ad ogni momento, più o meno felice, più o meno difficile, di questo cammino, incoraggiandomi, spronandomi e accompagnandomi, sempre. A lui, il mio Amore e tutta la vita.